International Journal of Antennas and Propagation

Beamforming Techniques for Wireless MIMO Relay Networks

Guest Editors: Athanasios G. Kanatas, Demosthenes Vouyioukas, Gan Zheng, and Laurent Clavier

Beamforming Techniques for Wireless MIMO Relay Networks

International Journal of Antennas and Propagation

Beamforming Techniques for Wireless MIMO Relay Networks

Guest Editors: Athanasios G. Kanatas, Demosthenes Vouyioukas, Gan Zheng, and Laurent Clavier

Editorial Board

Contents

Hindawi Publishing Corporation
International Journal of Antennas and Propagation
Volume 2014, Article ID 354714, 2 pages
http://dx.doi.org/10.1155/2014/354714

Editorial

Beamforming Techniques for Wireless MIMO Relay Networks

Athanasios G. Kanatas,[1] Demosthenes Vouyioukas,[2] Gan Zheng,[3] and Laurent Clavier[4]

[1] *Department of Digital Systems, School of ICT, University of Piraeus, 18534 Piraeus, Greece*
[2] *Department of Information and Communication Systems Engineering, University of the Aegean, 83200 Karlovassi, Samos Island, Greece*
[3] *School of Computer Science and Electronic Engineering, University of Essex, Wivenhoe Park, Colchester CO4 3SQ, UK*
[4] *IEMN, UMR CNRS 8520 and IRCICA, USR CNRS 3380 and Telecom Lille, Institut Mines Telecom, Lille, France*

Correspondence should be addressed to Athanasios G. Kanatas; kanatas@unipi.gr

Received 12 December 2013; Accepted 12 December 2013; Published 22 July 2014

The continuous increase in mobile data traffic creates the need for radical innovations in the mobile broadband system design. The demand for high-speed and interference-free transmission and reception is inevitable and one *sine qua non* condition is the efficient spatial reuse. However, increasing traffic within a fixed limited bandwidth creates more interference in the system and degrades the signal quality.

Multiple-input multiple-output (MIMO) techniques offer many benefits in practical wireless systems including capacity and spectral efficiency increment, fading mitigation, and improved resistance to interference. Beamforming is a multi-antenna technique that significantly reduces interference and improves system capacity.

An emerging research trend considers relays in terrestrial and satellite networks as the most promising proposal for achieving significant performance gains. Enhanced reliability and extended cell coverage are two of the advantages the relay networks offer. Relay networks encompass amplify-and-forward (AF) and decode-and-forward (DF) protocols, full- and half-duplex operation, experience fading and interference, and incorporate power constraints.

Although beamforming techniques at the source and/or the destination in a relay network have been examined, their use in MIMO relay networks has been recently proposed and is expected to overcome crucial obstacles in terms of capacity and interference. It is thus expected to contribute to the performance of the network, while combining various attributes of networks' design parameters.

The objective of this special issue is to provide the technology development and an in-depth description of the state-of-the-art on the area of beamforming and MIMO relay networks. We received 11 paper submissions and finally accepted 5 according to the reviewers' comments and associate editors' suggestions. The accepted papers cover the topics of radiation antenna pattern design for LTE base stations and relays, integrating MIMO systems and MISO beamforming, along with opportunistic MIMO beamforming power management issues for effective Quality of Service (QoS) fulfillment. Moreover, the special issue includes a survey article that presents the state-of-the-art and the major trends of the applied beamforming techniques on MIMO relay networks.

Specifically, two papers are concentrated on antenna design; one paper proposes effective radiation pattern (ERP) method that is incorporated into a multicell bad urban 4 G LTE operational scenario. It employs beamforming for both the base stations (BSs) and the relay nodes (RNs) in order to demonstrate the effects of the radio channel spatial characteristics on system level measures (SIR, capacity) as well as the validity of the proposed method. The other one is focused on a novel MIMO transmitter built on parasitic antenna arrays that shapes directly the radiation pattern with the aid of analog tunable loads attached to the parasitics, which is able to provide complex loading values even with negative real part and thus high order modulation schemes.

Two papers deal with beamforming methods and their performance with distinctive approaches; one paper studies

the optimum placement of the antenna elements in a given area that can maximize the ergodic capacity of a multi-input single-output (MISO) beamforming system. It is found that it is highly related to the power azimuth spectrum (PAS) distribution and power elevation spectrum (PES). The next paper explores a transmit power management mechanism where multiuser MIMO opportunistic beamforming with adaptive modulation strategy is performed by the system, satisfying the Quality of Service (QoS) for the scheduled user.

Finally, a comprehensive survey, mainly focused on the performance of the adopted beamforming techniques on MIMO relay networks, is presented. The main objective is to provide an account of recent research activity under various network performance challenges. The paper focuses on recently developed procedures for interference modeling and mitigation, beamforming channel modeling, channel estimation and feedback, complexity and power consumption, adaptive beamforming for multiuser relaying, degrees of freedom, diversity issues, and spectral efficiency in cooperative and opportunistic systems.

As long as different beamforming methods and MIMO network topologies and techniques have been considered, pertaining the challenges of beamforming implementation in MIMO relay networks, we sincerely hope that this special issue can further help the readers to understand beamforming in the context of wireless MIMO and relay systems and enhance their study for its potential application on the forthcoming 5 G system.

Acknowledgments

We hope that this special issue will attract the attention of other researchers in this area. We would like to express our appreciation to all the authors and reviewers for their great support that made this issue possible.

Athanasios G. Kanatas
Demosthenes Vouyioukas
Gan Zheng
Laurent Clavier

Hindawi Publishing Corporation
International Journal of Antennas and Propagation
Volume 2014, Article ID 879127, 10 pages
http://dx.doi.org/10.1155/2014/879127

Research Article

A Single RF MIMO Loading Network for High-Order Modulation Schemes

Bo Han,[1,2] Vlasis I. Barousis,[1] Antonis Kalis,[3] Constantinos B. Papadias,[1] Athanasios G. Kanatas,[4] and Ramjee Prasad[2]

[1] *Athens Information Technology (AIT), Peania, 19002 Athens, Greece*
[2] *Center for TeleInFrastructur (CTIF), Aalborg University (AAU), 9220 Aalborg, Denmark*
[3] *SignalGeneriX, 59627 Limassol, Cyprus*
[4] *Department of Digital Systems, University of Piraeus, 18534 Piraeus, Greece*

Correspondence should be addressed to Bo Han; hab@es.aau.dk

Received 20 July 2013; Accepted 12 October 2013; Published 22 July 2014

Academic Editor: Demosthenes Vouyioukas

Recently, a novel MIMO transmitter architecture has been introduced that requires only a single radio-frequency (RF) chain and is built on parasitic antenna arrays. MIMO transmission in this case is achieved by shaping directly the radiation pattern with the aid of analog tunable loads attached to the parasitics. As it has been shown, such a single RF MIMO system can support all PSK modulation formats with purely imaginary loading values. This paper extends its capabilities and proposes a novel architecture for parasitic antennas that is able to provide *complex* loading values, even with a negative real part. Definitely, this will extend the flexibility of parasitic antennas to multiplex successfully over the air more complex signaling formats, for example, QAM signals. The bit error rate evaluation shows that the proposed architecture could be very promising in emerging devices and also illustrates its robustness under possible loading perturbations that might have been raised due to nonidealities in the design.

1. Introduction

The continuously increasing demand for higher data rates and reliable communication has excited the research interest to investigate novel MIMO architectures even for compact mobile devices. This is imposed by the considerable hardware complexity and the often bulkier dimensions of conventional MIMO architectures. Indeed, the existence of multiple radio-frequency (RF) chains hinders the wide deployment of conventional MIMO technology in mobile devices, mainly due to the additional hardware burden and power consumption. Another hindering factor is the correlation among the closely spaced antenna elements due to the strict size constraints. A variety of techniques have already dealt with the aforementioned problems. Indicatively, antenna selection algorithms [1, 2] select a subset of appropriate antenna elements to be connected to the available RF chains [3–5]. Although these techniques offer some complexity savings, often they cause significant performance degradation as compared to the conventional MIMO systems. Another approach known as antenna subarray formation applies mainly to the receiver's side and is based on the fundamental idea that every available RF chain is fed with a linear combination of the responses of a selected subset of antenna elements [6, 7]. Commonly, all those approaches cope with the problem of implementation complexity algorithmically, by activating appropriate antenna elements based on their responses. Another popular approach lies in antenna design and particularly on the investigation of novel multielement antenna configurations with strict size constraints [8].

An alternative perspective of MIMO technology, on which this paper focuses, was recently introduced [9–11]. This architecture is able to provide multiplexing over the air with a single RF chain and is known as single RF MIMO. Instead of the conventional trend of using arrays with multiple active elements, the proposed scheme is built on parasitic antenna arrays with a single active, that is, single feeding, port. Such antennas consist of an active element

surrounded by multiple parasitics in close proximity and are known as electronically steerable parasitic antenna radiators (ESPARs) [12, 13]. Due to the strong mutual electromagnetic coupling among all elements, the feeding of the active element induces strong currents to all parasitics. In this way, all parasitics participate in the radiation mechanism affecting the shape of the far field pattern. Further current control, or equivalently beam-shape control, is possible with the aid of low cost tunable analog circuits attached to all parasitic elements. Tuning those circuits, henceforth called loads, the effective coupling among all neighbor elements changes and this causes a corresponding change to all currents and consequently to the radiation pattern. It should be strongly emphasized that in applications with quite strict size constraints, for example, mobile devices, single RF MIMO often achieve even higher capacity performance as compared to their conventional counterparts with significant hardware complexity [14–16]. Therefore it is evident that single RF MIMO emerges as a novel and promising technology, able to bring the MIMO benefits to mobile devices. A proof-of-concept experiment of this architecture can be found in [17, 18]. Furthermore, the authors in [19] investigate an efficient methodology to enable multiplexing of 16-PSK symbols assuming *purely* imaginary loads. Those loads are realized with varactor diodes that are commonly used in ESPAR antenna designs. These components are a special kind of electronic diodes whose bias voltage controls their capacitance and thus they provide a tunable *pure* imaginary load.

However, the loading restriction to only imaginary values definitely limits the tuning capabilities of ESPAR antennas, implying that higher modulation schemes cannot be supported. Although it has been shown (both theoretically and experimentally) that MIMO is possible with a single RF chain, a challenging and persisting problem is the design of novel and low cost analog loading circuits that will be attached to the parasitics. This largely dictates the capability of ESPAR antennas to support higher modulation schemes as it will improve their beam-shaping abilities.

This is the main objective of this paper. In particular, this paper enables ESPAR antennas to multiplex high-order modulated signals, beyond PSK, over the air (e.g., QAM). This imposes the design of more sophisticated circuits, as compared to those in [19], which will provide *complex* loading with positive or negative real part. This in turn extends the capabilities of parasitic antennas and enables them to produce the required patterns, according to the single RF MIMO concept. We demonstrate the advanced loading flexibility of our approach using a simple 2-element ESPAR antenna, that is, a sole active element and a parasitic that is connected to the novel loading circuit. It is clearly shown that the proposed architecture succeeds to multiplex over the air multiple symbols emerging from a 16-QAM constellation, as it is able to produce the set of required radiation patterns.

This paper is organized as follows. Section 2 provides a brief description of the radiation characteristics of ESPAR antennas at the beamspace domain and also describes the procedure for determining all required loading values, given a certain modulation format. Sections 3 and 4 present in detail the functionality of the architecture that implements the required loading values for the parasitics. The performance of the proposed loading architecture and the consequent single RF MIMO transmitter is evaluated in terms of bit error rate in Section 5. Finally, Section 6 summarizes the key conclusions of the paper.

2. Beamspace Domain Representation of ESPAR Antennas

2.1. A Brief Review. As it is mentioned in Section 1, ESPAR antennas take advantage of the strong couplings among the elements and beamforming is possible by tuning the loading values that are attached to the parasitics. By doing so, the port currents change in a controllable manner. For a given current vector $\mathbf{i}$, the radiation pattern is

$$P(\vartheta,\varphi) = \mathbf{i}^T \mathbf{a}(\vartheta,\varphi) = \sum_{n=0}^{M-1} i_n a_n(\vartheta,\varphi), \tag{1}$$

where M is the number of ESPAR elements and $\mathbf{a}(\vartheta,\varphi)$ is the $(M\times 1)$ steering vector of the array. The $(M\times 1)$ current vector is related to the loading values as

$$\mathbf{i} = u_s(\mathbf{Z}+\mathbf{X})^{-1}\mathbf{v}. \tag{2}$$

In (2) $\mathbf{Z}$ is the $(M \times M)$ electromagnetic coupling matrix of the ESPAR antenna, $\mathbf{X} = \text{diag}\left(R_s \;\; x_1 \;\; \cdots \;\; x_{M-1}\right)$ is the load diagonal matrix that adjusts the radiation pattern, and R_s is the output impedance of the sole source impedance, while $\mathbf{v} = \left[1 \;\; 0 \;\; \cdots \;\; 0\right]^T$ is a $(M\times 1)$ selection vector and u_s is the feeding signal to the active port.

It is understood that in contrast to conventional multiport antenna arrays, ESPAR antennas do not offer spatial degrees of freedom (DoFs) as there exists a single active element. Thus, the conventional way of assigning multiple transmit symbols to different active elements is not applicable and at first glance MIMO communication is not possible. However, thanks to the tunable parasitics and the consequent beamforming abilities of ESPAR antennas, a vector of transmitted symbols can be encoded directly to a single radiation pattern. This functionality can be viewed clearly through the beamspace representation of ESPAR antennas, as explained in detail in [14–16]. According to that representation and considering without loss of generality propagation over the azimuth plane, that is, $\vartheta = \pi/2$, the radiation pattern of an ESPAR antenna given in (1) can be written as a linear combination of M basis patterns or aerial degrees of freedom (ADoFs) as

$$P(\varphi) = \sum_{n=0}^{M-1} w_n \Phi_n(\varphi). \tag{3}$$

It has been shown that the shape of all basis patterns depends on the interelement distance, while the coefficients w_n depend on the interelement distance and the currents (due to electromagnetic coupling the currents are also distance-dependent).

More details about the beamspace domain representation of ESPAR antennas can be found, for example, in [14] and the references therein.

Equation (3) reveals the functionality of the single RF MIMO transmitter: letting the coefficients be the complex symbols for transmission of an arbitrary signal constellation, (3) shows that M symbols have been attached, that is, mapped, to different basis patterns. Thus, symbols are not driven to diverse active antenna elements as in the conventional case, but they modulate orthogonal radiation patterns. In this way, at every symbol period the shape of the transmit pattern changes according to the symbol vector for transmission. Although this functionality looks very similar to beamforming, indeed it is a multiplexing operation defined at the beamspace domain. The ESPAR receiver in turn assesses the impinging signals by switching among orthogonal patterns within a symbol period [14]. A similar single RF receiver is proposed in [11]. Therefore, MIMO transmission so far has been emulated at the beamspace domain with single RF transceivers at both link ends. However, this paper focuses on the design of the single RF transmitter and therefore the bit error probability in Section 5 has been derived assuming a conventional MIMO receiver. It is also understood that the basis patterns in (3) remain orthogonal to each other as long as there is a reasonable amount of multipaths with different angles of departure. Otherwise, the radiation patterns are not sampled adequately in the angular domain and this will raise some amount of correlation among the basis patterns.

It should be strongly noted that although (3) implies that theoretically the number of symbols that can be multiplexed is equal to the number of all elements, [14, 15] mention that the interelement distance affects the *effective* number of ADoFs, that is, the number of basis patterns with significant contribution to the total radiated power that can practically be exploited for transmission. In this paper, an ESPAR antenna with $M = 2$ elements will be considered at 2.4 GHz, with a small interelement distance, where both basis patterns are strong and beam-shaping is possible [16].

2.2. Application to an ESPAR with 2 Elements. For an ESPAR antenna with $M = 2$ elements the basis patterns are given by [16]

$$\begin{aligned} \Phi_0(\varphi) &= \frac{1}{k_0}, \\ \Phi_1(\varphi) &= \frac{\left(e^{jb\cos\varphi} - 2\pi I_0(jb)/k_0^2\right)}{k_1}, \end{aligned} \tag{4}$$

where

$$\begin{aligned} k_0 &= \sqrt{2\pi}, \\ k_1 &= \sqrt{2\pi + \frac{\left(\pi/k_0^2 - 1\right) 8\pi^2 I_0^2(jb)}{k_0^2}}, \end{aligned} \tag{5}$$

and the coefficients in (3) are given by

$$\begin{aligned} w_0 &= i_0 k_0 + \frac{2\pi i_1 I_0(jb)}{k_0}, \\ w_1 &= i_1 k_1, \end{aligned} \tag{6}$$

where $b = 2\pi d$, d is the interelement distance normalized to wavelength, and $I_0(\cdot)$ is the zero-order modified Bessel function of the first kind. As it has been already stated, in case of small interelement spacing d, both basis patterns are strong and therefore multiplexing over the air is possible according to (3) [16]. Letting the coefficients in (6) be the complex symbols for transmission of an arbitrary signal constellation, it is evident that at each signaling period the desired symbol vector is produced by tuning the currents at the elements. This in turn can be achieved by adjusting appropriately the loading at the parasitic, as it will be explained next.

2.3. Loads Values for All Possible Symbol Vectors. A common assumption in the literature is that usually the tunable loads at the parasitic elements are implemented with varactor diodes, where their bias voltage controls the capacitance. Although this is a low cost implementation approach, often the pure imaginary load restricts the beam-shape abilities of the ESPAR antenna and thus the capability of the antenna to produce all the necessary radiation patterns dictated by (3). This fact becomes particularly evident as the constellation size becomes higher.

Although the authors in [19] succeed to encode any PSK modulated symbols onto the radiation patterns using purely imaginary loading, imposing a higher constellation, for example, QAM, imaginary loads can no longer produce the whole desired set of possible radiation patterns. To alleviate this problem, this section defines *complex* loading values that correspond to all possible transmit symbol vectors, or equivalently to all possible radiation patterns emerging from a 16-QAM modulation.

Recalling (3), when $M = 2$ the pattern becomes

$$P(\varphi) = w_0\left(\Phi_0(\varphi) + \frac{w_1}{w_0}\Phi_1(\varphi)\right). \tag{7}$$

Equation (7) describes the triggering operation of the transmit ESPAR antenna. The first symbol w_0 is driven directly to the sole RF port, while the ratio w_1/w_0 determines the shape of the pattern. Therefore, the schematic of the single RF MIMO transmitter is the one depicted in Figure 1 that includes the ESPAR antenna and the triggering unit. At each signaling period a symbol vector $[w_0 \;\; w_1]$ is determined. Then, the tuning procedure maps the symbol ratio w_1/w_0 to a complex load x_1 that should be applied to the parasitic element, while the first symbol w_0 is fed to the active element. In this way the ESPAR is configured to the desired pattern and MIMO transmission is achieved as explained in Section 2.

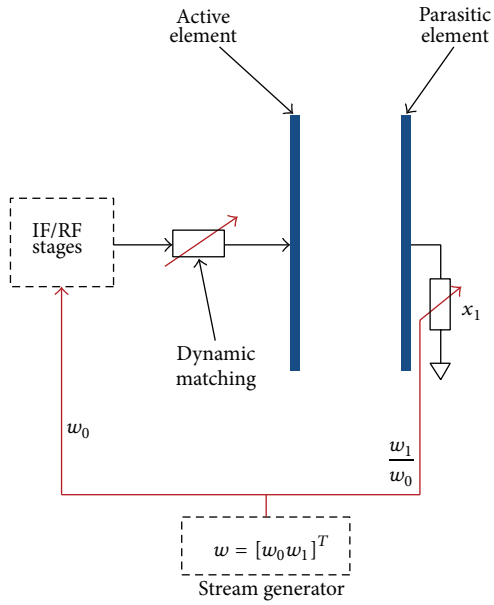

Figure 1: Topology of the proposed single RF MIMO transmission system.

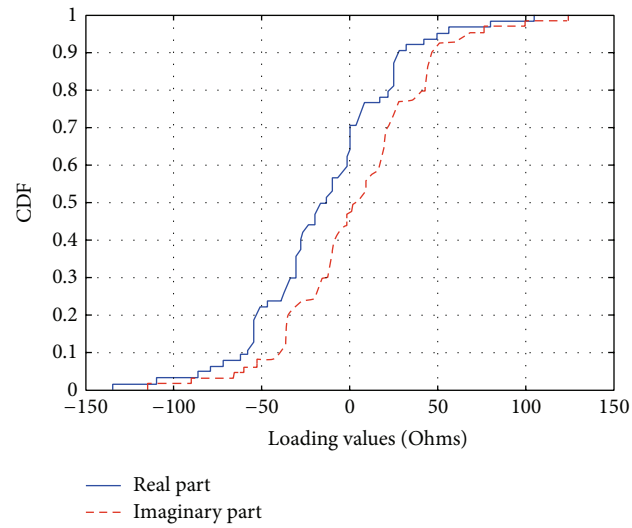

Figure 2: CDF pf the loading values that correspond to all possible 16-QAM symbol vectors.

In case of the ESPAR antenna with $M = 2$ elements, the transformation of the symbols to the load values are found by expanding (2) as

$$\left(\begin{bmatrix} Z_{11} & Z_{12} \\ Z_{21} & Z_{22} \end{bmatrix} + \begin{bmatrix} 50 & 0 \\ 0 & x_1 \end{bmatrix}\right)[i_0 \;\; i_1]^T = [u_s \;\; 0]^T. \quad (8)$$

From (8), and assuming $Z_{21} = Z_{12}$, we can get the required load value x_1 by

$$x_1 = -\left(\frac{i_0}{i_1} Z_{21} + Z_{22}\right). \quad (9)$$

According to (6), the above value can be rewritten as

$$x_1 = -\left(\left[\frac{w_0}{w_1} - \frac{2\pi I_0(jb)}{k_0 k_1}\right]\frac{k_1}{k_0} Z_{21} + Z_{22}\right), \quad (10)$$

where Z_{21} is mutual coupling of the two antenna elements. According to the constellation of the 16-QAM, there are totally 256 possible values of the ratio w_1/w_0. However, evaluating all of them, one observes that only 53 different loading values are required according to (10).

Figure 2 shows the cumulative distribution function (CDF) of the real and imaginary parts of the loads, as computed by (10), for all different 16-QAM transmit symbol vectors. It is mentioned that the mutual couplings in (10) are those that correspond to a real antenna design that is explained in Section 5. It is observed that the real part of the antenna load might be positive or negative. Therefore, if we were to take full advantage of the parasitic array capabilities, the loading circuit controlling the parasitic antenna loads should be able to provide a complex loading, which can be realized with a novel active circuit design. In this paper we describe such a design approach, which is the subject of the next sections.

3. Negative Resistance Circuit

3.1. System Level Requirement. From the aforementioned requirements, it is evident that an ESPAR antenna with 2 elements could multiplex two 16-QAM symbols given that the loading values are allowed to be complex with the real, that is, the resistive, part ranging from negative to positive values. Apparently, this can be achieved by replacing the varactor-based loading unit that has been used widely so far by a novel active circuit design. To emphasize this novel approach, hereafter the parasitic elements will be characterized as *active-loaded parasitics*.

To the authors' best knowledge, the idea of active-loaded parasitics has been first introduced in [20]. In particular, the main idea therein was to design a unit able to generate 4 negative values that are found to be appropriate for multiplexing two QPSK signals. Although in [20] along with the desired real part the proposed unit inevitably generates an imaginary component too, it has been found that this does not influence the performance, as long as an equivalent constellation could be defined. On the contrary, as the modulation format becomes more complex the number of the required loading states increases and a similar equivalent constellation cannot be found easily. Therefore, this paper proposes a universal (in the sense that the same topology could be used for designing a similar circuit that supports other modulation schemes or an arbitrary precoding) transmitter architecture with ESPAR antennas, comprised of active-loaded parasitic elements and a single RF chain. It will be shown that the proposed alternative is able to multiplex high-order modulation symbol formats over the air.

To achieve that goal, we propose the architecture shown in Figure 3. The active circuit in this figure is responsible to generate a *constant* negative resistance, which corresponds to the minimum value required for the given modulation scheme. To compensate the imaginary component of the active circuit and adjust the loading to the desired complex

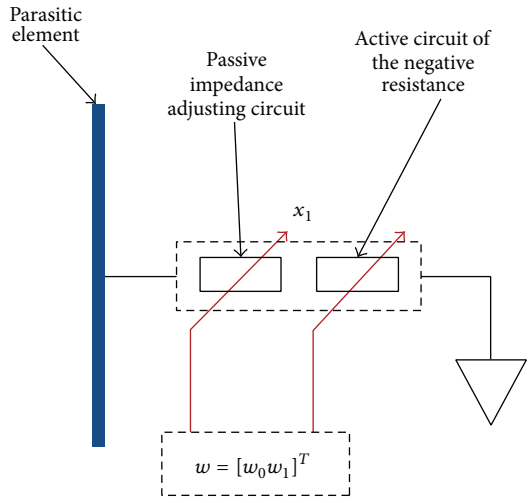

Figure 3: Topology of impedance control for the parasitic antenna.

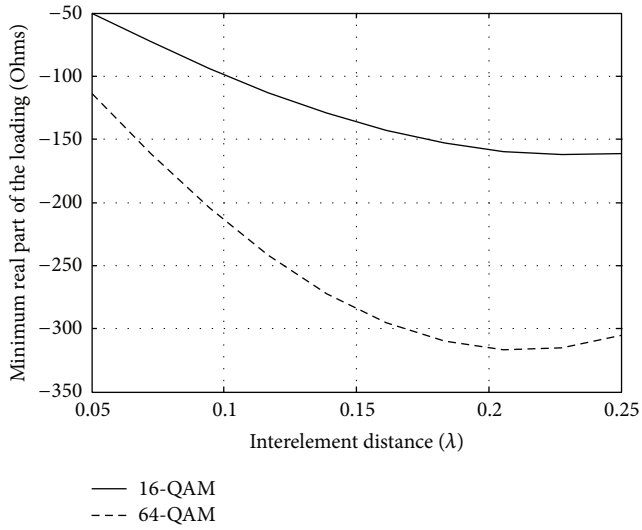

Figure 4: Minimum negative resistance value according to theory simulation.

value, a passive impedance adjusting circuit is also interpolated. In this way, the parasitic element is finally loaded with the desired complex loading value. In our design approach we initially estimate the lower bound of the loading. Recall that (10) gives the complex load as a function of the symbol ratio w_1/w_0 and the interelement distance d. Evaluating (10) for different interelement distances and assuming 16-QAM signaling one obtains Figure 4. In this figure, for each interelement distance all possible loading values are computed and the minimum one is plotted. As observed, the minimum value of x_1 is found to be below $-150\,\Omega$ for interelement spacings between $0.18\,\lambda$ and $0.25\,\lambda$. To provide a sense of the impact of the modulation order to the loading, Figure 4 includes also a curve that corresponds to the 64-QAM modulation scheme. Clearly, as the modulation scheme becomes more complex, the beam-shape requirements of the ESPAR become more demanding and this is reflected

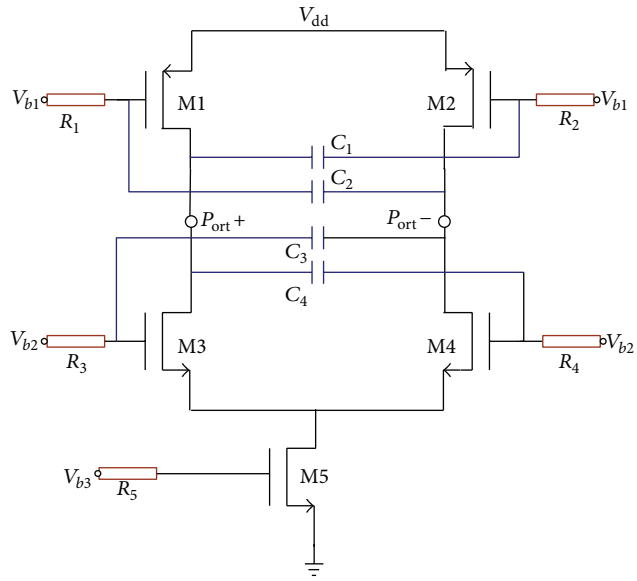

Figure 5: Negative resistance block using cross-coupling architecture.

to larger range of the required loading. It is noted that in this figure the mutual coupling between the two antenna elements is computed for each interelement distance using the theoretical formula presented in chapter 8 of [21]. Although this theoretical treatment assumes ideal dipoles in free space, it still provides a representative example of the dependence of the beam-shaping requirements with the modulation order. In Section 5, a realistic antenna design is assumed.

The simplest way to create an active circuit with tunable impedance is by using an operational amplifier (op-amp), which has a large open loop gain. However, commercial op-amps or low noise amplifiers (LNAs) usually provide a small open loop gain at high operating frequencies, for example, 1.9 GHz or 2.4 GHz. Taking also into account that usually such components are power hungry, they do not meet the low power requirements of mobile terminals. To satisfy the aforementioned constraints, next a novel circuit is described that is based on the complementary metal oxide semiconductor (CMOS) technology.

3.2. An Active Circuit Design for Generating Tunable Negative Resistance. Figure 5 shows the schematic of the proposed active circuit. The design is based on two cross-coupled transistor pairs under UMC 0.18 μm RF process. The PMOS transistors M1, M2 and the NMOS transistors M3, M4 are biased independently by voltages V_{b1}, V_{b2}, respectively. The individual biasing provides not only extra design flexibility, but also improved tuning capability. The NMOS transistor M5 works as a current source and it is designed with enlarged width W and length L to reduce the flicker noise. The DC-biasing components $R_1 - R_4$ are resistors with high value to provide isolation from the circuit that sets the biased voltages. The circuit is powered by $V_{dd} = 1.2$ V, which is a trend in portable applications. The tunable resistance is measured

between the ports $P_{\text{ort}}+$ and $P_{\text{ort}}-$ in Figure 5 and is given by the following equation [22]:

$$R_{\text{neg}} = \frac{-1}{\left(g_{mn} + g_{mp}\right)} = -\frac{V_{\text{gs}} - V_{\text{th}}}{2I_{\text{ds}}} = \frac{-\left(u_n + u_p\right)L}{u_n u_p C_{\text{ox}} W \left(V_{\text{gs}} - V_{\text{th}}\right)} = -\sqrt{\frac{\left(u_n + u_p\right)2n}{u_n u_p C_{\text{ox}}} \frac{L}{W} \frac{1}{4I_{\text{ds}}}}, \tag{11}$$

where g_{mn}, g_{mp} are the transconductances of NMOS transistor and PMOS transistor respectively, expressed as

$$g_{m(n,p)} = u_{(n,p)} C_{\text{ox}} \frac{W}{L} \left(V_{\text{gs}} - V_{\text{th}}\right) = 2\frac{I_{\text{ds}}}{V_{\text{gs}} - V_{\text{th}}}. \tag{12}$$

Moreover, $\mu_{(n,p)}C_{\text{ox}}$ is a process related coefficient, W/L is the ratio of channel width and channel length of the transistor, I_{ds} is the current flowing though the transistor, V_{gs} is the voltage between gate and source, and V_{th} is the threshold voltage of the transistor. The smaller the current I_{ds}, the smaller the negative resistance we get. In submicrometer processes, the effect of the channel length should be taken into consideration and therefore [22]

$$I_{\text{ds}} = \frac{u_n u_p C_{\text{ox}}}{2\left(u_n + u_p\right)} \frac{W}{L} \left(V_{\text{gs}} - V_{\text{th}}\right)^2 \left(1 + \lambda_{\text{tr}} V_{\text{ds}}\right), \qquad R_{\text{neg}} = \frac{-\left(u_n + u_p\right)L}{u_n u_p C_{\text{ox}} W \left(V_{\text{gs}} - V_{\text{th}}\right)\left(1 + \lambda_{\text{tr}} V_{\text{ds}}\right)}, \tag{13}$$

where λ_{tr} is the coefficient related to the effect of the channels length and V_{ds} is the voltage between the source and drain of the transistor.

3.3. Simulated Negative Resistance Values. Based on the aforementioned theoretical analysis, we set the size of the transistors M1 and M2 to $W/L = 10/0.18$. Regarding the transistors M3 and M4 this value is set to $W/L = 45/0.18$, while the current source M5 operates with a bias current of 1 mA. The capacitors C1–C4 are set to 1 pF and the resistors $R_1 - R_4$ are 1 MΩ. The active circuit in Figure 5 has been characterized by the S parameters obtained in Advanced Design System (ADS) software, which is an electronic design software for RF, microwave, and high speed digital applications. Based on this design setup, a fixed negative resistance value is selected by setting appropriately the bias voltages. This value is shown in Figure 6 obtained in ADS as a function of frequency. The horizontal axis is the frequency in GHz and vertical axis is the impedance value in Ω. Two markers indicate the real and imaginary parts of the impedance, respectively. According to the simulation, the real part of the impedance below 2.5 GHz is found smaller than −230.6 Ω and the imaginary part smaller than −117.9 Ω. It is noted that for the selected frequency of operation at 2.4 GHz (see Section 5),

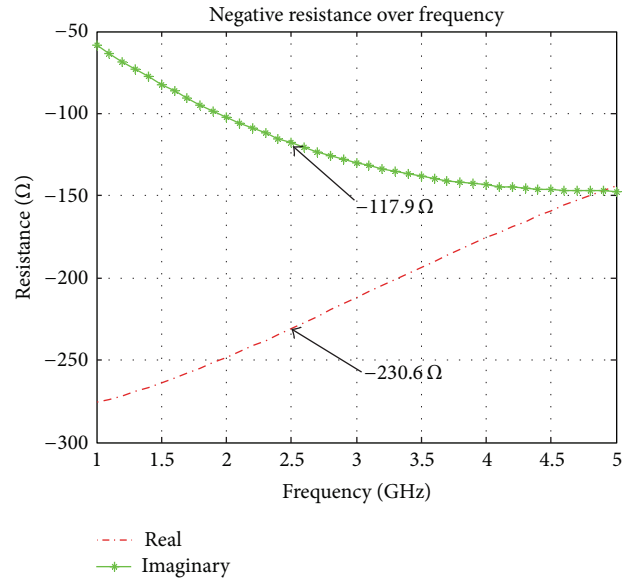

Figure 6: Simulated negative resistance values.

the corresponding impedance is finally adjusted to the desired loading by the impedance matching network presented at the next section. Compared with the loading requirements drawn in Figure 2, the result of the proposed negative resistance unit is more than sufficient. It is mentioned that as every active circuit, this also requires an external power supply that will provide the necessary biasing. However, the underlying power consumption is negligible as it has been found in [20] to be at the order of microwatts. Therefore, the design and the proposed architecture still remain energy efficient.

4. Loading Switching

4.1. Adjusting Stages. According to the proposed circuit architecture shown in Figure 2, in order to compensate with the imaginary component of the active circuit and adjust the load to the desired value, a switching passive impedance matching grid should be included. The adjusting unit is composed of 53 discrete values that are equal to the unique loading values as indicated in (10), where each one contains resistive R_{adj} and inductive L_{adj} components. As shown in Figure 7 the proposed adjusting unit consists of an 8 × 8 array and two 3-to-8 converters (although an 7 × 8 array with 3 redundant cells could be used, a 3-to-7 converter is not available widely in the market). The cells of this array hold 53 discrete values, while the remaining ones are unused. CMOS Port 1 is connected to the ports of the negative resistance circuit described in Figure 5, and the RF Port 2 is connected to the parasitic antenna. In this topology, only 6 control bits are required to select one out of the 53 values. Based on this implementation approach, each symbol vector is mapped to a 6-bit code-word and at each signaling period the appropriate one applies to retrieve the correct value of the load matrix. An example of such a selection is shown in Figure 7.

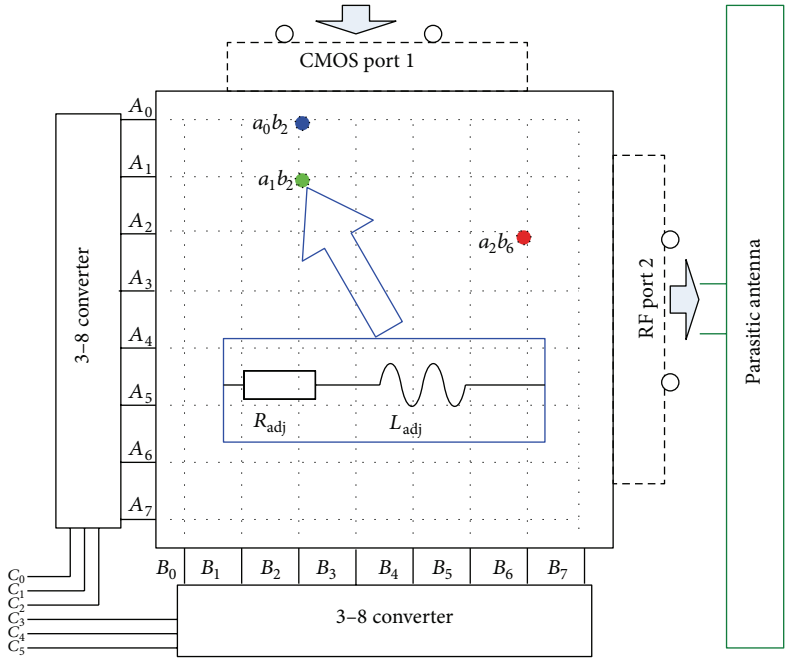

Figure 7: Topology of the proposed digitally controlled adjusting network.

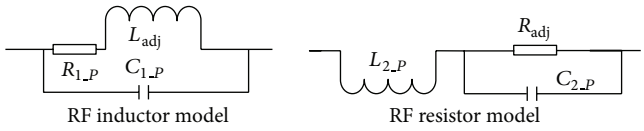

Figure 8: Small circuit model of resistor and inductor at high frequency.

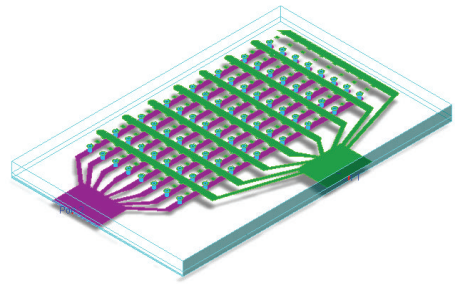

Figure 9: 3D view of the proposed load switching array produced in ADS design software.

It should be noted however that the proposed solution assumes instantaneous transitions between consecutive loading states. Although in practical designs the switching speed can be at the order of nanoseconds, in a real system the transmitted signal must satisfy specific bandwidth constraints. Therefore, a smoother and controllable transition between different loading states is needed. However, this issue deserves further study and is out of the scope of this paper.

4.2. Performance and Tolerance Simulation. Although we have a way to define the required loading values, at high frequencies additional nonidealities due to parasitic effects have to be also considered, as indicated in Figure 8 [23]. According to that figure, the impedance of the resistor and the inductor including the parasitic effects is given by

$$Z_{\text{res}} = j\omega L_{2\_P} + \frac{1}{j\omega C_{2\_P} + 1/R_2},$$
$$Z_{\text{ind}} = \frac{j\omega L_1 + R_{1\_P}}{1 + j\omega C_{1\_p}\left(R_{1\_P} + j\omega L_1\right)}. \quad (14)$$

The practical nonidealities that count not only for the parasitic effects but also for the mounting pad influence have been simulated in ADS. For completeness, the resulting model as obtained in ADS is shown in Figure 9. Taking into account this model, we observed a variation from the desired values in the order of around 2.5 Ω. Similar variations have been also reported in the literature, for example, [23]. It is noted that this deviation is representative for all loading states. It should be worthy to note that the adjusting matching network in Figure 7 has been proposed as an easy-to-implement solution, with fixed and predefined impedance values. Applying a deembedding technique (e.g., [24, 25]), one could easily compensate possible parasitic effects during the design procedure by taking them into account and optimizing the final impedance values on the grid. Therefore, it is understood that the treatment of the parasitic effects, at least to some extent, is a matter of implementation. In Section 5, however, we illustrate the impact of possible loading perturbations that might be present on the performance in terms of bit error probability.

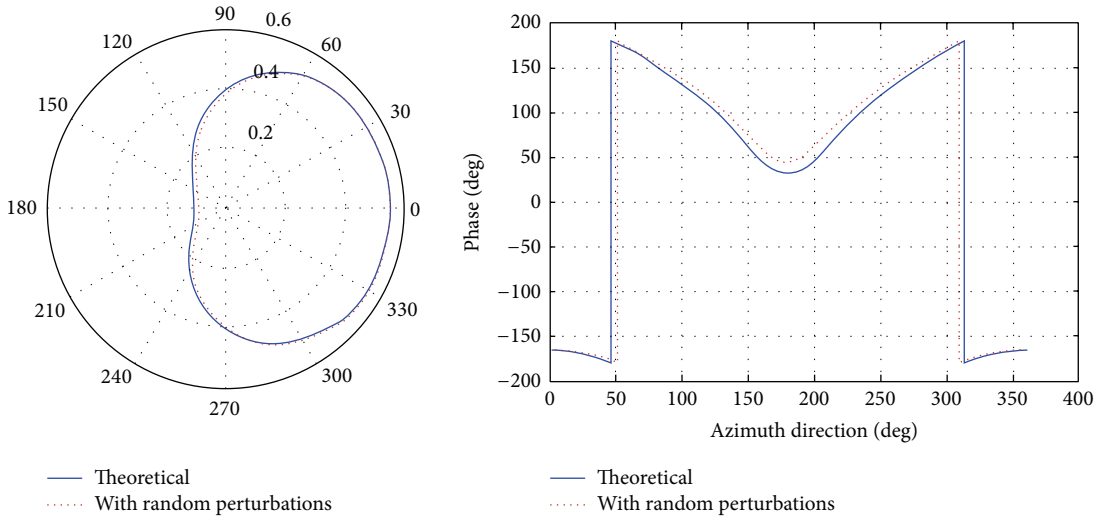

Figure 10: Theoretical and practical radiation patterns gains and phase.

5. Performance Evaluation

The performance of the proposed single-RF MIMO architecture is evaluated with a realistic ESPAR antenna, which has been designed in IE3D (this is a full-wave, method-of-moments based electromagnetic simulator solving the current distribution on 3D and multilayer structures of general shape and is provided by Mentor Graphics) using a metal thickness of 0.0254 mm and an FR4 substrate with thickness of 1.6 mm and dielectric constant of $E_r = 4.45$. The active element is selected as a folded-dipole, while the parasitic is a conventional dipole, while their interelement spacing is selected as $d \approx 0.23\,\lambda_{\text{eff}}$, $\lambda_{\text{eff}} = \lambda_0/\sqrt{E_r}$, where λ_0 is the wavelength in vacuum, that is, 125 mm at 2.4 GHz. The existence of small perturbations due to nonidealities on the loading states might change the shape of the desired pattern given in (3). Indicatively, Figure 10 shows a comparison between a desired pattern, that is, the theoretical, and the corresponding one with an extra deviation at the real and imaginary parts of the loading that represents the effect of nonidealities. As observed, both patterns are very identical, especially regarding the amplitude component. This high accuracy is achieved in all cases.

Figure 11 offers a valuable comparison of the bit error probability when a conventional zero-forcing receiver with two antenna elements is utilized and the ESPAR antenna at the transmitter (as described in Figure 1) multiplexes two 16-QAM signals. As observed, the performance using the theoretical loading values is compared against the case of two different ranges of loading deviation, that is, 3 and 4 Ohms (i.e., more than the one found with ADS), which model any possible and inevitable nonidealities. Reasonably, the loading deviations change slightly the currents at the ports of the ESPAR elements and in turn the actual signal constellation. Consequently, this causes a performance degradation in high E_b/N_o regime, but since it is expected that the mobile devices in future wireless systems will operate in the low E_b/N_o regime, the system remains robust and those nonidealities can be ignored.

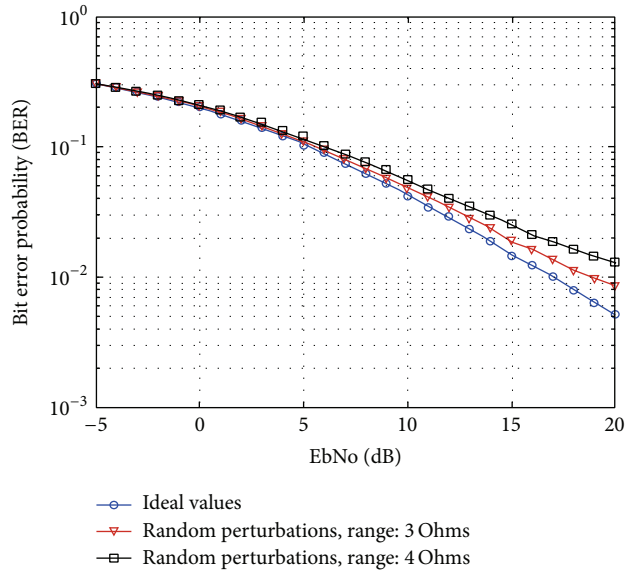

Figure 11: Bit error probability performance, under various loading conditions.

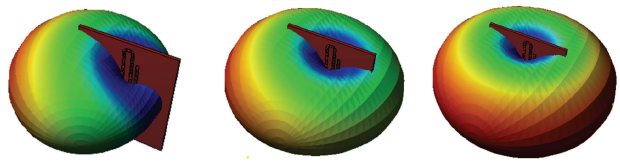

Figure 12: Three indicative radiation patterns obtained from IE3D.

Eventually, the end-to-end performance could be further improved by using more robust receiving techniques such as ordered successive cancellation (OSUC) zero-forcing, or even more complex ones [26]. For completeness, Figure 12 illustrates 3D examples of radiation patterns obtained in IE3D

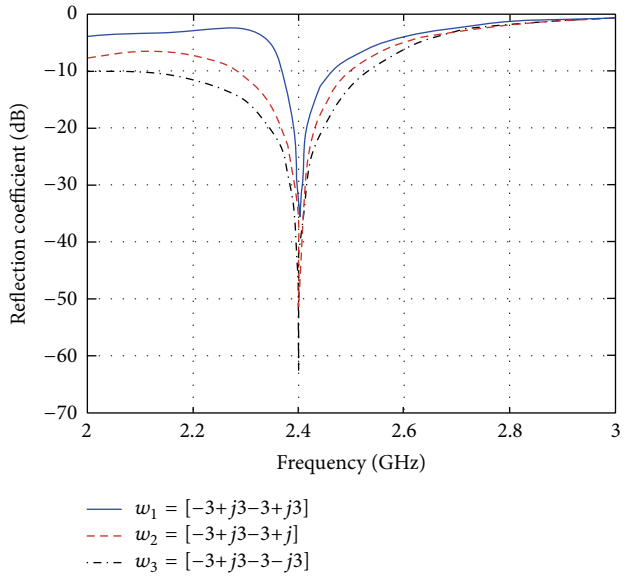

FIGURE 13: Simulated indicative return loss of the first 16 load values.

software, where each of them corresponds to a different 16-QAM symbol vector for transmission. Also, Figure 13 shows the return losses of the antenna for each of the patterns in Figure 12, as they are computed in IE3D antenna design software. As expected, the curve of the return loss for a certain pattern is different, since it depends on the loading values. Clearly, at 2.4 GHz the reflection coefficient is almost zero, as expected. As it has been verified, the same trend applies for all possible radiation patterns.

6. Conclusion

This paper presents a novel loading architecture that supports a reliable MIMO transmission with the aid of a single RF chain and a parasitic antenna array with closely spaced elements. Instead of the conventional trend of using purely imaginary loads, complex loading values with positive or negative real part are generated via an active circuit design. The consequent additional flexibility is found to improve significantly the beam-shaping abilities of the parasitic antenna, which as it has been shown succeeds to multiplex 16-QAM signals over the air. Therefore, MIMO transmission is emulated with a single RF chain. The remarkable hardware savings and the reduced antenna dimensions constitute the proposed architecture a strong candidate for battery-charged and lightweight devices. Although this architecture is demonstrated for 16-QAM signals, clearly the same design procedure can be used to support an arbitrary signaling format, an arbitrary precoding scheme, or power control policy.

Conflict of Interests

The authors declare that there is no conflict of interests regarding the publication of this paper.

Acknowledgments

The authors acknowledge the valuable contribution of Mr. Eleftherios Roumpakias, who is a Research Engineer in Broadband Wireless Sensor Networks (B-WiSE) Lab at Athens Information Technology (AIT), Greece. This work is supported by European Commission Founded SmartEN (Grant no. 238726) Marie Curie ITN FP7 Program. This work is also supported under the collaboration between Aalborg University and Athens Information Technology.

References

[1] A. Gorokhov, D. A. Gore, and A. J. Paulraj, "Receive antenna selection for MIMO spatial multiplexing: theory and algorithms," *IEEE Transactions on Signal Processing*, vol. 51, no. 11, pp. 2796–2807, 2003.

[2] A. Gorokhov, D. Gore, and A. Paulraj, "Receive antenna selection for MIMO flat-fading channels: theory and algorithms," *IEEE Transactions on Information Theory*, vol. 49, no. 10, pp. 2687–2696, 2003.

[3] P. D. Karamalis, N. D. Skentos, and A. G. Kanatas, "Selecting array configurations for MIMO systems: an evolutionary computation approach," *IEEE Transactions on Wireless Communications*, vol. 3, no. 6, pp. 1994–1998, 2004.

[4] D. A. Gore and A. J. Paulraj, "MIMO antenna subset selection with space-time coding," *IEEE Transactions on Signal Processing*, vol. 50, no. 10, pp. 2580–2588, 2002.

[5] P. J. Voltz, "Characterization of the optimum transmitter correlation matrix for MIMO with antenna subset selection," *IEEE Transactions on Communications*, vol. 51, no. 11, pp. 1779–1782, 2003.

[6] P. Theofilakos and A. G. Kanatas, "Capacity performance of adaptive receive antenna subarray formation for MIMO systems," *EURASIP Journal on Wireless Communications and Networking*, vol. 2007, Article ID 56471, 2007.

[7] P. Theofilakos and A. G. Kanatas, "Maximising capacity of MIMO systems with receive antenna subarray formation," *Electronics Letters*, vol. 44, no. 20, pp. 1204–1206, 2008.

[8] J. Villanen, P. Suvikunnas, C. Icheln, J. Ollikainen, and P. Vainikainen, "Performance analysis and design aspects of mobile-terminal multiantenna configurations," *IEEE Transactions on Vehicular Technology*, vol. 57, no. 3, pp. 1664–1674, 2008.

[9] A. Kalis, A. G. Kanatas, and C. B. Papadias, "A novel approach to MIMO transmission using a single RF front end," *IEEE Journal on Selected Areas in Communications*, vol. 26, no. 6, pp. 972–980, 2008.

[10] A. Kalis and C. Papadias, "An ESPAR antenna for beamspace-MIMO systems using PSK modulation schemes," in *Proceedings of the IEEE International Conference on Communications (ICC '07)*, pp. 5348–5353, June 2007.

[11] R. Bains and R. R. Müller, "Using parasitic elements for implementing the rotating antenna for MIMO receivers," *IEEE Transactions on Wireless Communications*, vol. 7, no. 11, pp. 4522–4533, 2008.

[12] R. F. Harrington, "Reactively controlled directive arrays," *IEEE Transactions on Antennas and Propagation*, vol. 26, no. 3, pp. 390–395, 1978.

[13] C. Sun, A. Hirata, T. Ohira, and N. C. Karmakar, "Fast beamforming of electronically steerable parasitic array radiator antennas: theory and experiment," *IEEE Transactions on Antennas and Propagation*, vol. 52, no. 7, pp. 1819–1832, 2004.

[14] V. I. Barousis, A. G. Kanatas, and A. Kalis, "Beamspace-domain analysis of single-RF front-end MIMO systems," *IEEE Transactions on Vehicular Technology*, vol. 60, no. 3, pp. 1195–1199, 2011.

[15] V. I. Barousis and A. G. Kanatas, "Aerial degrees of freedom of parasitic arrays for single RF front end MIMO receivers," *Progress in Electromagnetics Research B*, vol. 35, pp. 287–306, 2011.

[16] V. Barousis, A. Kalis, and A. G. Kanatas, "Single RF MIMO systems: exploiting the capabilities of parasitic antennas," in *Proceedings of the 74th IEEE Vehicular Technology Conference (VTC-Fall '11)*, pp. 5–8, September 2011.

[17] O. N. Alrabadi, J. Perruisseau-Carrier, and A. Kalis, "MIMO transmission using a single RF source: theory and antenna design," *IEEE Transactions on Antennas and Propagation*, vol. 60, no. 2, pp. 654–664, 2012.

[18] O. N. Alrabadi, C. Divarathne, P. Tragas et al., "Spatial multiplexing with a single radio: proof-of-concept experiments in an indoor environment with a 2.6-GHz prototype," *IEEE Communications Letters*, vol. 15, no. 2, pp. 178–180, 2011.

[19] O. N. Alrabadi, C. B. Papadias, A. Kalis, and R. Prasad, "A universal encoding scheme for MIMO transmission using a single active element for PSK modulation schemes," *IEEE Transactions on Wireless Communications*, vol. 8, no. 10, pp. 5133–5142, 2009.

[20] B. Han, V. Barousis, A. Kalis, and A. G. Kanatas, "Active parasitic arrays for low cost compact MIMO transmitters," in *Proceedings of the IEEE 5th European Conference on Antennas and Propagation (EUCAP '11)*, vol. 1, pp. 3663–3667, April 2011.

[21] C. Balanis, *Antenna Theory, Analysis and Design*, John Wiley & Sons, 2005.

[22] B. Razavi, *RF Microelectronics*, Prentice Hall, 1998.

[23] C. Bowick, J. Blyer, and C. Ajluni, *RF Circuit Design*, Newnes Elsevier, 2008.

[24] B. Han, M. Liu, and N. Ge, "A UWB down convert circuit and measurement," in *Proceedings of the IEEE International Conference on Microwave and Millimeter Wave Technology (ICMMT '10)*, vol. 1, pp. 1472–1475, May 2010.

[25] T. Hirano, J. Hirokawa, M. Ando, H. Nakano, and Y. Hirachi, "De-embedding of lumped-element characteristics with the aid of EM analysis," in *Proceedings of the IEEE International Symposium on Antennas and Propagation Society (AP-S '08)*, vol. 1, pp. 1–4, July 2008.

[26] A. Paulraj, R. Nabar, and D. Gore, *Introduction To Space-Time Wireless Communications*, Combridge University Press, 2003.

Hindawi Publishing Corporation
International Journal of Antennas and Propagation
Volume 2013, Article ID 454916, 10 pages
http://dx.doi.org/10.1155/2013/454916

Research Article

The Optimal Antenna Layout for Maximum Ergodic Capacity of MISO Beamforming System

Qianya Wang and Hongwen Yang

School of Information and Communication Engineering, Beijing University of Posts and Telecommunications (BUPT), Beijing 100876, China

Correspondence should be addressed to Qianya Wang; wangqianya.bupt@gmail.com

Received 21 June 2013; Revised 14 September 2013; Accepted 12 October 2013

Academic Editor: Demosthenes Vouyioukas

The performance of the multiantenna systems can be deeply affected by the antenna layout, that is, the placement of the antenna elements in a given area. This paper focuses on the optimal antenna layout which can maximize the ergodic capacity of a multi-input single-output (MISO) beamforming system. Since the optimization problem cannot be solved analytically, we use simulated annealing (SA) algorithm to search for the optimal antenna layout. The results show that the optimal antenna layout depends highly on the power azimuth spectrum (PAS) distribution and power elevation spectrum (PES) distribution. In the three-dimensional (3D) space uniformly scattering environment, the optimal antenna layout will locate the antenna elements on the surface of a sphere. When the scattering is concentrated in a two-dimensional (2D) plane, the circular layout is the optimal and finally, when there is no scattering (single plane wave), the optimal layout is the nonuniform linear array.

1. Introduction

multiple-input multiple-output (MIMO) systems have received significant attention for their capability of increasing channel capacity and improving the transmission reliability [1, 2]. Beamforming (BF) is one particular way of utilizing multiple antenna elements [3, 4]. In a beamforming antenna array, the radiated electromagnetic field can be patterned to have high antenna gain in desired direction by controlling the phase and amplitude of the signal field at each antenna element. Antenna beamforming has found a diverse range of applications due to its simplicity and effectiveness [5–8].

For a practical system, it is typical that multiple antenna elements have to be installed in a limited space area. The constrained space area will inevitably introduce the correlation between antenna elements and such correlation will affect the performance of multiantenna system. There are already many published works discussing the relation between the antenna correlation and the performance of multiple antenna systems in terms of ergodic capacity, outage capacity, bit error rate, and so forth [9–14]. However, to our knowledge, there are relatively few reports [15–22] on the relation between the multiple antenna system performance and the antenna layout, that is, the placement of the antenna elements. It is well known that, given the power azimuth spectrum (PAS) distribution and power elevation spectrum (PES) distribution [23], the performance of the multiantenna system is completely determined by the antenna spatial correlation matrix with its entries determined by the relative distance of the antenna elements. Hence, it is clear that the performance of the multiple antenna system is a function of antenna layout. In case of 2-dimensional (2D) deployment of multiple antenna elements and uniform PAS, it is reported [19, 20] that the optimal antenna layout which can maximize MIMO capacity is the near circular array, but both of them considered a propagation model including PAS only. For short-range communications, [21] has investigated the optimal antenna placement of 2×2 MIMO taken into consideration the joint effects of path loss and phase difference. In [22], empirical results for the effects of antenna placement on vehicle-to-vehicle link performance in vehicular ad hoc networks have been reported.

This paper focuses on the 3-dimensional (3D) deployments of multiple transmit antenna elements. In particular,

we are interested in the optimal antenna elements placement which can maximize the ergodic capacity of a multiple-input single-output (MISO) BF system. Since it is difficult (if not impossible) to find the optimal solution analytically, simulated annealing (SA) algorithm [24–26] is used to search for the optimal antenna layouts for different PAS and PES. The results show that the optimal antenna layout is highly dependent on the PAS and PES distribution. In the 3D space uniformly scattering environment, the layout with antenna elements located on a surface of sphere will obtain the best ergodic capacity. When the spherical power spectrum (SPS) [23] degrades to 2D distribution (with only PAS or PES), the circular layout is the optimal. While there is no angle spreading, the nonuniform linear array is the best.

The rest of the paper is organized as follows. The next section introduces the system model including the 3D spatial correlation model and the ergodic capacity expressed as the function of eigenvalues of antenna correlation matrix. In Section 3, we use the simulated annealing to search for the optimal antenna layouts for some representative PAS and PES. Section 4 concludes the paper.

Throughout the paper, the following notations are adopted. All the matrices and the vectors are denoted by boldfaced capital letters and boldfaced small letters, respectively. $(\cdot)^H$ and $(\cdot)^T$ denote the complex conjugate transpose and transpose operator, respectively. $|\cdot|$ is the absolute value and $\|\cdot\|$ is the two-norm operator. $E\{\cdot\}$ represents the expectation. $\mathrm{CN}(0, \mathbf{A})$ denotes a complex circular-symmetric Gaussian random vector with zero mean and variance matrix $\mathbf{A}$.

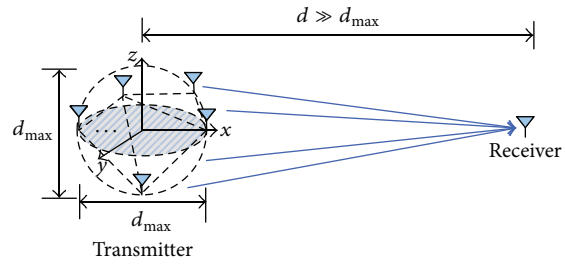

(a) MISO system

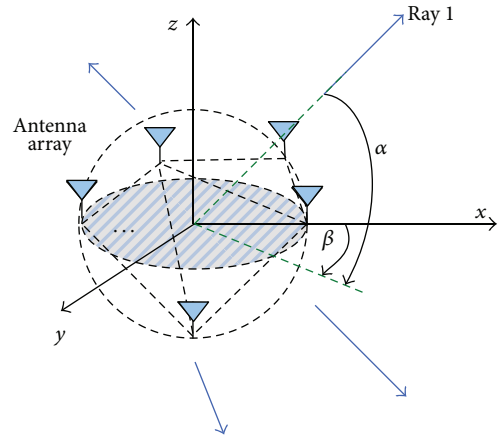

(b) Electromagnetic waves (rays) departing from different directions. For each ray, α denotes the elevation and β denotes the azimuth

Figure 1: System model.

2. System Model

2.1. MISO Beamforming System. Consider an MISO system shown in Figure 1(a) with L transmit antennas and a single receive antenna, where $d_{\max}$ is the maximum allowable separation distance between any two antenna elements and d is the distance between the transmitter and receiver. For most applications, d is much larger than $d_{\max}$. Suppose that all the antennas are mounted with the same orientation in 3D space, as shown in Figure 1(a); we can reasonably assume that the path loss, shadowing, and the antenna gain (due to the antenna pattern) are the same for all antenna elements.

Based on the principle of reciprocity, the characteristics of an antenna array will keep the same whatever it is used for transmitting or receiving. Consider the transmit antenna array shown in Figure 1(b); the electromagnetic waves (rays) will depart from the array in different directions, due to the scattering in the environment. For each ray, we use α to denote the elevation and β the azimuth. The total energy is distributed along these directions and the distribution is denoted, respectively, by $P_e(\alpha)$ and $P_a(\beta)$, namely, the power azimuth spectrum (PAS) and the power elevation spectrum (PES) [14, 27].

The MISO channel is modeled as a $L \times 1$ vector $\mathbf{h} = (h_1, h_2, \ldots, h_L)^T$, where $h_l\,(l = 1, 2, \ldots, L)$ is the channel coefficient from the lth transmit antenna to the receive antenna. Based on this assumption, we can model $\mathbf{h}$ as a zero mean complex circular-symmetric Gaussian vector $\mathrm{CN}(0, \mathbf{R})$, where $\mathbf{R}$ is the transmit antenna correlation matrix defined as

$$\mathbf{R} = E\left[\mathbf{h}\mathbf{h}^H\right]. \tag{1}$$

The received signal at the receiver is

$$r = \mathbf{h}^T\mathbf{w}s + n, \tag{2}$$

where n is the zero mean complex additive Gaussian white noise (AWGN) with variance N_0 and s is the scalar data symbol with $E[|s|^2] = E_s$. Before transmission on antenna l, the symbol is weighted by a complex number w_l. The weights for all transmit antennas can be collected into a $L\times 1$ BF vector $\mathbf{w} = (w_1, w_2, \ldots, w_L)^T$.

Assuming perfect channel state information (CSI) at the transmitter, then the optimal BF weighting vector is given by

$$\mathbf{w} = \frac{\mathbf{h}^H}{\|\mathbf{h}\|}, \tag{3}$$

and the instantaneous signal to noise ratio (SNR) at the output of receiver is given by

$$\gamma = \frac{E_s}{N_0}\|\mathbf{h}\|^2 = \gamma_0\|\mathbf{h}\|^2, \tag{4}$$

where $\gamma_0 = E_s/N_0$.

2.2. Correlation between Antenna Elements. The elements of $\mathbf{R}$ defined in (1) are the correlation coefficient of a pair of transmit antenna elements. With the classical multipath model [28–31], for any two transmit antennas located at $\mathbf{p} = (x, y, z)$ and $\mathbf{p}' = (x', y', z')$, the 3D spatial correlation is given by

$$\begin{aligned} R(\mathbf{p}, \mathbf{p}') &= \int_{-\pi/2}^{\pi/2} \int_{-\pi}^{\pi} \exp\left\{ j\frac{2\pi}{\lambda} \left[(x - x') \cos\alpha \cos\beta \right.\right. \\ &\quad + (y - y') \cos\alpha \sin\beta \\ &\quad \left.\left. + (z - z') \sin\alpha \right] \right\} \\ &\quad \times P_e(\alpha) P_a(\beta) \, d\alpha \, d\beta, \end{aligned} \tag{5}$$

where λ is the wavelength and $P_e(\alpha)$ and $P_a(\beta)$ are the PAS and PES with α and β defined in Figure 1(b).

An antenna layout is a set of L antenna positions: $\mathbf{P} = \{\mathbf{p}_1, \mathbf{p}_2, \ldots, \mathbf{p}_L\}$ where $\mathbf{p}_l = (x_l, y_l, z_l)$ is the 3D Cartesian coordinates of the lth antenna element. Given the PAS and PES, the antenna correlation matrix $\mathbf{R}$ can be completely determined by $\mathbf{P}$ through (5).

2.3. Ergodic Capacity. The instantaneous capacity, in nats per symbol, for MISO BF system is given by

$$C = \ln(1 + \gamma), \tag{6}$$

where γ is defined in (4). The ergodic capacity [31] is defined as the expectation of (6), which is

$$\overline{C} = E[\ln(1 + \gamma)] = \int_0^{\infty} [\ln(1 + x)] f_\gamma(x) \, dx, \tag{7}$$

where $f_\gamma(x)$ is the probability density function (p.d.f.) of γ.

If the correlation matrix $\mathbf{R}$ is known, then $f_\gamma(x)$ is given by [32, 33] as

$$f_\gamma(x) = \sum_{l=1}^{L} \frac{\sigma_l^{L-2}}{\prod_{k \neq l} (\sigma_k - \sigma_l)} \exp\left(-\frac{x}{\gamma_0 \sigma_l}\right), \tag{8}$$

where $0 < \sigma_1 < \cdots < \sigma_l < \cdots < \sigma_L$ are the distinct eigenvalues of $\mathbf{R}$. Substituting (8) into (7), the ergodic capacity is given as

$$\begin{aligned} \overline{C} &= \sum_{l=1}^{L} \frac{\sigma_l^{L-2}}{\prod_{k \neq l} \sigma_k - \sigma_l} \int_0^{\infty} \ln(1 + x) \exp\left(-\frac{x}{\gamma_0 \sigma_l}\right) dx \\ &= \sum_{l=1}^{L} \frac{\sigma_l^{L}}{\prod_{k \neq l} (\sigma_k - \sigma_l)} \exp\left(\frac{1}{\gamma_0 \sigma_l}\right) E_1\left(\frac{1}{\gamma_0 \sigma_l}\right), \end{aligned} \tag{9}$$

where $E_1(x)$ is the exponential integral function, defined as

$$E_1(x) = \int_x^{\infty} \frac{e^{-t}}{t} dt. \tag{10}$$

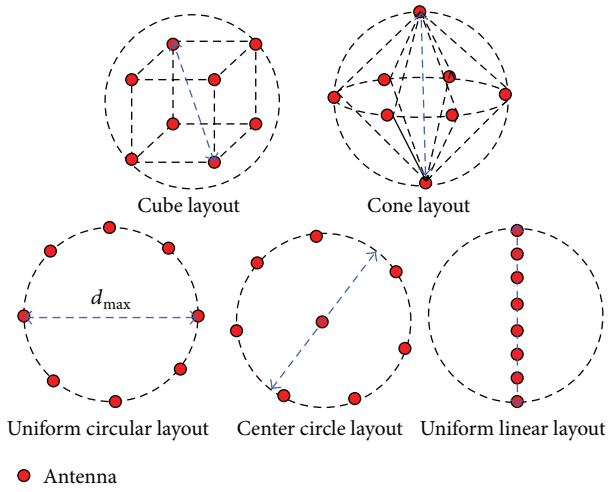

Figure 2: Reference regular antenna layouts.

Note that (9) is valid only when the eigenvalues $\sigma_1, \sigma_2, \ldots, \sigma_L$ are distinct. However, it can be easily verified that the discontinuous point of $\overline{C}$ at $\sigma_k \neq \sigma_m, k \neq m$ is the removable discontinuity; that is,

$$\lim_{\sigma_k \to \sigma_m^+} \overline{C} = \lim_{\sigma_k \to \sigma_m^-} \overline{C}. \tag{11}$$

Hence, in case that $\mathbf{R}$ has identical eigenvalues, the right-hand side of (9) can be evaluated with the left or right limits around the discontinuity.

From (9), we know that $\overline{C}$ is a function of $\mathbf{R}$. On the other hand, $\mathbf{R}$ is given by (5). Hence, for fixed PAS and PES, $\overline{C}$ is completely determined by the antenna layout $\mathbf{P} = \{\mathbf{p}_1, \mathbf{p}_2, \ldots, \mathbf{p}_L\}$. Our objective is to find the optimal $\mathbf{P}$ which can maximize $\overline{C}$ under the diameter constraint $d_{\max}$. The optimization problem can be formally stated as

$$\begin{aligned} \mathbf{P}^{\text{opt}} = \underset{\mathbf{P} \in \mathbf{R}^{L \times 3}}{\text{argmax}} \left\{ \overline{C}(\mathbf{P}) \right\} \quad &\text{s.t. } |\mathbf{p}_l - \mathbf{p}_{l'}| \leq d_{\max}, \\ &\forall 1 \leq l, \, l' \leq L, \, l \neq l'. \end{aligned} \tag{12}$$

The constraint condition $|\mathbf{p}_l - \mathbf{p}_{l'}| \leq d_{\max}$ implies that the antenna elements should be placed within a sphere of diameter $d_{\max}$.

3. The Optimal Antenna Layout

The optimization problem shown in (12) is too difficult to be solved directly, so in this section, we use simulated annealing (SA) [24–26] to search for the optimal transmit antenna layout. A brief description on SA and the related SA parameters used in this paper are presented in the Appendix.

We consider the 8×1 MISO BF system. With $L = 8$ antennas, some of the regular antenna placement patterns are illustrated in Figure 2 for reference.

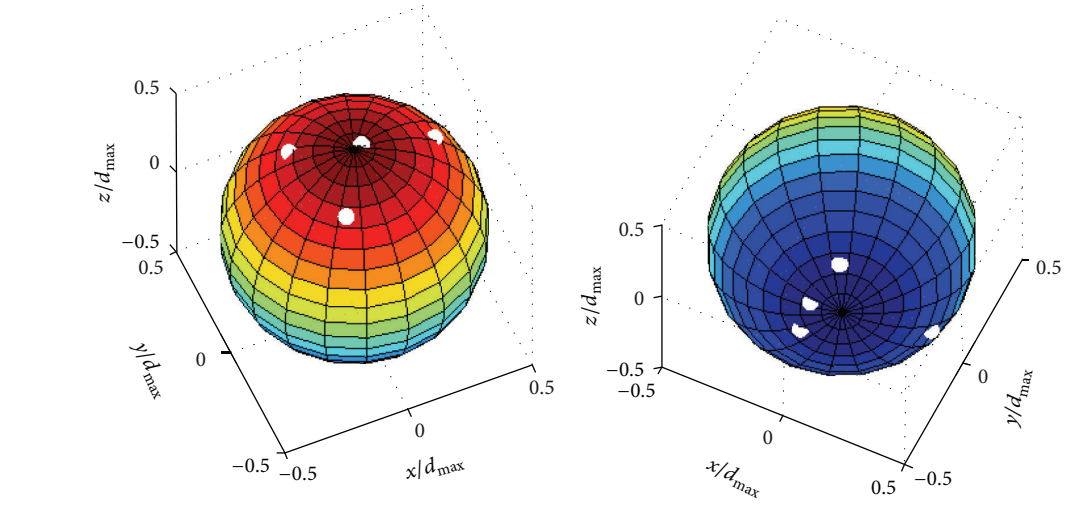

(a) $d_{max} = 0.2\lambda$

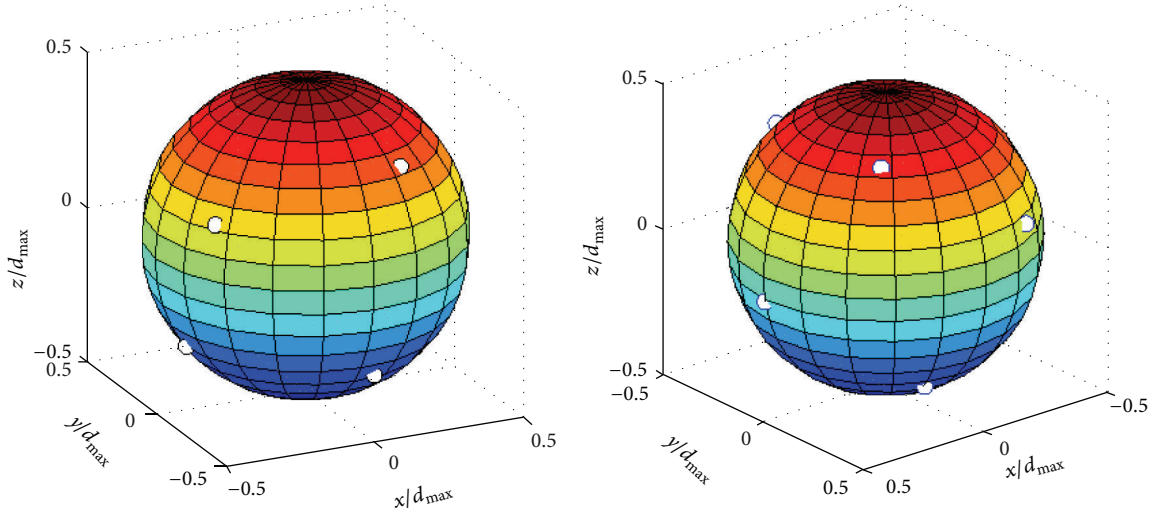

(b) $d_{max} = 0.6\lambda$

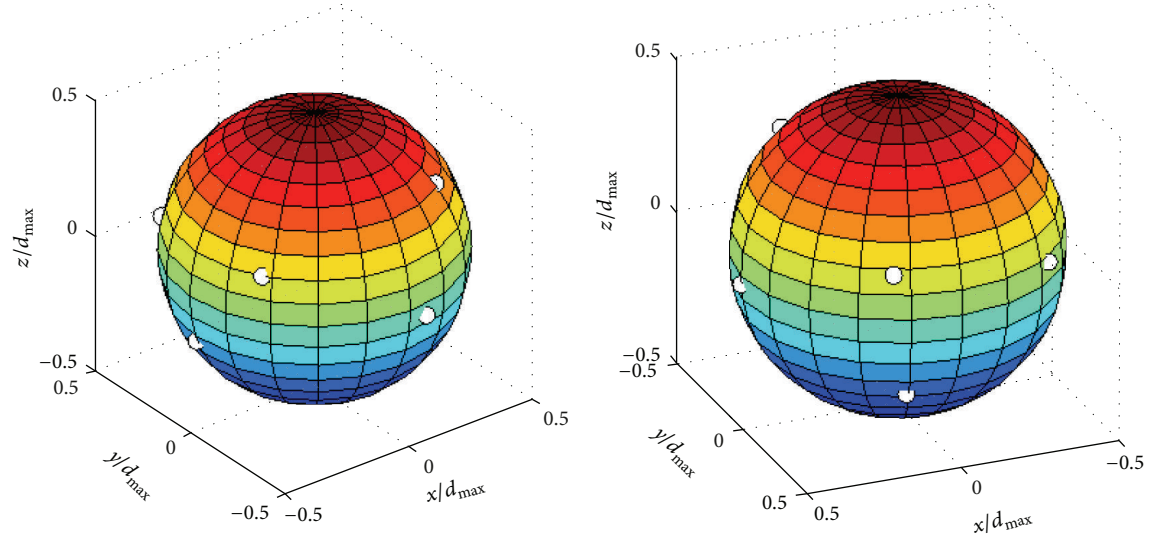

(c) $d_{max} = \lambda$

Figure 3: The optimal layout for Scenario I.

The optimal antenna layout will certainly depend on the angle spreading of the radio wave. For simplicity, we consider the uniform distribution PAS and PES, which are defined as

$$P_e(\alpha) = \frac{1}{2\Delta_\alpha} \left(\alpha_0 - \Delta_\alpha \le \alpha \le \alpha_0 + \Delta_\alpha\right)$$
$$P_a(\beta) = \frac{1}{2\Delta_\beta} \left(\beta_0 - \Delta_\beta \le \beta \le \beta_0 + \Delta_\beta\right), \quad (13)$$

where Δ_α and Δ_β are the range of α and $\beta \cdot \alpha_0$ and β_0 denote the center of angle of departure (AoD). Without loss of generality, we set $\alpha_0 = \beta_0 = 0$. Substituting (13) into (5), the spatial correlation of transmit antenna is given as

$$R\left(\mathbf{p}, \mathbf{p}'\right) = \frac{1}{4\Delta_\alpha\Delta_\beta} \times \int_{\Delta_\alpha}^{\Delta_\alpha} \int_{\Delta_\beta}^{\Delta_\beta} \exp\left\{j\frac{2\pi}{\lambda}\left[\left(x - x'\right)\cos\alpha\,\cos\beta + \left(y - y'\right)\cos\alpha\,\sin\beta + \left(z - z'\right)\sin\alpha\right]\right\} \mathrm{d}\alpha\,\mathrm{d}\beta. \quad (14)$$

Five propagation scenarios are considered in this paper, as shown in Table 1. Scenario I is the 3D whole space uniformly scattering environment. In Scenario II, the elevation of the departing rays is compressed to a very narrow domain, the scattering range converges like a 2D thin plane. Scenario III represents the narrow spreading situation where the angle spreading of departing rays for both azimuth and elevation has been compressed in the ±10° range. In this case, the departing rays converge like a thin beam. Scenario IV and Scenario V are the degraded cases of Scenario II and Scenario III.

3.1. The Optimal Layouts for Scenario I. Figure 3 shows the optimal antenna layout for Scenario I with diameter constraint as $d_{\max} = 0.2\lambda$, $d_{\max} = 0.6\lambda$, and $d_{\max} = \lambda$, respectively. For each $d_{\max}$ value, two subfigures are presented which are the two different side views of the same antenna placement layout. An interesting observation is that the optimal antenna layout will always place the antenna elements on the surface of the sphere.

In Figure 4, we compare the ergodic capacity of the optimal layout with that of regular layouts listed in Figure 2. We can see that the cube and the cone layout are near optimal. Specifically, when $d_{\max} \le 0.4\lambda$, the ergodic capacity of cube layout is almost the same as that of optimal layout and the cone layout is very close to optimal. When $d_{\max} > 0.4\lambda$, the cone layout is more close to the optimal layout than the cube layout.

3.2. The Optimal Layouts in Scenario II. Figure 5 shows the optimal antenna layout for Scenario II where the angle spread is uniform in the azimuth plane and is narrow in elevation (constrained in ±10° in elevation plane). Comparing

Table 1: PAS and PES for different propagation scenarios.

	PES Δ_α	PAS Δ_β
Scenario I	90°	180°
Scenario II	10°	180°
Scenario III	10°	10°
Scenario IV	0°	180°
Scenario V	0°	0°

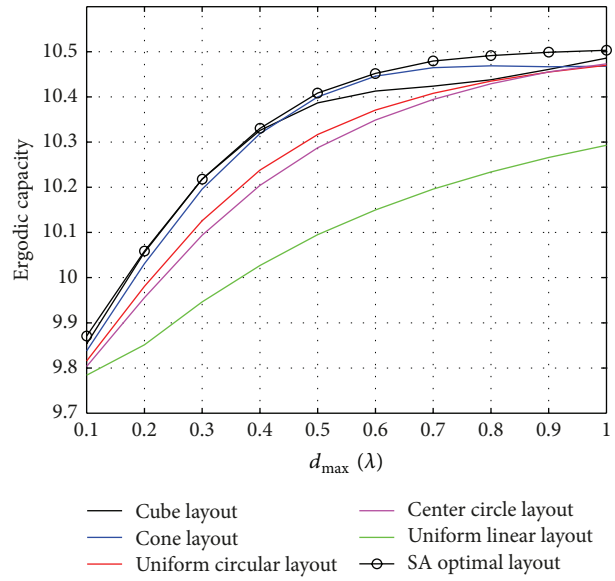

Figure 4: Capacity difference between the optimal layout and the reference regular layouts for Scenario I with $\gamma_0 = 20$ dB.

Figures 5 and 3, we can see that the angle spread of the departing rays has serious impact on the optimal antenna layout. Since the rays mainly depart from the horizontal plane, the optimal layout is essentially a ring with its normal line pointing in the z-direction. Figure 5(b) is an exception where 7 antennas have formed a ring in horizontal plane while the 8th antenna is placed at the norm line of the ring.

If we force the 8th antenna in Figure 5(b) at the norm line of the ring to the center of the horizontal plane ring and keep the positions of the rest 7 antennas, we will arrive at a layout similar to the center-circle layout shown in Figure 2. Figure 6 shows the capacity difference between the layout in Figure 5(b) and the center-circle layout. The results show that the capacity difference is very slight, since the angle spread in elevation is narrow (constrained in ±10° in elevation plane). In other words, although the optimal layout suggested by SA is Figure 5(b) for $d_{\max} = 0.6\lambda$, which is quite different with Figures 5(a) and 5(c) where the optimal solution is a plane, we know from Figure 6 that forcing the highest point to the x-y plane will lead to almost no loss. What is implicit here is that, with a very narrow angel spreading at elevation, the optimization can focus only on the x-y plane. In fact, we will see later that if the angle spread in elevation is even

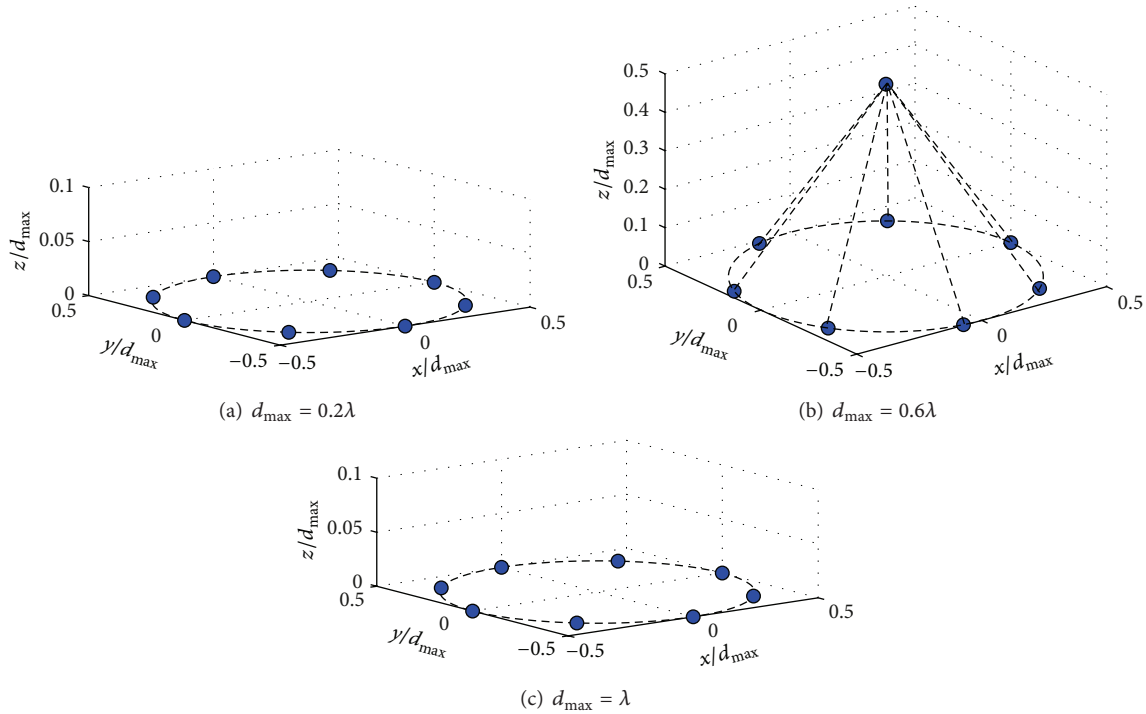

(a) $d_{\max} = 0.2\lambda$ (b) $d_{\max} = 0.6\lambda$

(c) $d_{\max} = \lambda$

FIGURE 5: The optimal layout for Scenario II.

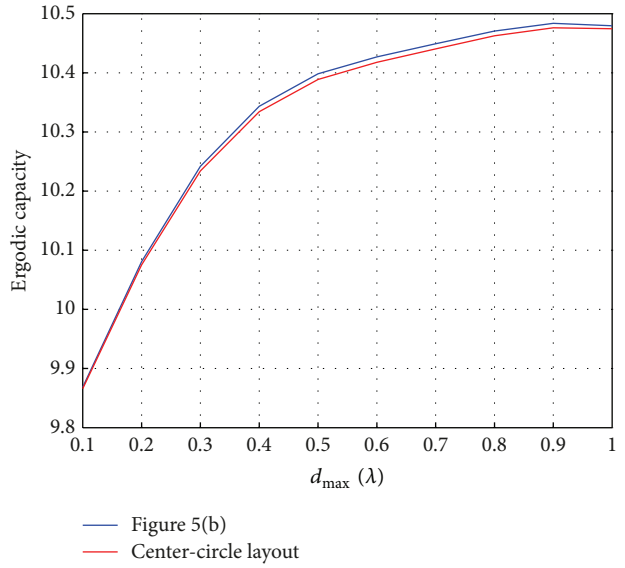

FIGURE 6: Capacity difference between the layout in Figure 5(b) and the corresponding center-circle layout. $\gamma_0 = 20$ dB.

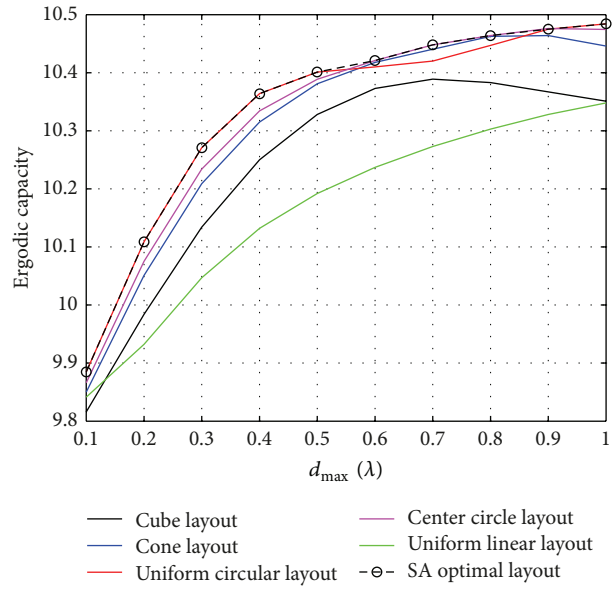

FIGURE 7: Capacity difference between the optimal layout and the reference regular layouts for Scenario II. $\gamma_0 = 20$ dB.

smaller as to zero, the z-axial coordinate will no more affect the performance.

In Figure 7, we compare the ergodic capacity of the optimal layout under Scenario II with that of regular layouts listed in Figure 2. Unsurprisingly, the uniform circle layout and the center circle layout are near optimal. Specifically, when $d_{\max} \leq 0.5\lambda$, the ergodic capacity of the uniform circle layout is almost the same as that of optimal layout. When $d_{\max} > 0.5\lambda$, the center circle layout is more close to the optimal layout than the uniform circle layout.

3.3. The Optimal Layouts in Scenario III. Figure 8 shows the optimal antenna layout for Scenario III where the angle spread is narrow in both azimuth and elevation (constrained in $\pm 10^\circ$ in azimuth and elevation plane). Comparing

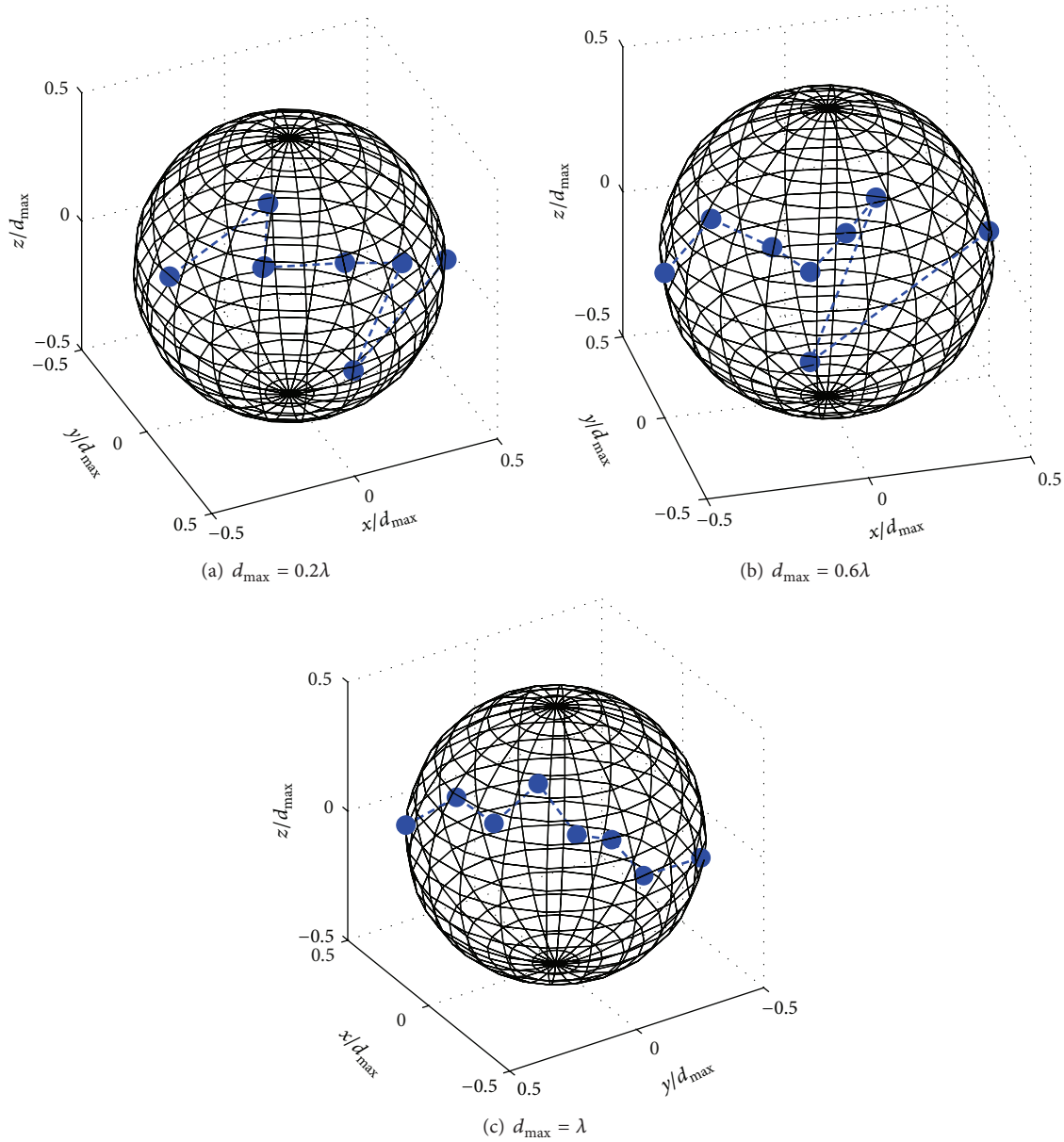

Figure 8: The optimal layout for Scenario III.

Figures 8, 5, and 3, we can see that the optimal antenna layout dimension is highly dependent on the power azimuth spectrum (PAS) distribution and power elevation spectrum (PES) distribution. In this case, the departing rays converge to a thin beam which is approximately a single plane wave. The optimal layout in this case is different with all the results in the two scenarios mentioned previously, the antennas no longer distribute on the sphere surface. The eight antennas are some like eight nodes on a knotted rope, but each of them has its own vibration amplitude and these amplitudes are irregular.

In Figure 9, we compare the ergodic capacity of the optimal layout under Scenario III with that of regular layouts listed in Figure 2. We can see that when the angle spreading is very narrow both in elevation and azimuth, the uniform linear array is the one closet to the optimal, among the layouts listed in Figure 2.

3.4. The Optimal Layouts in Scenario IV. Scenario IV is the degraded case of Scenario II. The range of PES has been further compressed by setting Δ_α in (13) to zero, resulting in that the $P_e(\alpha)$ becomes the Dirac impulse function and the double integral in (14) simplifies to a single integral as shown in (15). The z-axial coordinate disappears from (15) implying that the z-axial coordinate will no more affect the antenna spatial correlation. The 3D antenna layout optimization problem is then reduced to a 2D optimization problem. With

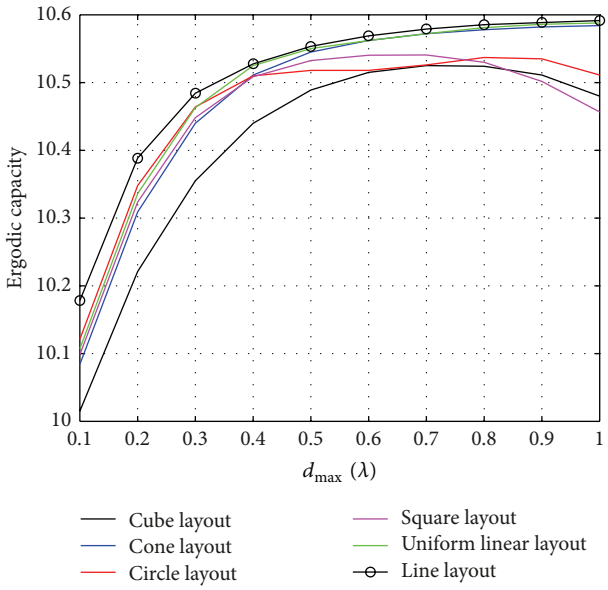

FIGURE 9: Capacity difference between the optimal layout and the reference regular layouts for Scenario III. $\gamma_0 = 20$ dB.

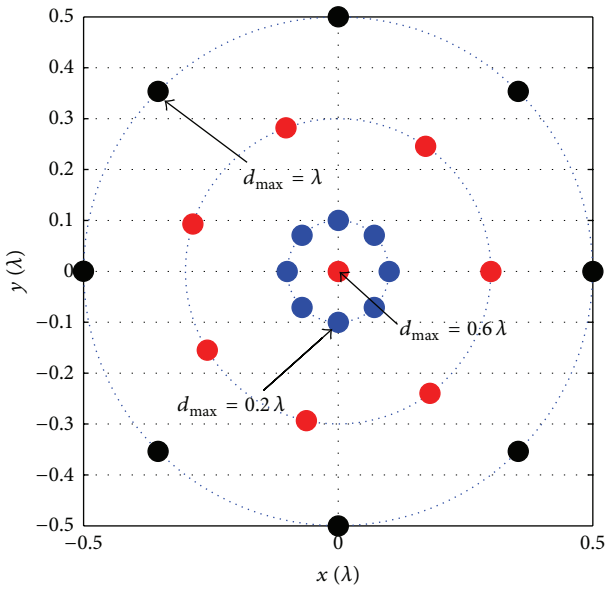

FIGURE 10: The optimal layout for Scenario IV with various $d_{\max}$.

a constraint that the antenna elements must be placed within a circle of diameter $d_{\max}$:

$$R\left(\mathbf{p},\mathbf{p}'\right) = \frac{1}{2\Delta_\beta}\int_{\Delta_\beta}^{\Delta_\beta} \exp\left\{j\frac{2\pi}{\lambda}\left[\left(x-x'\right)\cos\beta + \left(y-y'\right)\sin\beta\right]\right\} \mathrm{d}\beta. \quad (15)$$

Figure 10 shows the optimal antenna coordinates for Scenario IV which is the output of SA. The points in red, blue or black denote, respectively, the optimal antenna locations for different $d_{\max}$ constraints. In case that $d_{\max} = 0.2\lambda$ and $d_{\max} = \lambda$, the antennas are almost uniformly distributed on a circle while in the case of $d_{\max} = 0.6\lambda$, one antenna is placed at the center of the circle and the rests are nonuniformly distributed on the circle.

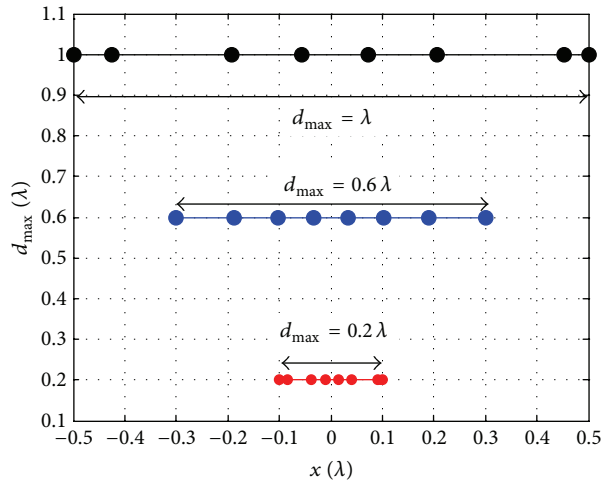

FIGURE 11: Optimal layout for Scenario V with various $d_{\max}$.

3.5. The Optimal Layouts in Scenario V. Scenario V is the degraded case with both Δ_α and Δ_β set to zero. Now the double integral in (14) disappears and it reduces to (16). This indicates that the optimal layout does not depend on z-axial and y-axial coordinates and the original 3D antenna layout optimization problem is reduced to a 1D optimization problem with a constraint that all antennas should be placed in a interval of length $d_{\max}$:

$$R\left(\mathbf{p},\mathbf{p}'\right) = \exp\left[j\frac{2\pi}{\lambda}\left(x-x'\right)\right]. \quad (16)$$

Figure 11 is the optimal layout obtained through SA. The points in red, blue, or black correspond to three difference $d_{\max}$ constraints. We can see that the optimal layout in this case is the nonuniform linear array.

In summary, in the three-dimensional (3D) space uniformly scattering environment, the optimal antenna layout will locate the antenna elements on the surface of a sphere. For practical consideration, the cube layout is a good choice for $d_{\max} \le 0.4\lambda$ and the cone layout is better for $d_{\max} > 0.4\lambda$. When the scattering is concentrated in a two-dimensional (2D) plane, the circular layout is the optimal. For practical consideration, we may consider the uniform circular layout for $d_{\max} \le 0.5\lambda$ and the center circle layout for $d_{\max} > 0.5\lambda$. While the scattering is very narrow in both elevation and azimuth, the optimal layout is nearly a nonuniform linear array. The uniform linear layout is near optimal particularly when $d_{\max} > 0.4\lambda$.

(1) Generate a random initial configuration of antennas $\mathbf{P_0}$, and $\mathbf{P}^{\text{opt}} = \mathbf{P_0}$, compute the cost function value $f(\mathbf{P}_0)$;
(2) Set the initial temperature $T(0) = T_0$ and the iterations $i = 1$;
(3) Do while $T(i) > T_{\text{end}}$
  (1) for inner loop $m = 1 \sim K$
  (2) Do some small random perturbation to the $\mathbf{P}^{\text{opt}}$ that yields a nearby solution $\mathbf{P}_{\text{new}}$. Compute $f(\mathbf{P}_{\text{new}})$ and $\Delta f = f(\mathbf{P}_{\text{new}}) - f(\mathbf{P}^{\text{opt}})$
  (3) if $\Delta f \leq 0$, $\mathbf{P}^{\text{opt}} = \mathbf{P}_{\text{new}}$;
  (4) if $\Delta f > 0$, $u = \exp(-\Delta f/T(i))$; generate a random variable $c = \text{random}[0, 1]$, if $c < u$, $\mathbf{P}^{\text{opt}} = \mathbf{P}_{\text{new}}$.
  (5) end for
(4) $i = i + 1$;
(5) $T(i + 1) = T(i)$;
(6) End Do while
(7) Output $\mathbf{P}^{\text{opt}}$

Algorithm 1: Process of SA algorithms.

4. Conclusions

This paper investigates the problem of arranging the transmit antennas to attain the maximum ergodic capacity in an MISO beamforming system. Since the optimization problem cannot be solved analytically, we use simulated annealing (SA) algorithm to search for the optimal antenna layout. The results show that the optimal antenna layout dimension is highly dependent on the power azimuth spectrum (PAS) distribution and power elevation spectrum (PES) distribution.

Appendix

Simulated annealing [24–26] is a technique for combinatorial optimization problems, such as minimizing functions of many variables. For our purposes, a combinatorial optimization problem is one in which we seek to find some configurations of antenna layout $\mathbf{P} = \{\mathbf{p_1}, \mathbf{p_2}, \ldots, \mathbf{p}_L\}$ in (12) that minimizes the $f(\mathbf{P}) = -\overline{C}$ in (9), which is defined as the cost or objective function of SA in this paper. SA starts with a random or feasible initial solution and moves step by step towards a solution $\mathbf{S}^{\text{opt}}$ giving hopefully the minimum (or close to the minimum) of the cost function.

When the configuration of antenna layout $\mathbf{P} = \{\mathbf{p_1}, \mathbf{p_2}, \ldots, \mathbf{p}_L\}$ is at a feasible solution, we attempt some small random perturbation to the configuration that yields a nearby solution. This process can continue starting from the new configuration until no further improvements are obtained, at which point the process terminates. This strategy seems reasonable, but it has a serious problem: it is easily trapped in local minimum, solutions that look good in some small neighborhood of the cost surface but are not necessarily the global optimum. To avoid this problem, the acceptance function is used to decide the acceptance probability.

The probability of accepting a move that causes an increase Δf in $f(\mathbf{P}) = -\overline{C}$ is determined by the acceptance function. Like most researchers, we use the Metropolis acceptance function [24] $\exp(-\Delta f/T)$, where T is a control parameter corresponding to the temperature in analogy with physical annealing. Because $\Delta f > 0$ and $T > 0$, $\exp(-\Delta f/T)$ is always smaller than 1. We generate a random number c uniformly distributed on the interval $[0, 1]$ and compare $\exp(-\Delta f/T)$ with c. If $\exp(-\Delta f/T) > a$, then the move is accepted; otherwise, the move is rejected.

Table 2: Parameters for SA algorithms.

Cost function	$-\overline{C}$ in (9)
Initial temperature	$T_0 = 100$;
Cooling schedule	$T(t) = 0.9T(t - 1)$
Ending temperature	$T_{\text{end}} = 0.0001$
Inner loop	$K = 100$

The initial temperature T_0 is set to be 100, and the ending temperature T_{end} equals 0.0001. The cooling schedule will be the simplest possible: $T_{\text{new}} = bT_{\text{old}}, 0 < b < 1$, where the initial temperature and cooling rate b are determined empirically to give good results and we let b be 0.9 in this paper. At each temperature, we perform 100 moves. The stopping criterion is to terminate annealing when the cost improvement seen across five successive temperatures or the temperature is cooler than the ending temperature. The key SA parameters in this paper are listed in Table 2 and the detailed process of SA is shown in Algorithm 1.

Acknowledgment

This paper was supported by National Natural Science Foundation of China (no. 61072059).

References

[1] G. J. Foschini and M. J. Gans, "On limits of wireless communications in a fading environment when using multiple antennas," *Wireless Personal Communications*, vol. 6, no. 3, pp. 311–335, 1998.

[2] J. H. Winters, "On the capacity of radio communication systems with diversity in Rayleigh fading environments," *IEEE Journal on Selected Areas in Communications*, vol. 5, no. 5, pp. 871–878, 1987.

[3] T. K. Y. Lo, "Maximum ratio transmission," *IEEE Transactions on Communications*, vol. 47, no. 10, pp. 1458–1461, 1999.

[4] W. Li, X. Huang, and H. Leung, "Performance evaluation of digital beamforming strategies for satellite communications," *IEEE Transactions on Aerospace and Electronic Systems*, vol. 40, no. 1, pp. 12–26, 2004.

[5] Y. Yang, B. Bai, W. Chen et al., "A low-complexity crosslayer algorithm for coordinated downlink scheduling and Robust beamforming under a limited feedback constraint," *IEEE Transactions on Vehicular Technology*, no. 99, pp. 1–13, 2013.

[6] P. A. Dighe, R. K. Mallik, and S. S. Jamuar, "Analysis of transmit-receive diversity in Rayleigh fading," *IEEE Transactions on Communications*, vol. 51, no. 4, pp. 694–703, 2003.

[7] J. Choi, "Opportunistic beamforming with single beamforming matrix for virtual antenna arrays," *IEEE Transactions on Vehicular Technology*, vol. 60, no. 3, pp. 872–881, 2011.

[8] S. Lee, S. Moon, H. Kong, and I. Lee, "Optimal beamforming schemes and its capacity behavior for downlink distributed antenna systems," *IEEE Transactions on Communications*, vol. 99, pp. 1–10, 2013.

[9] A. Maaref and S. Aissa, "Closed-form expressions for the outage and ergodic shannon capacity of MIMO MRC systems," *IEEE Transactions on Communications*, vol. 53, no. 7, pp. 1092–1095, 2005.

[10] A. Zanella, M. Chiani, and M. Z. Win, "Performance of MIMO MRC in correlated Rayleigh fading environments," in *Proceedings of the IEEE Vehicular Technology Conference (VTC '05)*, vol. 3, pp. 1633–1637, Stockholm, Sweden, June 2005.

[11] M. R. McKay, I. B. Collings, and P. J. Smith, "Capacity and ser analysis of MIMO beamforming with MRC," in *Proceedings of the IEEE International Conference on Communications*, vol. 3, pp. 1326–1330, June 2006.

[12] M. T. Ivrlac, W. Utschick, and J. A. Nossek, "Fading correlations in wireless MIMO communication systems," *IEEE Journal on Selected Areas in Communications*, vol. 21, no. 5, pp. 819–828, 2003.

[13] M. di Renzo and H. Haas, "Bit error probability of SM-MIMO over generalized fading channels," *IEEE Transactions on Vehicular Technology*, vol. 61, no. 3, pp. 1124–1144, 2012.

[14] R. Nordin and M. Ismail, "Impact of spatial correlation towards the performance of MIMO downlink transmissions," in *Proceedings of the 18th Asia Pacific Conference on Communications (APCC '12)*, pp. 390–395, October 2012.

[15] G. Singh, P. Mishra, and R. Vij, "Performance evaluation of ML-VBLAST MIMO decoder using different antenna configuration using rican and Rayleigh channel," in *Proceedings of the IEEE Conference on Communication Systems and Network Technologies (CSNT '13)*, pp. 174–179, April 2013.

[16] J.-A. Tsai, R. M. Buehrer, and B. D. Woerner, "BER performance of a uniform circular array versus a uniform linear array in a mobile radio environment," *IEEE Transactions on Wireless Communications*, vol. 3, no. 3, pp. 695–700, 2004.

[17] Y. Masoudi, S. Lotfi, E. Laleh, and F. Fathy, "Mobile antenna placement using combination of genetic algorithm and Learning automata," in *Proceedings of the IEEE Conference on Communication Systems and Network Technologies (CSNT '13)*, pp. 22–28, April 2013.

[18] P. Uthansakul, D. Assanuk, and M. Uthansakul, "The use of genetic algorithm for designing MIMO antenna placement," in *Proceedings of the International Conference on Computer and Information Application (ICCIA '10)*, pp. 414–417, December 2010.

[19] Q. Wang, H. Yang, and L.-Y. Dai, "MIMO capacity with different antenna layout," in *Proceedings of the 2nd International Conference on Networks Security, Wireless Communications and Trusted Computing (NSWCTC '10)*, vol. 1, pp. 45–48, April 2010.

[20] Q. Wang and H. Yang, "Optimal antenna layout under uniformly scattering environments," in *Proceedings of the International Conference on Wireless Communications and Signal Processing (WCSP '10)*, pp. 1–5, October 2010.

[21] X. Pu, S. Shao, and Y. Tang, "Optimal 2×2 antenna placement for short-range communications," *IEEE Communications Letters*, vol. 17, no. 8, pp. 1560–1563, 2013.

[22] S. Kaul, K. Ramachandran, P. Shankar et al., "Effect of antenna placement and diversity on vehicular network communications," in *Proceedings of the 4th Annual IEEE Communications Society Conference on Sensor, Mesh and Ad Hoc Communications and Networks (SECON '07)*, pp. 112–121, June 2007.

[23] W. Fan, F. Sun, and P. Kyösti, "3D channel emulation in multi-probe setup," *Electronics Letters*, vol. 49, pp. 623–625, 2013.

[24] R. A. Rntenbar, "Simulated annealing algorithms: an overview," *IEEE Circuits and Devices Magazine*, vol. 5, no. 1, pp. 19–26, 1989.

[25] Q. Ji-Yang, "Application of improved simulated annealing algorithm in facility layout design," in *Proceedings of the 29th Chinese Control Conference (CCC '10)*, pp. 5224–5227, July 2010.

[26] J. Tian and M. Gao, "Soft measurement modeling based on improved simulated annealing neural network for sewage treatment," in *Proceedings of the WRI World Congress on Software Engineering (WCSE '09)*, vol. 4, pp. 486–489, May 2009.

[27] W. Yue-yu and G. Li-li, "Spatial correlation in three-dimensional receiver antenna array channel model," *Computer Engineering*, vol. 34, no. 12, pp. 9–12, 2008 (Chinese).

[28] R. H. Clarke, "A statistical theory of mobile-radio reception," *The Bell System Technical Journal*, vol. 47, pp. 957–1000, 1968.

[29] W. C. Jakes, *Microwave Mobile Communication*, John Wiley & Sons, New York, NY, USA, 1974.

[30] T. L. Fulghum, K. J. Molnar, and A. Duel-Hallen, "The Jakes fading model for antenna arrays incorporating azimuth spread," *IEEE Transactions on Vehicular Technology*, vol. 51, no. 5, pp. 968–977, 2002.

[31] A. Goldsmith, *Wireless Communications*, Cambridge University Press, New York, NY, USA, 2004.

[32] R. K. Mallik and M. Z. Win, "Channel capacity of adaptive transmission with maximal ratio combining in correlated Rayleigh fading," *IEEE Transactions on Wireless Communications*, vol. 3, no. 4, pp. 1124–1133, 2004.

[33] M. Kang and M.-S. Alouini, "Impact of correlation on the capacity of MIMO channels," in *Proceedings of the International Conference on Communications (ICC '03)*, vol. 4, pp. 2623–2627, May 2003.

Hindawi Publishing Corporation
International Journal of Antennas and Propagation
Volume 2013, Article ID 745018, 21 pages
http://dx.doi.org/10.1155/2013/745018

Review Article

A Survey on Beamforming Techniques for Wireless MIMO Relay Networks

Demosthenes Vouyioukas

Department of Information and Communication Systems Engineering, University of the Aegean, Samos, 83200 Karlovassi, Greece

Correspondence should be addressed to Demosthenes Vouyioukas; dvouyiou@aegean.gr

Received 24 July 2013; Accepted 3 October 2013

Academic Editor: Laurent Clavier

One of the major challenges the mobile broadband community faces is the exponential increase in mobile data traffic, even more so, for cell-edge users. Thus, in a multitier network, the demand for high-speed and interference-free transmission and reception is inevitable. Beamforming (BF) is an advanced technology that offers a significantly improved solution to reduce the interference levels and improve the system capacity. Accordingly, the establishment of relays in mobile data networks has emerged spectral efficiency enhancements and cell capacity gains from an overall system perspective. This paper provides a comprehensive survey focused on the performance of adopted beamforming technique on MIMO relay networks that is expected to overcome crucial obstacles in terms of capacity and interference. The main objective is to point out the state-of-the-art research activity on BF techniques in MIMO relay networks, under various network performance challenges. Thereby, it focuses on recently developed procedures for interference modeling and mitigation, BF channel modeling, channel estimation and feedback, complexity and power consumption, adaptive BF for multiuser relaying, degrees of freedom, diversity issues, and spectral efficiency, in cooperative and opportunistic systems. Different network topologies have been considered and categorized, pertaining the challenges of BF implementation in MIMO relay networks.

1. Introduction

Next-generation wireless networks are bound to offer a dramatic increase in data rate compared to the currently deployed networks. One major limiting factor towards this goal is the interference that arises due to the increased temporal and spectral reuse of resources. As a result, novel techniques that exploit the spatial domain will contribute significantly in the efficient operation of future networks. Among them, multiple-input multiple-output (MIMO) antenna configurations, cooperative relays, and beamforming (BF) have been very active research fields in the recent years, as they allow increased flexibility in interference mitigation.

Equipping transmitters and receivers with MIMO capabilities can achieve increased diversity and multiplexing gains. It was the seminal work of [1] which presented capacity results of MIMO systems in Gaussian channels that sparked great interest by the academia and the industry. The gains in capacity offered by MIMO topologies led to their inclusion in current and future wireless standards, namely, IEEE 802.11n, 802.16e, 3GPP LTE, and LTE-advanced. MIMO systems take advantage of the rich scattering observed in urban environments that offers independent propagation paths for the emitted signals. So, the designer of a MIMO system can target loading each antenna with a different information carrying signal, thus increasing the multiplexing gain or loading the same signal on all the antennas, thus improving the diversity gain. The capacity bounds of MIMO channels were the topic of [2] where realistic assumptions about time-varying channels and channel correlation were considered and results were given also for the multiple-access channel (MAC) and the broadcast channel (BC). The authors in [3] presented an overview of single-user (SU) MIMO and multiuser (MU) MIMO techniques and discussed the advantages offered by the latter at the cost of channel state information (CSI) at the transmitter in order to form accordingly the antenna beams. More recently, [4] provided an extension to multicell

networks where MIMO nodes cooperate to exploit intercell interference. Cooperative techniques were introduced, such as base station (BS) cooperation and schemes that employed relays.

In general, the literature on cooperative relaying has seen a tremendous rise in contributions in recent years. Through cooperative relaying, coverage extension, increased reliability, and diversity can be harvested. The first study of the capacity of the relay channel was conducted in [5]. In addition, various relaying strategies such as amplify-and-forward (AF), decode-and-forward (DF), and compress-and-forward (CF) were investigated in the seminal work of [6]. Optimization efforts for AF MIMO relay systems are depicted in [7], providing an overview of the fundamental results and practical implementation issues in designing AF MIMO relay systems. Relays are attractive as they improve three critical parameters of wireless networks. By allowing multihop transmission, transmitters are brought closer to the receiver, thus reducing the path loss attenuation of the signal. In addition, shadowing can be overcome by installing relay nodes in places where obstacles affect single-hop communications. Furthermore, multipath fading is mitigated through the provision of independent propagation paths. For example, even when one relay is employed, the signal propagates through a two-hop path and also through the direct path between the source and the destination. Also, cooperative relaying offers increased diversity [8], even when cooperative relays choose not to transmit but rather choose to cooperatively listen [9], thus improving the performance in terms of outage and error probability. Additionally, when multiple relays are available, selecting the best one according to instantaneous CSI was proven to be outage optimal in [10] compared to the case where multirelay transmissions are performed. More recently buffer-aided relays were examined [11] and relay selection schemes that aim at improved spectral efficiency were presented in [12, 13].

The third technique that is examined in this survey is beamforming. This technique uses BF matrices at the transmitters and the receivers, which form the antennas' beam patterns in such a way as to optimize a specific design criterion, such as mean square error (MSE) or signal-to-noise ratio (SNR). The implementation of BF requires the use of digital signal processors (DSPs) to shape accordingly the beam patterns that are emitted by the antennas. In the context of single-hop mobile communications, the article in [14] presented space-time processing to combat cochannel interference (CCI) and intersymbol interference (ISI). Another early work was [15], which proposed joint BF and power control in order to minimize the total transmitted power in the network while satisfying a signal-to-noise-plus-interference ratio (SINR) threshold at the receivers. An overview of smart antennas is given in [16] where switched beam, adaptive beam, and spatial division multiple-access (SDMA) are discussed. Moreover, digital signal processing algorithms such as direction-of-arrival (DoA) and adaptive BF were presented in [17].

This survey provides a detailed presentation of works that study BF techniques in networks where relays with MIMO capabilities are deployed. More specifically, the increased degrees of freedom (DoF) in exploiting the spatial resources are the main topic of the presented works. This area has seen a significant increase in contributions recently but a survey depicting its importance and categorizing these works has not been published except from a few articles, which provide quick overviews of some techniques. In [18], the authors present BF schemes for scenarios where MIMO AF relays assist the communication in single and multiuser networks either through one-way or two-way relaying. In another article [19], relay classification is performed and BF techniques are presented for various combinations of regenerative versus nonregenerative, full-duplex versus half-duplex, and one-way versus two-way. The author discusses the formulation of transmit-receive BF matrices, amplification matrices for nonregenerative relays, self-interference for full-duplex relays, and successive interference cancellation for the two-way case. Here, descriptions and categorizations for various network topologies and communication strategies are given. More specifically, articles that investigate BF schemes for single and multiuser communications are presented and their main contributions are highlighted. Also, a classification based on various relaying topologies such as single and multiple relaying as well as opportunistic relay selection is provided and the corresponding BF schemes are discussed. As the included works consider channel models and fading distributions that are examined in depth in the context of MIMO relaying, there is no channel modeling literature review in the context of this survey as emphasis is given on BF schemes and their various implementations.

This survey is organized by taking into consideration the different network topologies where BF techniques can be employed and its structure is as follows. In Section 2, the challenges of BF implementation in MIMO relay networks are given. More specifically, the design parameters that include MSE minimization and SNR maximization under various power constraints are presented. Also, overhead due to channel estimation and feedback is discussed. Another challenge that is often observed in MIMO networks is antenna correlation, thus its effect on the design of BF matrices is herein presented. In Section 3, BF schemes for single-user communications are presented. Various different cases are presented, such as single and multiple relay topologies with and without relay selection. In Section 4, networks where multiuser communications take place are investigated and scenarios where single or multiple relays assist the communication for one or two-way communications are described. Discussion and open issues are the subject of Section 5, while conclusions are given in Section 6.

Notation. In this work, $(\cdot)^T$, $(\cdot)^H$, $(\cdot)^*$, $|\cdot|$, $\|\cdot\|_2$, and $\|\cdot\|_F$ denote transpose, Hermitian transpose, complex conjugation, the determinant of a complex number, the Euclidean norm, and the Frobenius norm, respectively. Upper (lower) boldface letters will be used for matrices (vectors).

2. Challenges

To better illustrate the challenges that are presented in this section, the system model of [20] is adopted and extended

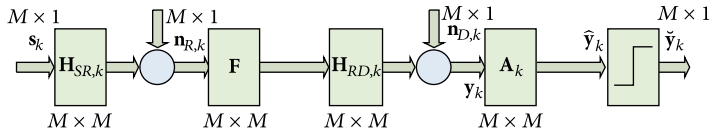

Figure 1: Block diagram of the two-hop relay equalization.

for two-hop topologies, as shown in Figure 1 [21], where a two-hop equalization process is depicted. The majority of works consider single-carrier transmission and reception but a multicarrier technology such as OFDM provides a more general system model. Furthermore, by focusing on a specific subcarrier, denoted by k, present works that use single-carrier block-fading channel models can be included. A network where a source communicates with a destination through an AF half-duplex relay is taken into consideration. However, the reader should note that adjustments should be made in the system model for the cases of DF and CF types of relaying, as there is no amplification in the analog domain by the relay. Furthermore, it is assumed that the source, the relay, and the destination have M_S, M_R, and M_D antennas, respectively, and for simplicity $M_S = M_R = M_D = M$. The received signal at the destination is

$$\mathbf{y}_k = \mathbf{H}_{RD,k}\mathbf{F}\mathbf{H}_{SR,k}\mathbf{s}_k + \mathbf{H}_{RD,k}\mathbf{F}\mathbf{n}_{R,k} + \mathbf{n}_{D,k}, \quad 1 \le k \le N, \tag{1}$$

where $\mathbf{H}_{RD,k}$ is the $M \times M$ channel matrix of the RD link, $\mathbf{F}$ is the $M \times M$ amplification matrix at the relay, $\mathbf{s}_k$ is the $M \times 1$ transmitted signal vector from the source, $\mathbf{H}_{SR,k}$ is the $M \times M$ channel matrix of the SR link, and $\mathbf{n}_{R,k}$, $\mathbf{n}_{D,k}$ are $M \times 1$ additive white Gaussian noise (AWGN) vectors at the relay and the destination, respectively.

The transmitted signal vector from the source is defined as

$$\mathbf{s}_k = \mathbf{B}_k\mathbf{x}_k = \sum_{i=1}^{L_k} \mathbf{b}_{k,i}\mathbf{x}_{k,i}, \tag{2}$$

where $\mathbf{x}_k$ are the L_k transmitted symbols as L_k established substreams are assumed and $\mathbf{B}_k$ is the $M \times L_k$ BF matrix at the source which can be designed jointly with the relay-amplify matrix $\mathbf{F}$ or separately and this holds also for the receiver's processing matrix $\mathbf{A}_k$. The transmitted symbols are assumed to satisfy the constraint $L_k \le M$ as each node has M antennas. At the destination, the received signal vector, assuming an equalizer, is expressed as

$$\widehat{\mathbf{y}}_k = \mathbf{A}_k^H\mathbf{y}_k. \tag{3}$$

In [21], equalization is performed first by designing the amplification matrix $\mathbf{F}$ at the relay and then for the overall channel through the MIMO equalizer $\mathbf{A}_k$. Another approach would consider joint optimization of $\mathbf{F}$ and $\mathbf{A}_k$. Various criteria can be considered in the optimization process and they are discussed as follows.

2.1. Performance Criteria. In the works that investigate the formulation of BF matrices, various performance criteria have been proposed. More specifically, transmit and receive BF matrices are derived through optimization problems that are subject to various performance criteria.

(a) Minimization of the Mean Square Error (MMSE). Many works take into consideration this important metric, which aims at the minimization of the estimation errors at the destination under a target SNR. Articles presenting problems with MMSE are included in [21–30]. In [20], a multicarrier system has been presented and the MSE for the kth carrier is defined as the trace of the covariance matrix of the error vector $\mathbf{e}_k \triangleq (\widehat{\mathbf{x}}_k - \mathbf{x}_k)$, where $\widehat{\mathbf{x}}_k$ is the estimation of $\mathbf{x}_k$. As a result, the problem of MSE minimization requires BF matrices to provide

$$\min \mathbf{E}_k\left(\mathbf{B}_k, \mathbf{F}, \mathbf{A}_k\right) \triangleq \min \mathbf{E}\left[\left(\widehat{\mathbf{x}}_k - \mathbf{x}_k\right)\left(\widehat{\mathbf{x}}_k - \mathbf{x}_k\right)^H\right]. \tag{4}$$

The MSE of the substreams are the diagonal elements of $\mathbf{E}_k$, so for the (kth, ith) substream, its MSE value will be located at the ith diagonal position. As a result, MSE values can be denoted through the trace of $\mathbf{E}_k$.

(b) Minimization of the Sum of MSE. In [31, 32], two end nodes communicate simultaneously through a MIMO AF relay. So, the minimization of MSE at both directions is considered; thus the optimization target is transformed into the minimization of the sum of MSE as follows:

$$\begin{aligned}&\min \mathbf{E}_{1k}\left(\mathbf{B}_{1k}, \mathbf{B}_{2k}, \mathbf{F}, \mathbf{A}_{1k}, \mathbf{A}_{2k}\right)\\ &\quad + \min \mathbf{E}_{2k}\left(\mathbf{B}_{1k}, \mathbf{B}_{2k}, \mathbf{F}, \mathbf{A}_{1k}, \mathbf{A}_{2k}\right)\\ &\quad \triangleq \min \mathbf{E}\left[\left(\widehat{\mathbf{x}}_{1k} - \mathbf{x}_{2k}\right)\left(\widehat{\mathbf{x}}_{1k} - \mathbf{x}_{2k}\right)^H\right]\\ &\quad + \min \mathbf{E}\left[\left(\widehat{\mathbf{x}}_{2k} - \mathbf{x}_{1k}\right)\left(\widehat{\mathbf{x}}_{2k} - \mathbf{x}_{1k}\right)^H\right],\end{aligned} \tag{5}$$

where indices 1 and 2 are used to denote matrices and signals which correspond to the two end nodes which are concurrently communicating through the relay.

(c) Maximization of SINR. Other works form optimization problems by considering the maximization of the SNR or SINR in the cases of multiuser and two-way relaying networks. From [20], the SINR for the ith spatial substream of the kth subcarrier, (kth, ith) substream, is given in relation to MSE as

$$\mathrm{SINR}_{k,i} = \frac{1}{\mathrm{MSE}_{k,i}} - 1, \tag{6}$$

where $\mathrm{MSE}_{k,i}$ is the MSE of the (kth, ith) substream and corresponds to the ith diagonal element of $\mathbf{E}_k$.

It is obvious that the maximization of the SINR is equivalent to the minimization of the MSE. The articles which optimize the BF matrices under the maximization of SNR are [21, 33–39].

When interference arises, SNR is replaced by SINR by considering streams that interfere in the reception of the desired signal. Many works consider zero-forcing (ZF) as in [28, 40–43]. The goal of ZF is to cancel the interference at the receiver and is based on the ZF filter, which uses the pseudoinverse matrix of the channel matrix between the communicating nodes as follows:

$$\mathbf{Z} = \mathbf{H}^{+} = \left(\mathbf{H}^{H}\mathbf{H}\right)^{-1}\mathbf{H}^{H}. \tag{7}$$

(d) Maximization of Capacity. Various articles target capacity maximization, as is the case in [21, 27, 44–57]. The relation of the maximization of mutual information to MSE is given as [20]

$$I = -\log|\mathbf{E}|. \tag{8}$$

From this equation, it is concluded that the maximization of the mutual information derives from the minimization of the MSE.

(e) Maximization of the Distance of Network-Coded Symbols. Other works employ network coding (NC) and consider the maximization of the minimum symbol distance as a design criterion. In two-way relay networks, uncoded symbols are transmitted simultaneously by the two end nodes and received by the relay. Next, the relay broadcasts an NC version of the two symbols, such as an XOR combination, in order for the end nodes to decode their signal of interest. The minimum distance of the different network-coded symbols is given as [58]

$$d_{\min}^{(\mathrm{NC})} = \min\left(a_1, a_2\right) \cdot d_{\min}, \tag{9}$$

where a_1, a_2 are the BF gains of each end node, chosen to align the signal subspaces at the relay and $d_{\min}$ is the minimum distance of the transmit constellation S, which contains M-QAM symbols. These works include [58, 59].

2.2. Power Constraints. A critical parameter in designing BF schemes is the power constraint imposed on different nodes in the system. Power constraints are practical considerations as network nodes may be battery-operated and regulatory authorities define maximum power levels for transmission in wireless systems. The following focus on the kth subcarrier as most works consider single-carrier transmissions in their system models.

(a) Power Constraint at the Relay(s). Many works impose various types of power constraints at the relays depending on their number and whether or not multi- or single-relay transmissions take place. For single-relay topologies, [23, 27, 28, 40, 45, 51, 52] impose a power constraint at the single relay expressed by

$$\left\|\mathbf{F}\mathbf{H}_{SR,k}\mathbf{B}_k\right\|_2^2 + \sigma_{R,k}^2\|\mathbf{F}\|_F^2 \le P_{2,k}. \tag{10}$$

When multiple relays are used, individual and sum-power constraints are imposed. The algorithms in [33, 42, 60] impose an individual power constraint of the form

$$\left\|\mathbf{F}\mathbf{H}_{SR_j,k}\mathbf{B}_k\right\|_2^2 + \sigma_{R_j,k}^2\|\mathbf{F}\|_F^2 \le P_{2,R_j,k} \tag{11}$$

at each relay j, while [21, 22, 43, 44, 46, 56, 61] employ sum-power constraints of the form

$$\sum_{j=1}^{N_R}\left\|\mathbf{F}\mathbf{H}_{SR_j,k}\mathbf{B}_k\right\|_2^2 + \sigma_{R_j,k}^2\|\mathbf{F}\|_F^2 \le P_{2,k}. \tag{12}$$

Finally when one relay is selected from a set of available relays, [62] sets a power constraint at the selected relay, that is, similar to the constraint of the single relay topologies.

(b) Power Constraint at the Source and the Relays. Other works search for BF matrices under power constraints at both the source(s) and the relay(s). In networks where a single relay is available, [24–26, 34, 48, 49] have individual power constraints for the source and the relay, and the source's constraint is defined as $\|\mathbf{B}_k\|_2^2 \le P_1$. In a multiple-relay scenario, [61] considers individual constraints for the source and the relays that operate under a sum-power constraint. Also, for similar use, cases [33, 38, 39] impose joint power constraints at the source and the relays expressed by

$$\|\mathbf{B}_k\|_2^2 + \sum_{j=1}^{N_R}\left\|\mathbf{F}\mathbf{H}_{SR_j,k}\mathbf{B}_k\right\|_2^2 + \sigma_{R_j,k}^2\|\mathbf{F}\|_F^2 \le P_k. \tag{13}$$

In topologies where relay selection is performed, [36] imposes a separate power constraint at the source and the selected relay while [47] has individual power constraints at the source and the selected set of relays. For multiple-source scenarios where a single relay is available, the works in [29, 31, 53–55, 58, 59] consider individual and separate power constraints at the sources and the relay. In networks where multiple relays are employed, [41, 63, 64] have individual power constraints at the sources and a sum power constraint at the relays,while [50] imposes individual sum-power constraints at the sources and the relays.

(c) Power Constraint at the Receiver Side. In this category, for multiple source-destination pairs, the target is the minimization of the interference which is received at each destination as in [21, 42]. For a similar setup, the maximization of the desired signal power is the goal of [57].

2.3. Complexity. Many works present optimal BF schemes; however, in practical setups, these techniques are very difficult to implement due to the induced computational complexity. As a result, there have been a number of suboptimal methods that do not significantly degrade the network's

performance. For the optimization of the BF vectors, there are several published papers, providing reduced complexity and thus enhancing some of the aforementioned performance criteria.

For single-user communications, various works provide efficient algorithms for the calculation of the BF matrices. In [33, 61], the authors provide two suboptimal methods which optimize the source BF vectors and can be used in networks with larger scale than the three-node networks under study. The first suboptimal solution is based on the gradient method that finds the local optimum, and the second uses max-min optimization that leads to a semidefinite programming problem whose solution can be obtained. Furthermore, the authors of [22] provide two suboptimal techniques, which offer simpler solutions to the power allocation problem at the relays. In the first, equal power allocation to all the frequencies is employed while the second performs equal power allocation to all the frequencies and the relays, thus significantly reducing the amount of channel estimation overhead. Also, in [24], the optimization problem that is formed by the transceiver design is nonconvex and the authors provide a decomposition method that transforms the optimization problem into a master problem and a subproblem. The master problem is formulated as a relay-precoder design problem, whereas the subproblem is a source-precoder design problem. By solving the subproblem, the source precoder is obtained and then the solution is transferred to the master problem for the derivation of the relay precoder.

Other works provide reduced complexity BF algorithms for multiuser communication networks. In [38, 39], the system performance is improved through a low-complexity BF vector optimization technique that targets the maximization of the effective channel gains. By considering the relaying functionality of the two destinations as an auxiliary mechanism, the low-complexity algorithm focuses on the maximization of the broadcast channel gains. This is achieved by initializing the combining vectors according to a blind algorithm and then by updating them as the eigenvectors corresponding to the largest eigenvalue for the two SD channels. Moreover, in [48], a MIMO broadcast relay channel is studied targeting sum-rate maximization. It is shown that the problem of finding the input covariance matrices and the relay BF matrix is nonconvex and in order to solve it the authors propose to examine the dual multiple access relay channel (MARC). By matching the relay BF matrix to the left and right singular vectors of the first and second hop channels, the solution to this problem is tractable and sum-rate optimization is performed for this case. The MIMO broadcast relay channel is also the topic of [49] and the goal is to maximize the weighted sum rate. However, finding the source precoding matrix $\mathbf{B}$ and the relay BF matrix $\mathbf{F}$ is a non-linear and nonconvex problem. To achieve a tractable solution, the authors set an equivalent problem that aims to minimize MSE. This problem consists of four variables, $\mathbf{B}$, $\mathbf{F}$, the receive matrix $\mathbf{A}_k$ of user k, and the weight matrix $\mathbf{W}_k$ of user k. By keeping three of the four variables fixed, the problem is convex with respect to the remaining variable and has a closed-form solution. Another work [50] examines the relay interference broadcast channel and targets the end-to-end rate maximization. The proposed low-complexity algorithm is performed through a three-step procedure. During the first step, the precoders at the relays are designed in order to maximize the second-hop sum rates. In the second step, using the knowledge of the second-hop rates and the time-sharing value, that is, the fraction of time where each hop is performed, the source precoders are designed and an approximation of the optimal end-to-end rate is achieved. In the last step, power control is employed to balance any rate mismatch. The uplink case of a cellular network is studied in [26] where multiple users communicate with one BS through one RS. This algorithm is proposed when the number of the transmitted independent streams from the users is greater than or equal to their number of antennas, that is, for fully loaded scenarios.

For networks where multiple source-relay-destination links are present, various less complex algorithms have been proposed. In [56], the authors study a two-hop topology with multiple MIMO relays. As the optimal sum-rate maximization BF strategy introduces increased complexity, a reduced complexity suboptimal scheme is presented. This iterative algorithm decouples the effective channels and aligns their channel gains at the same level, thus offering a tractable solution to the sum-rate maximization problem. Moreover, another scheme based on interference neutralization is given which cancels the interference at the last hop. Moreover, in [57], the authors present an approximation in the computation of the end-to-end rate in a multisource multidestination network with relays. Through this approximation, the relationship between the two-hop channel gains are taken into account and suboptimal solutions can be achieved when designing the relay BF matrix. In this way, rate mismatch is avoided as the dominance of a specific two-hop is considered and the end-to-end sum rates are improved.

When two or more end nodes communicate with each other simultaneously, two-way communication occurs and many other works present suboptimal algorithms in such cases. In [58], the authors study a two-way MIMO relay network that employs network coding. More specifically, they aim to improve the network's performance by maximizing the minimum distance of the NC symbols. As the derivation of the global optimum depends on the individual constellation and their mapping rule, a closed-form solution for the transmit precoders at the end nodes is not known. In order to reduce the complexity of optimization, a suboptimal precoding strategy that consists of elements of three different precoders is proposed. The resulting precoding strategy adapts between precoding with subspace alignment, precoding with subspace separation, and precoding with maximum ratio transmission. In addition, [29] considers linear MMSE receivers in a two-way MIMO relay network. As the joint source, relay, and receiver matrices optimization depends on multiple matrix variables, a suboptimal relay precoding matrix design is presented. The suboptimal algorithm is proposed in cases where the relay has more or equal number of antennas than both end nodes. To reach to a tractable solution, the main problem is decomposed into subproblems, which are solved using the projected gradient algorithm.

Furthermore, in [31], a simplified algorithm is proposed which computes transmit and receive BF matrices at the end nodes of a two-way network. This is achieved by computing the receive BF matrices given all other BF vectors and then computing the transmit BF matrices through one-step SVD decomposition. Finally, the relay BF matrix is obtained. The authors of [53] give a suboptimal solution to the sum-rate optimization problem in a two-way MIMO relay network. As the original problem is nononvex, a decomposition into three separate subproblems is proposed to find the transmit, receive, and relay BF matrices. However, the problem of finding the relay BF matrix is nonconvex and an approximation is given based on the power iteration technique. Also, [54] examines a two-way MIMO relay network where suboptimal schemes to compute the relay BF matrix structure are presented. The first is based on the combination of maximal ratio reception and maximal ratio transmission while the second on ZF reception and ZF transmission. Finally, in [27], a multiuser two-way relay network is examined where precoding design aims to suppress co-channel interference. In contrast to BS precoding design with a fixed RS precoder, the design of the RS precoder with a fixed BS precoder is nonconvex. As a result, the authors propose an iterative algorithm that finds a local optimal solution either through eigenvalue decomposition or through randomization, which leads, in a quasioptimal solution.

All the aforementioned papers are categorized accordingly in Table 1 with respect to their network configuration, depicting the complexity in quantitative way (whenever possible) and elsewhere in qualitative way, and the utilized suboptimal optimization method, along with the detailed configuration and the relay strategy scheme that they adopt.

2.4. Channel Estimation and Feedback. The formulation of transmit and receive BF matrices is based on successful channel estimation and the feedback of CSI to the nodes that perform BF. The works presented in this subsection consider cases where full CSI is not available and, so, efficient methods that are based on partial CSI are devised to allow BF techniques to take place. Furthermore, the operation of BF with reduced CSI exchange minimizes additional overhead to the network and allows increased QoS.

In scenarios where only a single destination is present, the following works aim to give BF algorithms with reduced CSI exchange, in order to provide scalable methods for more complex network topologies. In [65], clusters of multiple-antenna relays assist the communication of a multiple-antenna source and a single-antenna destination. In addition, transmit maximal ratio combining BF (TMRC-BF) is employed at the relays which double the duration of the effective channel through which the transmitted signal propagates. As a result, additional overhead is needed due to pilot signals that are used to estimate the channel. By using the real value property of the equivalent channel, the pairing of relay clusters is proposed in conjunction with corresponding pilot designs. Simulations for MSE performance reveal that when the pilot SNR is not less than 5 dB below the pilot SNR during TMRC-BF, optimal performance can be achieved. In [34], a modified quantization scheme at the destination is presented in order to reduce the amount of CSI feedback. This scheme is based on the fact than in the extreme cases where the SD link or the SRD link is weak, no feedback or only the knowledge of the right singular vector of the direct link is required at the relay to determine the source BF vector. The article in [66] proposes antenna selection in order to reduce the overhead of feedback compared to multiple-antenna BF. The authors map this scenario to a case where a dominant channel is present or when diversity is preferred compared to multiplexing gain. The antenna selection with limited feedback is described where narrowband tones are transmitted from each source and relay antennas and at the end the destination is able to perform MMSE. This selection process requires $\log_2(M_S M_R)$ bits of feedback, where M_S and M_R are the number of antennas at the source and relay, respectively, and $M_R + 2M_S$ are time slots for SNR estimation; thus the minimization of SNR estimation time is important in this scheme. From the analysis, it is shown that full diversity order can be achieved.

When relay selection takes place, instantaneous channel-gain values are needed and CSI availability is critical for the performance of the selection algorithm. In [35], the authors consider the relay selection scheme as a special case of BF where limited feedback equal to $\log_2(m)$, where m is the number of relays, is needed. The compared schemes include relay selection and multiple-relay BF with various amounts of feedback ranging. From the results, it is concluded that the selection scheme achieves better performance than BF for limited feedback cases in AF relay networks. Also, in [36], partial relay selection (PRS) is employed in order to reduce the CSI requirements of the optimal opportunistic relay (OR) selection. More specifically, the selection process is based on the quality of the SR links. In this way, no additional CSI feedback from the RD links is required. Comparisons with OR with full CSI indicate that when $\min(M_{r,1}M_d, M_{r,2}M_d) \geq M_s M_{r,1} + M_s M_{r,2}$, where M_s, M_d and $M_{r,q}$ are, respectively, the numbers of antennas at the source, destination, and the qth relay, PRS and OR achieve the same diversity gain.

For a network where one BS serves multiple users, the authors in [67] study user selection based only on partial CSI of transmit correlation. As a result, in each transmission, one user is served by the BS and one by the RS, and their selection is based on an orthogonal pair of users which has the largest phase difference of the transmit correlation, in order to reduce the interference received by each user and maximize the achievable sum rate of multiuser dual-hop MISO relay channels.

2.5. Antenna Correlation. Another challenge for MIMO BF is the correlation between the antennas at each node. Such scenarios are of great importance as colocated antennas in small devices such as smartphones result in spatial correlation in transmission and reception.

In [68], a network with a MIMO source, a single-antenna fixed gain relay, and a MIMO destination is explored. The analysis takes into account the correlation between the antennas at the source and at the destination using the Kronecker correlation model. Closed-form expressions are derived for

Table 1: Classification of articles based on network topology, with their corresponding complexity and suboptimal optimization method used.

Reference article	Complexity	Suboptimal optimization method	Configuration/relay strategy
		Single relay/single user	
[24]	The cost function that expresses the minimization of MSE is a nonlinear function of the two precoding matrices at the source and the relay, resulting in a nonconvex optimization problem	Source-precoder subproblem is solved by applying Karush-Kuhn-Tucker (KKT) conditions to single relay-precoder optimization	S: single MIMO R: single AF MIMO D: single MIMO
[54]	MRR-MRT: proportional to MF-based receive and transmit beamforming to maximize the total signal power ZFR-ZFT: proportional to ZF-based receive and transmit beamforming to remove the interference	Relay BF matrix calculations based on: (i) Maximal-Ratio Reception and Maximal-Ratio Transmission (MRR-MRT) (ii) Zero-Forcing Reception and Zero-Forcing Transmission (ZFR-ZFT)	S: single-antenna, single source R: single AF two-way single-pair MIMO D: single-antenna, single user
[31]	$O(N^3)$, N: number of antennas at the source	Optimal beamforming at all nodes based on the minimization of the sum MSE adopting KKT conditions	S: single MIMO R: single AF two-way single-pair MIMO D: Single MIMO
[53]	The sum-rate maximization problem in this two-way AF single-relay network is not convex and an approximate solution can be derived through decomposition	Joint optimization of the transceivers at both sources and relay in terms of sum-rate maximization and based on KKT conditions	S: single MIMO R: single AF two-way single-pair MIMO D: single MIMO
[58]	The global optimum regarding the maximization of the distance of network-coded symbols is complicated to be found, as it depends on the symbol constellation and the corresponding mapping rule. Moreover, for general MIMO channels between the two sources and the relay, a closed-form solution has not been derived	Design of a hybrid precoder combining three different classes of suboptimal precoders, with additional constraints of subspace alignment, subspace separation, and the maximal ratio transmission Define the optimal precoding vectors within each class in terms of maximizing the minimum distance between different network coding symbols	S: single MIMO R: single AF two-way single-pair MIMO D: Single MIMO
		Multiple relays/single user	
[22]	For each relay: $\log_2(N_c)\, NN_c/2 + N^2N_c$ N_c: iid symbols N: number of antennas at the relay	(i) frequency domain (FD) based processing at the relays (ii) equal power allocation (EPA) across all frequencies (iii) equal power allocation (EPA) across all frequencies and relays	S: single-antenna, single source R: multiple AF MIMO D: single-antenna, single user
[33]	The optimization of the source BF matrix is nonconvex	Gradient algorithm for finding local optimum of the source BF vector	S: single MIMO R: Multiple AF MIMO D: single-antenna, single user
[29]	The joint source, relay and receive matrices optimization problem that aims at two-way MSE minimization is non-convex. The global optimum cannot be achieved with reasonable complexity (nonexhaustive searching)	Iterative algorithm for joint source, relay, and receive matrices optimization for two-way sum MSE minimization	S: single MIMO R: multiple AF two-way single-pair MIMO D: single MIMO
[61]	Depending on the imposed power constraints, the optimization problems for each optimal case induce different complexity. When multiple relays are employed, the optimization is nonconvex for the case of joint relay power constraints and joint source-relay power constraints	Max-min optimization of the source BF vector under joint relay and jointed source-relay power constraints: (i) transformation method (ii) gradient method (iii) relaxation method	S: single MIMO R: multiple AF MIMO D: single-antenna, single user

Table 1: Continued.

Reference article	Complexity	Suboptimal optimization method	Configuration/relay strategy
		Single relay/multiple users	
[26]	Proportional to the beamforming algorithm for the fully loaded or overloaded uplink	Linear MMSE criterion for both downlink/uplink utilizing iterative beamforming algorithm: (i) equalizer design at the user/BS (ii) forwarding matrix design at the relay station (iii) precoder design at the BS/user	S: single MIMO R: single AF MIMO D: multiple MIMO users
[38, 39]	2^{2B} for each channel matrix (SR, RD, RR) B: bits	(i) blind algorithm (ii) broadcast channel optimization	S: single MIMO R: single AF MIMO D: multiple MIMO users
[48]	The formulated sum-rate optimization is non-convex and a global optimal solution cannot be obtained	Optimization of the dual multiple access relay channel (MARC) applying alternating minimization algorithm (AMA) that maximizes the network sum rate	S: single MIMO R: single AF MIMO D: multiple MIMO users
[49]	Proportional to two linear relay beamforming schemes	Weighted MMSE method for MSE minimization	S: single MIMO R: single AF MIMO D: single-antenna, Multiple users
[27]	$n_{BS} = (NK + 1)^2(K + 2)^{0.5}(2NK + K^2 + 2K + 4)\log(1/\varepsilon)$ $n_{RS} = l_{RS}(\max(M^2, K + 2)^4 M \log(1/\varepsilon) + n_{rd})$ N: number of BS antenna M: number of relay antenna K: number of MS single antenna l_{RS}: iteration number in Algorithms 1 and 2 n_{rd}: the complexity of randomization	(i) Iterative algorithm for RS precoding design with the BS precoder fixed (ii) Design of joint BS-RS precoding by solving the BS and RS precoding alternately	S: single MIMO R: single AF two-way multi-pair MIMO D: single-antenna, multiple users
		Multiple relays/multiple users	
[42]	(i) The complexity of the centralized adaptive BF is $O\left(J\left(\sum_k m_k^2\right)^2\right)$ per iteration J: is the number of sources and destination nodes m_k: is the number of antennas at the kth relay (ii) For the decentralized algorithm, the complexity per iteration is equal to $O(Jm_i^4)$ at the ith relay	(i) Centralized adaptive BF algorithm with the existence of a local processing center connected to all the relays and minimizing a cost function using state-space modeling approach (ii) Decentralized adaptive BF algorithm allowing each relay terminal to compute its beamforming matrix locally with limited amount of data exchange with the other relays, employing Kalman filtering to estimate its beamforming coefficients iteratively	S: single-antenna, Multiple sources R: multiple AF MIMO D: single-antenna, Multiple users
[43]	The optimization problem of meeting the QoS constraint with minimal relay power expenditure is non-convex	ZF-BF is used in order to reduce complexity by projecting the BF vector to a low dimensional space thus reducing the number of variables that are used for optimization	S: single-antenna, multiple sources R: multiple AF MIMO D: single-antenna, multiple users
[56]	As the problem of sum-rate maximization is NP-hard, the process of checking whether a set of SINR values are achievable in order to obtain the optimal solution is highly complex	(i) Sum-rate maximization through an iterative algorithm subject to a sum-power constraint of the relay BF matrices (ii) Interference neutralization beamforming scheme subject to a linear constraint on the desired signals	S: single-antenna, multiple sources R: Multiple AF MIMO D: single-antenna, multiple users

Table 1: Continued.

Reference article	Complexity	Suboptimal optimization method	Configuration/relay strategy
[50]	Proportional to three-phase cooperative algorithms with distributed implementation	Sum-utility maximization via matrix-weighted sum-MSE Minimization for end-to-end sum-rate maximization	S: multiple MIMO R: multiple AF MIMO D: multiple MIMO users
[57]	The sum-rate optimization problem is NP-hard and the global optimal solution cannot be derived with realistic computation complexity	Distributed two-hop interference pricing algorithm for relay beamforming design for maximizing end-to-end sum rates	S: multiple MIMO R: multiple AF MIMO D: multiple MIMO users

S: source, R: relay, D: destination.

the outage probability and BER performance. Moreover, the diversity order of the network is found to be dependent on the number of the source's antennas, a result that is in contrast to CSI-assisted relaying where the diversity order is equal to the minimum number of antennas between the source and the destination. Also, the case where the second hop is stronger reveals that the system's performance depends only on the antenna configuration at the source. The strong point of this work is that realistic assumptions are made and mapped to cases such as the uplink of a cellular network where antenna spacing causes correlation at the terminals or when two BSs communicate with the help of a single-antenna relay; that is, when these BSs have the same number of antennas, CSI-assisted relaying has a higher array gain and offers superior performance. In [37], the authors extend their previous published work [68] by examining the performance of two different relay protocols. The first is called channel-noise assisted (CNA) AF relaying that uses the statistics of the channel and the noise. The second protocol is called channel-assisted AF relaying and uses the statistics of the channels. The two protocols exhibit similar performance at high SNR. From the analysis, SER expressions are obtained and the diversity order and array gain for both protocols are extracted. The results indicate that antenna correlation is beneficial for cases where low SNR dominates the network while in the high SNR regime it is detrimental for the outage probability and SER. Finally, the achieved diversity order is equal to the minimum number of antennas between the source and the destination. The article in [69] studies a similar scenario with the above works, where a MIMO source communicates with a MIMO destination through a single-antenna relay. The analysis is given for two different systems. The first employs maximal ratio transmission (MRT) at the source and maximal ratio combining (MRC) at the destination and assumes general correlation structures. The second is based on transmit antenna selection (TAS) and assumes antenna correlation only at the destination. From the analysis closed-form expressions for outage probability, average symbol-error-rate (SER) and generalized higher moments of SNR are obtained for CSI-assisted and fixed-gain relaying. Also, a high SNR analysis is performed to gain an insight on the diversity of the system. It is concluded that CSI-assisted relaying outperforms the fixed-gain and this holds for the MRT/MRC system in comparison to the TAS system.

In a different setup, the authors in [63] study a multiple-access scenario where MIMO users want to communicate with MIMO BSs through MIMO relays. The antennas at all the nodes are considered correlated and modeled with Kronecker correlation. The challenge in this setup is that the BSs have perfect CSI while UEs and RTs have the channel covariance information (CCI). As a result, to maximize the system sum rate, the authors perform a joint optimization of the UEs covariance matrices and relay precoding matrices. From the analysis, the asymptotic sum-rate expression is derived for the large-system scenario where the antennas are increased in every network node with constant ratios. Moreover, results are obtained for various given signaling inputs, and an iterative algorithm is given which obtains the asymptotically optimal users and RS precoding matrices.

3. Beamforming for Single-User Communications

In this section, various works are presented that study MIMO BF techniques in cases where a single user is present in the network. Following, and for each scenario, an analytical description is performed evaluating the BF scheme.

3.1. Beamforming with Single Relay. In Figure 2, a network where a single relay is used to establish communication between a source and one user is depicted. Under the single-relay consideration and when capacity and power optimization arises, the authors in [45] provide the three basic modes for the three-terminal MIMO relay network, namely, the direct link (mode A), the relay without direct link (mode B), and the relay with direct link (mode C). A weighting matrix at the relay is designed in such a way as to minimize capacity loss. This is achieved by transforming the MIMO relay channel in parallel SISO relay subchannels and then, through waterfilling, power allocation is performed.

The Grassmannian codebooks are proved appropriate for the design of the source and relay BF based on the distributions of the optimal source and relay BF vectors [34]. The authors aim at SNR maximization through BF at the source and the relay. The explored scenarios include an SRD topology with and without the presence of the SD link. Moreover, when perfect CSI is available at the source

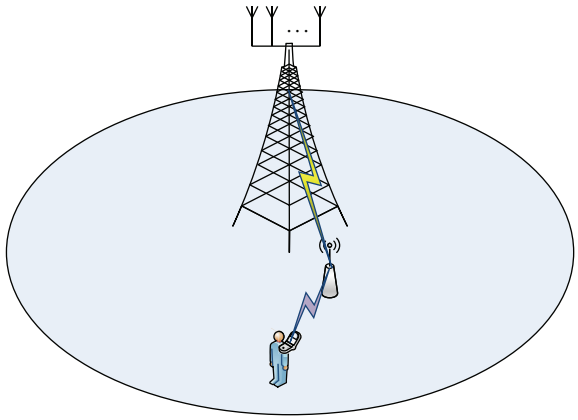

Figure 2: Single-relay communication.

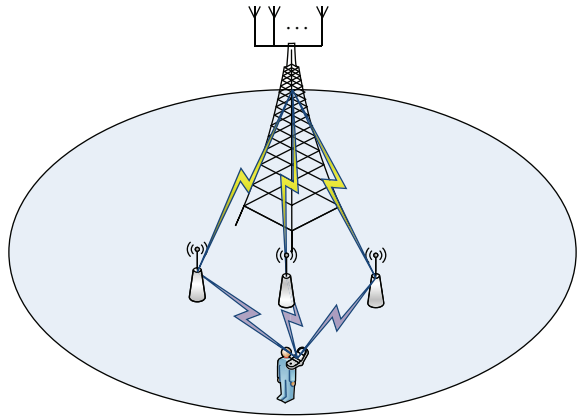

Figure 3: Multiple-relay communication.

and the relay, a mapping of the source and relay signals to the dominant right singular vectors of the SR and RD channel should be performed. On the other hand, when limited feedback is available, Grassmannian BF codebooks at the source and the relay should be adopted which quantize the optimal BF vectors. In order to reduce the complexity, a modified quantized scheme can be employed for the case where SD connectivity is feasible. Through this scheme, only one singular vector needs to be quantized resulting in significant reduction of feedback from the destination to the relay.

The optimization (minimization) of the MSE in a single-user single-relay scenario is considered in [23], where the authors consider the optimal BF in three stages. First, the MIMO relay performs receive BF by using the Hermitian transpose of the left singular matrix of the SR channel. Then, linear precoding takes place at the relay and, finally, transmit BF is performed through the use of the right singular matrix of the RD channel. The work in [25] extends the previous one by performing joint source-relay precoding design. As the derivation of the optimal relay amplification $\mathbf{F}$ and source precoding $\mathbf{B}$ matrices in closed form is intractable, an iterative algorithm is provided. The algorithm optimizes $\mathbf{F}$ for a given $\mathbf{B}$ under a relay power constraint. Also, $\mathbf{B}$ is optimized for a fixed $\mathbf{F}$ under power constraints at the source and the relay. Following the precoding technique, the authors in [24] propose a non-linear precoding scheme, which adopts a Tomlinson-Harashima precoder (THP) at the source, while the relay uses a linear precoder. Moreover, a direct SD link exists and the destination uses an MMSE receiver. The proposed scheme performs a joint source-relay precoder design and to make the solution tractable it decomposes the problem into one subproblem and a master problem, which provide the precoders of the source and the relay correspondingly. Comparison with the schemes of [21, 24] shows improved MSE performance from the proposed precoding method. Finally, the work in [70] studies the degrading effect of self-interference and provides precoding designs to mitigate it. More specifically, transmit and receive beams at the relay are formed in such a way to minimize the self-interference signal experienced at the receive antennas of the relay. This is achieved by pointing these beams to the minimum eigenmodes of the channel between transmit and receive relay antennas. Also, the authors provide the condition, which corresponds to the null-space projection scheme of the optimal eigen-BF, thus providing orthogonal subspaces to relay reception and transmission. The main contribution of this work is the formulation of precoding designs that allow the minimization of the degrading effects of self-interference.

3.2. Beamforming with Multiple Relays. Figure 3 illustrates the scenario where multiple relays are allocated for the communication between a source and one user. Moving forward and considering single-user BF for multiple-relay nodes, in [44], the authors compare signaling and routing techniques for various relaying protocols, namely, amplify-and-forward (AF), decode-and-forward (DF), and hybrid relaying, where the relay decodes only the necessary information to obtain CSI for the SR or RD channels. Several MIMO spatial multiplexing (SM) techniques are presented, which take advantage of CSI knowledge at the relay by coordinating the SR and RD channels eigenmodes. The authors compare SM to single signal BF (SSB), which exploits the spatial diversity of MIMO channels. If CSI is available at the transmitter, then SSB can be performed. In continuity, two cases of SSB are given for both DF and hybrid relaying. It is shown that, in the low SNR regime, SSB is preferable compared to spatial multiplexing due to its increased diversity. The main contribution of this article is the consideration of three types of relaying and the comparison of SM and SSB for various SNR regimes.

When a MIMO equalizer is introduced for implementing the BF matrix at the receiver, the authors in [21] study the SNR and MMSE designs under a global power constraint at the relays and at the receiver, in a network with MIMO source, multiple MIMO relays, and MIMO destination. For the MMSE approach, they provide two alternatives to formulate the relay matrix $\mathbf{F}$ and the MIMO equalizer $\mathbf{A}_k$ at the receiver. Firstly, they perform a two-step design where $\mathbf{F}$ is priorly formed and then $\mathbf{A}_k$ is derived. Secondly, they proceed in a joint formulation of $\mathbf{F}$ and $\mathbf{A}_k$. On the other hand, for the SNR

approach, they include two optimization cases, with a zero-forcing constraint and with the global power constraint. Furthermore, they form the BF matrices aiming to maximize the transmission rate. The simulations show that both approaches achieve similar BER performance when there is no power constraint at the relays. By targeting SNR maximization at the destination under different power constraints, the authors in [33, 61] study a network where a MIMO source communicates with a single-antenna destination through multiple MIMO AF relays. Three different power constraints are derived for the optimal BF-AF weights and for a given BF vector at the source. Firstly, for the individual and joint relay power constraints, closed-form solutions are given. Secondly, for the joint source-relay power constraint, a numerical method is presented which offers optimal power allocation for the source and the relays. In order to decrease implementation complexity, suboptimal methods for the joint relay and joint source-relay power constraints are presented. These methods are based on the transformation of the optimization problem into a nonconvex polynomial programming problem. Numerical results illustrate that the performance of the suboptimal methods follows closely that of the optimal one. By targeting minimization of the MSE or equivalently the maximization of the SINR under a sum power constraint, the study in [22] considers BF that is coupled with single-carrier frequency domain equalization in a three-node network. From the proposed algorithm, the optimal frequency-domain linear equalization (LE) and decision-feedback equalization (DFE) to the receivers is derived. The optimal relay BF matrices are formed under a sum power constraint. Moreover, complexity issues are considered by providing suboptimal power allocation algorithms without significant performance degradation.

3.3. Relay Selection. The case of relay selection is shown in Figure 4. In order to reduce synchronization requirements among the multiple transmitting relays, relay selection has been proposed in [10]. In addition, the selection of one relay or a subset of the available relays improves the spectral efficiency of the transmission as the amount of orthogonal channels is less than the number of the relays in the network for the same diversity gain. In [35], the authors illustrate the efficiency of relay selection through comparisons with BF schemes based on limited and unlimited CSI. They develop the outage probability of the optimal AF BF with unlimited feedback noting that due to its impractical assumptions it serves only as a performance bound to other more practical schemes. Moreover, the selection scheme is proven to be the unique optimal for AF BF as it minimizes noise amplification. Also, numerical comparisons are given for the cases of optimal codebook design and random BF with limited feedback. The compared schemes include relay selection, optimal BF, and BF with various amounts of feedback. It is concluded that the selection scheme outperforms the other BF schemes in limited feedback scenarios while alleviating synchronization concerns.

Partial relay selection (PRS) is employed in [36], where suboptimal relay selection is presented, as the only CSI considered in the selection algorithm is the quality of the SR links. Furthermore, transmit and receive BF is implemented at the source and the destination, while for the selected AF MIMO relay the linear precoder is optimized. Additionally, the outage probability of the proposed scheme is given in closed form and for the asymptotically high SNR the diversity gain is extracted. As a result, PRS and OR achieve the same diversity gain.

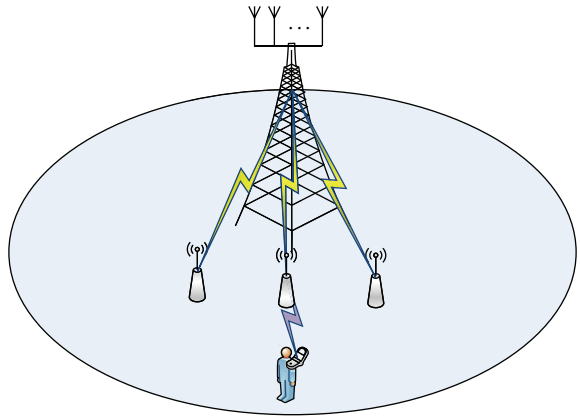

Figure 4: Communication with relay selection.

Another technique is the opportunistic selection of a semiorthogonal subset of relays [47]. The proposed scheme takes place in two steps. First, spatial eigen-mode combining between the forward and backward channels is performed. Then, for the selected subset, the algorithm proceeds in antenna pair selection for reception in the first hop and transmission in the second hop.

The best relay selection is studied in [62], where a single-user network is examined with the consideration of multiple MIMO relays. The proposed scheme selects the best relay that successively combines maximal ratio receiver combining in the first hop and BF in the second. In order for this process to take place, the authors consider that in two sequential time slots the channel coefficients remain constant. Simulations include comparisons with various relay numbers and antenna numbers on each relay, illustrating the reduction of the outage probability as these values increase. Along with the best relay selection, there are other selection techniques that incorporate, for example, max-rate selection with interference mitigation issues. The work in [46] considers a multihop backbone network where MIMO relays are employed. In each phase, a relay is selected based on maximum rate path routing and performs transmit BF. Additionally, mitigation of the multiple access interference that degrades the performance of the network is achieved through cancellation. The effects of interference mitigation transmit BF and spatial reuse on the performance of the proposed scheme are studied in a game theoretic approach, aiming at the optimal combination of these techniques.

Finally, the multi-relay network of [71] selects in each time slot two relays in order to achieve full-duplex operation through successive relaying. To this end, buffer-aided relay selection is combined with beamforming and two schemes

are proposed. The first scheme is inspired by the case of no IRI between the relays and adopts MRC at the receiving relay and MRT BF at the transmitting relay. As IRI is considered, this scheme utilizes an SINR criterion for the SR link and the relay-pair that maximizes the instantaneous end-to-end rate is chosen. The second scheme is based on ZF-BF to cancel the IRI at the receiving relay and to maximize the effective channel power gain of the RD link. Results illustrate that the SINR-based approach improves the rate performance of the network in the low SNR region while the ZF scheme has the best performance and approaches the upper bound of the IRI-free case.

4. Beamforming for Multiuser Communications

An alternative approach for transmitting the signal through the relays is to serve multiple users simultaneously. A relay broadcast channel (RBC) can be considered, which is a typical case for the so-called nondedicated relay system. A nondedicated relay system is when the mobile users can help each other by relaying information for their peers besides receiving their own data. An RBC is based on a broadcast channel (BC) where a BS transmits to multiple users simultaneously. Relay mechanism is presented into the BC in such a way that the users can benefit from each other by performing cooperative procedures. In addition, another case considered is that of two-way relaying as a multiuser scenario, where the two sources exchanging information could be single or multiple pairs of users that communicate and not necessarily a BS and a user.

There are several ways of exploiting this operation by employing MIMO techniques, as depicted in Figures 5–7. Several scenarios can exist, such as multiuser communication through a single relay, multiuser communication through multiple relays, two-way single pair communication, and two-way multi-pair communication.

4.1. Beamforming with Single Relay. When a single relay is concerned, as is the case in Figure 5, there are many studies that take into consideration some or all of the aforementioned challenges discussed in Section 2. Different power constraints, precoding techniques, and feedbacks are introduced to minimize MSE, maximize sum rate, and decrease complexity. The classification of the examined papers depends on whether users are equipped with multiple antennas or not.

On one hand, when only a MIMO BS and a MIMO RS are considered, a solution for the optimization problem is introduced in [49], which exploits the downlink performance, incorporating relay BF with source precoder matrix. It deals with a formation of MIMO relaying broadcast channel to multiple users at the downlink, based on weighted sum-rate criterion. Accordingly, the design of the source and relay matrices is based on non-linear and nonconvex Weighted MMSE (WMMSE) criterion. The WMMSE scheme can better deal with the multiuser interferences and noise, and the relation between downlink gains and source-relay

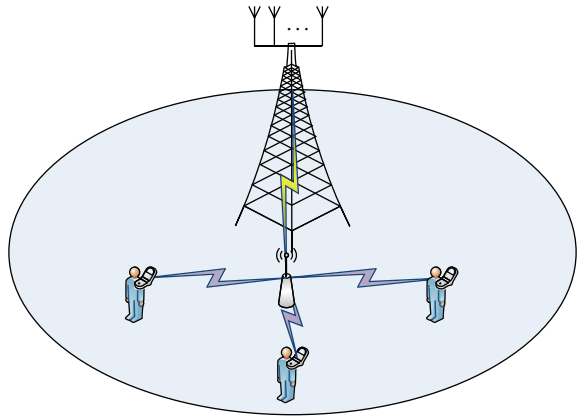

Figure 5: Multiuser communication through a single relay.

users channel gains. Because of the difficulty in solving the non-linear and nonconvex problem, decoupling it into two tractable subproblems solves an equivalent problem and an alternative optimization based on efficient linear iterative design algorithm is proposed, which always converges to a stationary point. Following the previous topology, the authors in [40] consider a MIMO relay-assisted multiuser downlink transmission with limited feedback and suggest two precoding schemes at the RS based on the ZF criterion and the MMSE criterion. These robust linear BF schemes take only channel direction information (CDI) feedback using a finite number of feedback bits to the RS and the effect of channel quantization errors for determining the BF vectors.

On the other hand, when all nodes have multiple antennas, the authors in [39] consider MIMO relay broadcast channels. For simplicity, a two-user system is taken into consideration. A precoding, relaying, and combining (cooperative) scheme is proposed, under an overall power constraint, and an optimal power allocation solution in a closed form is developed. Instead of considering time-division broadcast schemes, it is assumed that the BS transmits simultaneously to both users in the same frequency band. Precoding is used to steer the signals for the two users in different subspaces to avoid interuser interference, employing the zero-forcing criterion. The user with better conditions acts as an AF relay to the other user besides receiving its own signal. Based on the proposed scheme, an optimal power allocation solution is established so as to minimize the BER, which is equivalent to maximize the SNRs. Moreover, an optimization algorithm for the BF vectors is proposed in order to achieve the maximum effective channel gains, utilizing three different schemes for optimization of combining vectors: exhaustive search, blind algorithm, and broadcasting optimization. The proposed algorithm is shown to achieve a near optimal performance (compared with the exhaustive search algorithm) and maximum diversity gain. Nevertheless, there are several weaknesses: only a fixed relay direction has been considered, the BF and combining vectors have been determined in sequence, which is not optimal, and only one data stream for each user and flat fading channels have been taken into consideration.

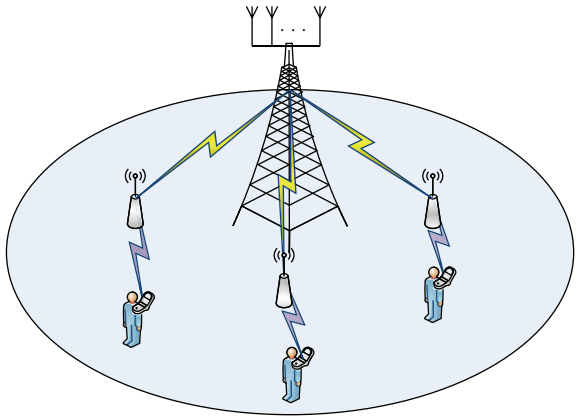

Figure 6: Multiuser communication through multiple relays.

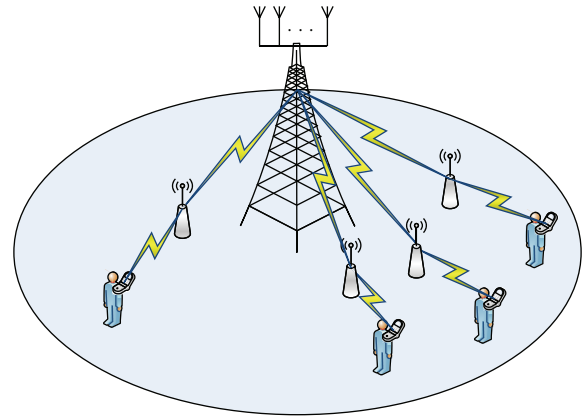

Figure 7: (Left) Two-way single pair communication, (right) two-way multi-pair communication.

Accordingly, a fully MIMO single-relay scheme is presented in [48] where the topology comprises a MIMO BS, where a dirty paper coding is applied, a fixed infrastructure-based half-duplex MIMO relay station (RS) with linear processing, and multiple users equipped with multiple antennas. A MIMO BRC and its dual multiple access relay channel (MARC) network (uplink-downlink duality) is used to transform the problem and solve a nonconvex problem which finds the input covariance matrices and the RS BF matrix that maximize the system sum rate. To make the problem tractable, the relay BF to the left and right singular vectors of the forward (RS-to-users) and backward (BS-to-RS) channels was matched. With this RS BF structure, the authors proposed an iterative algorithm for the sum-rate maximization for the dual MIMO MARC, where the MIMO-AF duality was proved for multiple-antenna-user networks. The proposed scheme follows an alternating-minimization convergent procedure over the input covariance matrices at the transmitter and the BF matrix at the relay. Also, the derivation of the mapping from the resulting covariance matrices for the MARC to the desired covariance matrices for the BRC is proposed. A valuable observation for better system performance is to have more antennas at the RS than at the BS.

Following the consideration of a fully MIMO single-relay topology, a linear BF design for amplify-and-forward relaying cellular networks is considered in [26]. The design is based on optimizing (minimizing) the sum mean square errors of multiple data streams, while joint design of the precoders, forwarding matrix, and equalizers for both uplink and downlink is considered and under individual power constraints. An iterative algorithm is proposed for the downlink so as to jointly design the precoder at BS, while forwarding matrix at RS and equalizers at mobile terminal. For the uplink, the duality of the BF design is demonstrated and the same downlink iterative algorithm can be applied. Additionally, a low-complexity algorithm has been developed for the uplink under a special case when the number of independent data streams from different mobile terminals is greater than or equal to their number of antennas (fully loaded or overloaded uplink systems). It is found that the resultant solution includes several existing algorithms for multiuser MIMO or AF relay network with single antenna as special cases and outperforms the suboptimal schemes. It is verified that for AF MIMO relaying systems, source precoder design is of great importance and offers additional design freedom for performance improvement.

Finally, when both single- and distributed-relaying schemes are considered and compared in [43], multiple single-antenna SD pairs communicate via one MIMO relay in a network where linear BF techniques are employed. The goal of BF is the sum-power minimization aiming at a target SINR at the destinations. The BF technique is based on ZF in order to cancel the interference at the destinations and the formulation of the relay BF matrix result in a least-squares problem that can be solved with convex optimization tools. From the numerical results, it is concluded that the MIMO relay with ZF-BF achieves the best performance compared to other schemes employing distributed single-antenna relays.

4.2. Beamforming with Multiple Relays. Interference management is maybe the most fundamental open problem in wireless networks. When multiple MIMO relays are concerned, as shown in Figure 6, thus enhancing the SD pairs equipped with multiple or single antennas, and incorporate beamforming techniques for throughput improving, interference issues appear. The following studies are inspired by this problem and confront the arising interference issues by introducing beamforming algorithms under different network topologies.

In regard with the first topology, where multiple SD pairs communicate through multiple MIMO AF relays, the authors of [42] develop two adaptive relay BF algorithms employing linearly constrained BF algorithms with minimum variance based on Kalman filtering. As a result, the received power at the destinations is minimized by considering the linear constraints on the relay BF matrices, thus avoiding severe degradation of the reception by noise and interference while preserving the desired signal at each destination. The main differentiation of these algorithms is that the first operates in a centralized fashion while the second is distributed. In the centralized approach, the relays have a common processing

center that receives all the CSI and computes the BF coefficients, which are fed back to the relays. In the distributed case, each relay computes its own BF coefficients through local channel estimation. Additionally, extensions to these algorithms are discussed through power control and QoS modification. Numerical results indicate similar performance of the proposed methods to the noniterative centralized second-order cone program (SOCP)-based algorithm at low and medium SNR regimes and with reduced computational complexity. The main contribution of this work is the reduced complexity of the two proposed algorithms compared to the SOCP-based BF algorithm and the formulation of a distributed BF algorithm.

Following the first topology, there are several papers dealing with a new cooperative interference management scheme named interference neutralization. Accordingly, in [55], illustrative examples are discussed in a network consisting of multiple sources, relays, and destinations. This technique is based on the concept of neutralizing the interference signal at the destination provided that this interference is propagated through various paths. In practice, these interfering signals are processed so that they have the same power level and neutralize each other by adding them at the destination. This processing can take place at the relay using a proper permutation. In addition, the use of lattice codes to achieve the neutralization effect is shown and the signal received after the summation of the interfering signals is the desired point on the scaled lattice. The main contribution of this work is the detailed description of interference neutralization. In [56], authors deal with the mitigation of the cochannel interference issues that arise when relays are equipped with multiple antennas operating in AF and half-duplex modes. Selecting a pair of multiple sources and multiple destinations, both of which are equipped with single antenna, enhances the network performance. A coordinated relay beamforming is considered to suppress interference and improve the date rates of two-hop interference networks, under the sum-rate maximization criterion. A suboptimal solution of interference neutralization beamforming is then introduced, which allows the interference to be canceled over the air at the last hop, where the relay beamformer is designed to neutralize interferences at each destination terminal.

Concerning the second topology, where a number of MIMO half-duplex relays aid the data transmission from a number of transmitters MIMO BSs to their associated MIMO users, the study in [50] conceived an interference management approach. This approach considers interference broadcast channels at relays and end users, where a number of MIMO half-duplex DF relays aid the data transmission from a number of transmitters MIMO BSs to their associated MIMO users. A typically linear precoding design at the transmitter and BF matrix at the relay is accomplished, so as to maximize the end-to-end sum rates. The proposed algorithm solves in a suboptimum way the transmit precoder design following three phases: (1) second-hop transmit precoder design, where the relays are designed to maximize the second-hop sum rates; (2) first-hop transmit precoder design, where approximate end-to-end rates that depend on the time-sharing fraction and the second-hop rates are used to formulate a sum-utility maximization problem to design the transmitters; this problem is solved by iteratively minimizing the weighted sum of mean square errors; (3) first-hop transmit power control, where the norms of the transmit precoders at the transmitters are adjusted to eliminate rate mismatch. The second hop is treated as the conventional single-hop interference broadcast channel and existing single-hop algorithms can be applied to find the stationary points of second-hop sum-rate maximization. The design of the first-hop precoders is devised by applying a naive approach ignoring the designed second-hop transmit precoders. The overall performance is subjected to the assumptions of each transmitting node (relay and BS) and has instantaneous and perfect local channel state information (CSI) and there is a feedback channel to send information from a receiving node to its serving node. Finally, the algorithm is implemented in a quite reverse mode; the relays are optimized for second-hop sum-rate maximization before the transmitters are designed for end-to-end sum-rate maximization. An interesting interference pricing scheme is employed in [57], where the authors investigate the two-hop interference channel and map it to a cellular network with relays. Interference pricing is employed to allow the relays to take into consideration the impact of interference on the end-to-end rate. In order to avoid rate mismatch in the two-hop transmission, an approximation is proposed in the computation of the end-to-end achievable rate, which incorporates the interaction of the two-hop channels, that is, which hop is dominant.

4.3. Two-Way Communication. In Figure 7, two-way relaying scenarios are shown for single and multiple pairs. Two-way communication considers two source nodes that exchange their information through an assisting relay node. When beamforming algorithms are engaged at the exchange scheme, the delivery of information can be completed in two time slots. In the first time slot, both source nodes simultaneously transmit signals to the relay node. In the second time slot, the relay node precodes the received signals along with various beamforming techniques and broadcasts the signals to both source nodes. Self-interference and cointerference issues arise and several multiple access and network coding techniques have been proposed for optimization of a two-way relay channel (TWRC) communication system. When one relay is dedicated to a single user, then a single-pair SD is accounted for, whereas when multiple users utilize one relay, a multiple-pair SD is taken into consideration.

4.3.1. Single Pair. The first set of papers deal with precoding at the relay node. In [32], the authors focus on designing the precoders and decoders based on the MSMSE criterion in a topology where multiple MIMO relays assist two MIMO sources. To simplify the optimization process, the decomposition of the primal problem into four subproblems is performed. These problems include the derivation of the optimal decoders at the sources, and the optimal relay precoding matrix, the optimal precoding matrix for the first source and then for the second source. It is noted that the solution of the second subproblem is one of the

main contributions of this work as it is converted into a convex problem that can be solved. Also, a simulation setup of the proposed scheme is presented and comparisons with suboptimal versions and a nonprecoded scheme are performed. In [29], the main task is the derivation of the optimal structure of the precoding matrices at the sources and the MIMO relay, when MMSE receivers are used as they reduce the complexity in comparison to joint ML detection. Since the joint optimization problem is proven to be nonconvex (Schur-concave/Shur-convex), an iterative algorithm is developed to find the optimal precoding matrices. The algorithm is initialized by finding a simplified relay precoding matrix, designed for the cases where relay antennas are twice (or greater) the number of the antennas of each source. Afterwards, for fixed precoding matrices at the relay and one source, the optimal matrix at the other source is designed. Finally, joint optimization can be performed by updating the relay precoding matrix with fixed matrices at the source and then update the sources' precoding matrices with a fixed relay matrix. Numerical results show the efficiency of the proposed algorithm in terms of normalized MSE and BER and with significantly lower complexity when the suboptimal relay matrix is selected.

Along with the precoding strategy, various network coding schemes found prolific field for increasing the spectral efficiency of the network, alleviating interference issues, and thus optimizing the single-pair BF performance. The work in [58] presents a three-node topology where the end nodes communicate through a MIMO relay. The relay follows a network coding strategy based on either digital network coding or physical network coding. As a result, the precoding strategy in the broadcast phase takes into consideration the maximization of the minimum distance of the network-coded symbols. For this reason, a hybrid precoder is proposed which switches among three suboptimal precoders, that is, with subspace alignment, with subspace separation, and with maximum ratio transmission. Numerical results include comparisons of the three suboptimal precoders with the hybrid precoder and a reference scheme where each end node does not cause interference to the reception of the other node's signal at the relay. The result proves the efficiency of the proposed scheme as it achieves a near-optimal frame error rate (FER) performance. The work in [54] studies a three-node topology with single-antenna source and a MIMO AF relay. To increase the spectral efficiency of the network, analogue network coding is performed which results in the cancellation of the self-interference at the sources caused by the previously transmitted messages. The authors derive the optimal BF matrix at the relay through SVD as well as its achievable capacity region. The capacity limits are extracted through the use of rate profiles, which regulate the ratio of the rate of a user to their sum rate as a predefined value. In addition, power minimization is performed at the relay given specific SNR at the receivers. In order to offer more practical schemes for this topology, two suboptimal approaches based on matched filter and ZF are presented. The results indicate that the matched filter approach is the scheme, which can offer the best performance considering its lower complexity compared to the optimal BF technique. In [30], relay selection is combined with two-way transmissions in a network consisting of two single-antenna sources that are assisted by K MIMO relays. The optimal relay selection criterion is extracted by considering the minimum PLNC decoding error probability. To perform the selection, each relay transformation matrix is decided according to [54] and then the one that provides the minimum decoding error probability is selected. Numerical results show the diversity gain achieved by relay selection through the proposed criterion.

A sum-rate maximizing technique is proposed in [53], which performs joint optimization at the relay. The authors aim at the maximization of the sum rate in a two-way communication scenario with a MIMO relay. To this end, a sum-rate maximizing technique is proposed which performs joint optimization at the relay. As the derivation of the optimal processing matrix is nonconvex, an approximate solution is proposed which consists of the iteration of three optimization problems for the transmit beamformer, the receive combiner, and the linear relaying matrix. Simulations compare the proposed scheme with other single and multiple antenna techniques in terms of sum-rate performance. It is concluded that the upper bound is achieved by the proposed BF scheme while it converges rapidly to the final solution. Alternatively, when the minimization of the sum mean square error (SMSE) is evolved, the authors in [31] jointly optimize the ideal BF vectors for the two communicating sources and the MIMO relay with the target of SMSE minimization, under individual power constraints at all the nodes. A simplification analysis is then conducted stating that the BF pairs, which minimize the SMSE, also maximize the SNR at both communicating nodes. In addition, a scheme, which optimizes the BF vectors in three consecutive steps, is given and is compared to the optimal one in terms of the number of iteration and BER. Results indicate that when the number of antennas is greater than two, the simplified scheme experiences only a small performance loss and can substitute the optimal one.

4.3.2. Multiple Pairs. Considering the multiple-pair two-way communication scheme, numerous works exist that have tried to improve all the above-mentioned challenges in Section 2. Regarding the channel estimation challenge, the authors in [51] consider multiple SD pairs that communicate through MIMO AF relays and adopt the two-way strategy. The nodes are assumed to be full-duplex and perfect CSI is available to all of them. In this context, two different cases are presented. The first is termed Y relay channel and consists of three users that want to unicast independent messages for different two users through the relay. For this setting, the achievable degrees of freedom (DoF) are extracted when the relay performs either analog network coding (ANC) or physical layer network coding (PLNC) and are proven to be equal to $2M$ if all the nodes have M antennas. The second case considers multiple two-way relay links that operate concurrently, thus naming this case as two-way relay X channels. By equipping the users with $M = 3$ antennas and the relay with $N = 4$ antennas, the DoF is found to be equal to 8. The main contribution of this article is the investigation

of the DoF in two-way relay networks. Correspondingly, the formulation of a general model for topologies where N single-antenna nodes communicate simultaneously (N-way) through a MIMO relay is presented in [64]. From the analysis it is extracted that for this general case there should be at least $N - 1$ antennas at the relays while the transmission should occupy N time slot. Moreover, the general BF matrix at the relay is constructed for various objective functions.

An interesting relaying scheme termed Quantify-and-Forward (QF) is considered in [41], where the authors investigate a topology consisting of K single-antenna pairs that perform two-way communication with the help of a MIMO relay, which is equipped with $M \geq 2K$ antennas. The relaying strategies include AF and QF and the corresponding BF techniques are derived. For AF relaying, two possibilities are considered; the first is BF with ZF transmitter and receiver and the second performs block diagonalization, which takes into consideration that intrapair interference can be cancelled. Also, the QF strategy, which can be seen as a case of analog network coding due to the signal separation, is performed at the relay. Furthermore, the received signals at the relay are quantized to a scalar that is a linear combination of the two-dimensional vectors transmitted by each pair. In the next phase, multicast aware BF is employed aiming to minimize distortion. Additionally, comparisons are performed between the proposed schemes and DF relaying in terms of the average sum rate showing improved performance in a wide range of SNRs. The main contribution of this work is the consideration of AF and QF strategies that do not require the knowledge of the codebooks of the mobiles by the relay. Also, through the QF scheme, simpler signal representation is achieved through signal separation at the relay.

The challenge of power minimization is the subject of [28]. The article studies a topology where $2K$ MIMO users communicate in pairs through a MIMO AF relay. The optimization problem is formulated for both ZF and MMSE criteria taking into consideration a power constraint at the relay and predetermined transmit-receive BF vectors which can be obtained from CSI. Also, four BF methods are presented which deal with different CSI conditions; firstly, eigen-BF that requires perfect CSI knowledge at the users in order to produce the eigen-BF vector; secondly, antenna selection that can be performed with partial CSI as only the CSI of the selected antenna is fed back to the relay; thirdly, random BF which does not assume CSI knowledge but needs synchronization information among the users and the relay; finally, equal gain BF that also does not need any CSI and no further information at the relay. Another area that the authors investigate is the power control for ZF systems. Two different cases are studied starting with local power control that distributes the multiuser power to the users according to their channel conditions and then global power control that for the high SNR regime divides network power to the users and the relay with the target of system SNR maximization. All the proposed BF methods are evaluated through simulations illustrating the tradeoff between improved performance and CSI overhead. The main contribution of this paper is the investigation of four different BF methods that can be chosen according to the availability of CSI in the network.

In [52], physical layer network coding is proposed in a topology where one MIMO BS with M antennas communicates with M single-antenna mobile stations through a MIMO relay that also has M antennas. The communication protocol is based on two-way relaying in order to enhance the spectral efficiency of the network. The BF method is based on interference alignment that aims to put the two messages, which are transmitted and received by each user, in the same spatial direction at the relay. In this way, cochannel interference, that is, the major degrading factor in this network, is mitigated. Moreover, the precoding designs for the matrices at the BS and the RS are given in detail, under individual power constraints and the minimization of CCI. Through analytic results, it is proven that the multiplexing gain achieved is equal to the number of the mobile stations while the diversity gain can be increased by employing multiple MIMO relays and by increasing the number of antennas at the BS and RS to be greater than M. Finally, simulations are performed to compare the proposed network coded scheme to time sharing network coding approaches, thus illustrating the improved performance of this scheme. The main contribution of this work is the interference alignment inspired network coding technique and the discussions of multirelay and increased antenna number cases.

Finally, while aiming to optimize the total MSE and sum rate and combat interference, different precoding schemes are applied for enhancing the uplink transmission performance [59]. This work investigates two-way relaying for a topology where a MIMO BS with an ML decoder, communicates with K single-antenna users through a common MIMO AF relay. The objective is to maximize the minimum symbol distance at the BS, that is, to improve the uplink performance. Moreover, three different precoding cases are presented which require varying complexity and a clean relay model that assumes negligible noise at the relay is introduced as well. Firstly, precoding at the BS is considered while the relaying only amplified the received signal under the imposed power constraint. Secondly, precoding at the RS under the aforementioned optimization target is proven to be nonconvex and to obtain a solution the transformation into another optimization problem is given which can be solved through bisection search to acquire the quasioptimal solution. The third precoding design considers joint precoding at the BS and the RS to further improve the system's performance. These precoding methods are compared via simulation and the joint scheme shows the best performance but at the cost of increased complexity in its practical implementation. Through the proposed methods, self-interference and cochannel interference are efficiently mitigated. The authors in [27] extend the study in [59] by considering a similar cellular multiuser two-way relaying topology and aiming to optimize the total MSE and sum rate. Linear precoding designs are given for BS precoding, RS precoding, and joint BS-RS precoding.

5. Discussion and Open Issues

This section provides a discussion based on the works that were presented throughout this survey and, in addition, some

Table 2: Classification of articles based on network topology, the optimization target with the corresponding power constraint, and the relaying topology.

Reference article	Network topology	Optimization target	Power constraint	Relaying topology
[21]	Single-user	MSE, SINR, Capacity	Relay (total), receiver (interference level)	Multirelay
[22]	Single-user	MSE	Relay (sum-power)	Multirelay
[23]	Single-user	MSE	Relay	Single-relay
[24]	Single-user	MSE	Source-relay (separate)	Single-relay
[25]	Single-user	MSE	Source-relay (separate)	Single-relay
[26]	Multiuser	MSE	Source-relay (separate)	Single-relay
[27]	Two-way multipair	MSE	Relay	Single-relay
[28]	Two-way multipair	MSE, SINR	Relay	Single-relay
[29]	Two-way single-pair	MSE	Sources-relay (separate and individual)	Single-relay
[30]	Two-way single-pair	MSE	Sources-relays (separate and individual)	Relay selection
[31]	Two-way single-pair	MSE	Sources-relay (separate and individual)	Single-relay
[32]	Two-way single-pair	MSE	Sources (individual)-relays (sum-power)	Multirelay
[33]	Single-user	SNR	Source-relay (joint)	Multirelay
[61]	Single-user	SNR	Source (individual)-relay (total), relay (joint and individual)	Multirelay
[34]	Single-user	SNR	Source-relay (separate)	Single-relay
[35]	Single-user	SNR	Source-relay individual	Relay selection
[36]	Single-user	SNR	Source-(selected) relay (separate)	Relay selection
[37]	Single-user	SNR	Relay	Relay selection
[38]	Multiuser	SNR	Source-relay (joint)	Single-relay
[39]	Multiuser	SNR	Source-relay (joint)	Single-relay
[40]	Multiuser	SINR	Relay	Single-relay
[41]	Two-way multipair	SINR	Sources-relay (separate and individual)	Single-relay
[42]	Multiuser	SINR	Relay (individual), receiver (interference level)	Multirelay
[43]	Multiuser	SINR	Relay (sum-power)	Multirelay
[44]	Single-user	Capacity	Relay (sum-power)	Multirelay
[45]	Single-user	Capacity	Relay	Single-relay
[46]	Single-user	Capacity	Relay	Relay selection
[47]	Single-user	Capacity	Sources-relays (separate sum-power)	Relay selection
[48]	Multiuser	Capacity	Source-relay (separate)	Single-relay
[49]	Multiuser	Capacity	Source-relay (separate)	Single-relay
[50]	Multiuser	Capacity	Sources-relays (separate sum-power)	Multirelay
[51]	Two-way multipair	Capacity	Relay	Multirelay
[52]	Two-way multipair	Capacity	Relay	Single-relay
[53]	Two-way single-pair	Capacity	Sources-relay (separate and individual)	Single-relay
[54]	Two-way single pair	Capacity	Sources-relay (separate and individual)	Single-relay
[55]	Multiuser	Capacity	Sources (individual)-relays (individual)	Multirelay
[56]	Multiuser	Capacity	Relays (sum-power)	Multirelay
[57]	Multiuser	Capacity	Receiver (interference levels)	Multirelay
[58]	Two-way single-pair	Minimum symbol distance	Sources-relay (separate and individual)	Single-relay
[59]	Two-way multipair	Minimum symbol distance	Sources-relay (separate and individual)	Single-relay

open research topics that are of great interest and have not yet been sufficiently examined by the community. Table 2 depicts the references that were presented in the context of this survey. More specifically, each article is classified based on network topology, the optimization target with the corresponding power constraint, and the relaying topology that was employed. In general, most works investigate beamforming with half-duplex relays to avoid self-interference but the performance of the network is limited by the half-duplex constraint. Single user network has been a very active research field as it is a simple communication paradigm that allows the proposed BF techniques to clearly expose their operation. It is observed that a lot of contributions have been made in the two-way communications, as it is a strategy that improves the spectral efficiency and can provide significant gains, if the interference between the communicating end nodes is efficiently mitigated. On the other hand, as it is also the case with one-way multiuser communications, relay selection has not been considered as an alternative cooperation strategy and this offers a possible research direction towards complexity reduction. From the optimization target's perspective, there are numerous works that aim at MSE minimization, SNR, or SINR increase and capacity improvement. As network-coding algorithms combined with beamforming have recently been developed, there are a few works, which aim at the maximization of the minimum distance of network-coded symbols.

Although the area of BF with MIMO relaying has seen a significant number of contributions, there are many open issues that need to be investigated in the future. An important parameter that has to be taken into consideration is the synchronization among the various network nodes, especially in topologies where multiple relays are employed. More specifically, synchronization based on consensus algorithms [72] and single-hop on-off keying orthogonal signaling technique [73] inspired by sensor networks, distributed solutions such as those proposed in the context of relay selection [10, 74] should be adjusted, so as to satisfy the needs of networks that implement BF.

An overall requirement for the efficient implementation of BF techniques is CSI. As the majority of studies in the field examine schemes where perfect CSI is assumed, there is a lot of research to be done for practical schemes that will be robust when CSI is partially available, or impairments such as delay and channel estimation uncertainties affect its exploitation. Moreover, distributed solutions must be developed that will make use of local CSI knowledge, as is the case in [36], and formulate accordingly the BF matrices based on partial state information. These limited CSI cases could be extended to other network topologies, such as broadcast channels and full-duplex relaying schemes, which are discussed subsequently. The exploitation of CSI is also studied in [75], which addresses the optimization problem for a three-hop wireless network, where collaborative AF relaying terminals appear at both the transmitter and receiver ends to form a virtual MIMO system. This work is a step towards extending previous published results, which considered collaborative-relay beamforming (CRBF) only on one side, giving rise to a dual-hop communications system.

Moreover, recently there has been an increased interest in full-duplex relaying. Novel BF techniques should benefit from the increased spectral efficiency of this relaying scheme. BF algorithms should consider the loop interference among the receive and transmit antennas of the relay and find ways to mitigate it, appropriately forming the precoding matrix at the source and the BF matrix at the relay. Further schemes based on half-duplex relays but aiming at recovering the half-duplex loss are two-way and successive relaying. In networks where two-way relaying is applied to improve spectral efficiency, network coding approaches have started to receive significant contributions [52, 54, 58], but there is enough space for additional work in this area. For successive relaying topologies, only [71] has proposed BF techniques and there is increased interest in this field for further research as the half-duplex loss can be recovered. Successive relaying networks perform concurrent transmissions by the source and one transmitting relay. As a result, interrelay interference arises and the BF matrix at the relay could be structured in such a way to minimize IRI, while achieving the performance target at the RD link. Likewise, the source precoding matrix should aim at increasing the SINR at the receiving relay, thus offering increased protection to the IRI from the transmitting relay.

Another field that has not been sufficiently researched until now is the BF designs for cognitive relay networks, where only few works have considered such topologies. In [76], various relay BF algorithms are proposed in a network where primary and secondary users coexist. BF aims at interference minimization to the primary users and rate maximization for the secondary users through iterative algorithms. Also in [77], the authors propose cognitive MIMO relay selection to maximize the capacity of the secondary user and by employing BF the interference to the primary user is minimized. As the exploitation of spatial resources is at the heart of BF, an adaptation of such a technique for networks consisting of primary and secondary users would provide additional gains in spectral efficiency. Moreover, a combination of game theory and BF matrix formulation in order to achieve a target spectral efficiency while keeping the interference of the secondary users towards the primary users at low levels is an interesting research approach.

Since BF aims at the minimization of undesired receptions in order to minimize interference, it can offer improved security at the physical layer. A limited number of works have proposed algorithms in this field. In [78], a topology where an untrusted AF MIMO relay that may try to decode the source's messages is studied. Two alternative solutions are developed; first, the relay is treated as an eavesdropper and does not assist the source-destination communication, while, in the second, BF matrices at the source and the relay are jointly designed in order to increase the secrecy rate. Moreover, in [79], a two-way relay network in the presence of an eavesdropper is studied and, through various BF schemes, the leakages are avoided and the secrecy sum rate of the two sources is increased.

Finally, regarding the formulation of precoding and BF matrices, other metrics, such as power consumption, should be considered. This is especially important, as relays

may be battery-operated and the BF matrices they will use must achieve increased energy efficiency. The article in [80] presents a cluster of distributed relays, which form a virtual multiple-input-single-output (MISO) system. The optimal number of relays that should participate in the communication in order to satisfy an outage threshold, in terms of energy efficiency, is investigated. Results indicate that cooperative BF outperforms direct communication in energy and spectral efficiency.

6. Conclusions

In this paper, various works in the field of beamforming with multiple-input multiple-output relays have been elaborated, as they constitute an utmost promising technique for reducing interference levels and enhancing system capacity of next generation mobile broadband systems. Moreover, aiming to outline the importance of BF for MIMO relay networks while providing an overall perspective on the area, this survey includes papers that constitute the state of the art in this field. In order to facilitate the design and optimization of BF algorithms, various challenges that should be explicitly considered were presented. More specifically, important design parameters, such as the performance criteria and the power constraints, were presented and classified. Also, a literature review regarding issues such as computational complexity, and channel state information acquisition and feedback as well as antenna correlation was provided. Furthermore, the articles included in the survey were categorized based on their network topology. Firstly, articles on single-user communications were discussed and were further categorized for cases of single and multiple relaying as well as relay selection. In continuity, multiuser topologies that studied the relay broadcast channel and two-way communications were presented.

Recent research on BF MIMO relays has made significant steps, but unfortunately more research and development work is necessary towards channel impairments, synchronization, and cognitive aspects. To this end, this paper highlighted significant benefits regarding the formulation of precoding and BF matrices, interference mitigation techniques, and relay selection methods. Finally, a discussion was given on the paper's findings and on the open issues, which constitute interesting research directions in the field of BF with MIMO relays.

Conflict of Interests

The author declares that there is no conflict of interests regarding the publication of this paper.

References

[1] E. Telatar, "Capacity of multi-antenna Gaussian channels," *European Transactions on Telecommunications*, vol. 10, no. 6, pp. 585–595, 1999.

[2] A. Goldsmith, S. A. Jafar, N. Jindal, and S. Vishwanath, "Capacity limits of MIMO channels," *IEEE Journal on Selected Areas in Communications*, vol. 21, no. 5, pp. 684–702, 2003.

[3] D. Gesbert, M. Kountouris, R. W. Heath Jr., C.-B. Chae, and T. Sälzer, "Shifting the MIMO paradigm," *IEEE Signal Processing Magazine*, vol. 24, no. 5, pp. 36–46, 2007.

[4] D. Gesbert, S. Hanly, H. Huang, S. Shamai Shitz, O. Simeone, and W. Yu, "Multi-cell MIMO cooperative networks: a new look at interference," *IEEE Journal on Selected Areas in Communications*, vol. 28, no. 9, pp. 1380–1408, 2010.

[5] T. M. Cover and A. A. E. Gamal, "Capacity theorems for the relay channel," *IEEE Transactions on Information Theory*, vol. 25, no. 5, pp. 572–584, 1979.

[6] J. N. Laneman, D. N. C. Tse, and G. W. Wornell, "Cooperative diversity in wireless networks: efficient protocols and outage behavior," *IEEE Transactions on Information Theory*, vol. 50, no. 12, pp. 3062–3080, 2004.

[7] L. Sanguinetti, A. A. D. 'Amico, and R. Yue, "A tutorial on the optimization of amplify-and-forward MIMO relay systems," *IEEE Journal on Selected Areas in Communications*, vol. 30, no. 8, pp. 1331–1346, 2012.

[8] C. La Palombara, V. Tralli, B. M. Masini, and A. Conti, "Relay-assisted diversity communications," *IEEE Transactions on Vehicular Technology*, vol. 62, no. 1, pp. 415–421, 2013.

[9] A. Bletsas, H. Shin, and M. Z. Win, "Cooperative communications with outage-optimal opportunistic relaying," *IEEE Transactions on Wireless Communications*, vol. 6, no. 9, pp. 3450–3460, 2007.

[10] A. Bletsas, A. Khisti, D. P. Reed, and A. Lippman, "A simple cooperative diversity method based on network path selection," *IEEE Journal on Selected Areas in Communications*, vol. 24, no. 3, pp. 659–672, 2006.

[11] A. Ikhlef, D. S. Michalopoulos, and R. Schober, "Max-max relay selection for relays with buffers," *IEEE Transactions on Wireless Communications*, vol. 11, no. 3, pp. 1124–1135, 2012.

[12] N. Nomikos, D. Vouyioukas, T. Charalambous, I. Krikidis, D. N. Skoutas, and M. Johansson, "Capacity improvement through buffer-aided successive opportunistic relaying," in *Proceedings of the IEEE Wireless Vitae Conference*, June 2013.

[13] N. Nomikos, T. Charalambous, I. Krikidis, D. N. Skoutas, D. Vouyioukas, and M. Johansson, "Buffer-aided successive opportunistic relaying with inter-relay interference cancellation," in *Proceedings of the IEEE International Symposium on Personal Indoor and Mobile Radio Communication*, September 2013.

[14] P. Balaban and J. Salz, "Dual diversity combining and equalization in digital cellular mobile radio," *IEEE Transactions on Vehicular Technology*, vol. 40, no. 2, pp. 342–354, 1991.

[15] F. Rashid-Farrokhi, K. J. R. Liu, and L. Tassiulas, "Transmit beamforming and power control for cellular wireless systems," *IEEE Journal on Selected Areas in Communications*, vol. 16, no. 8, pp. 1437–1450, 1998.

[16] S. Bellofiore, C. A. Balanis, J. Foutz, and A. S. Spanias, "Smart-antenna systems for mobile communication networks. Part 1: overview and antenna design," *IEEE Antennas and Propagation Magazine*, vol. 44, no. 3, pp. 145–154, 2002.

[17] S. Bellofiore, J. Foutz, C. A. Balanis, and A. S. Spanias, "Smart-antenna system for mobile communication networks Part 2: beamforming and network throughput," *IEEE Antennas and Propagation Magazine*, vol. 44, no. 4, pp. 106–114, 2002.

[18] S. Berger, M. Kuhn, A. Wittneben, T. Unger, and A. Klein, "Recent advances in amplify-and-forward two-hop relaying," *IEEE Communications Magazine*, vol. 47, no. 7, pp. 50–56, 2009.

[19] Y. Hua, "An overview of beamforming and power allocation for MIMO relays," in *Proceedings of the IEEE Military Communications Conference*, pp. 375–380, October 2010.

[20] D. P. Palomar, J. M. Cioffi, and M. A. Lagunas, "Joint Tx-Rx beamforming design for multicarrier MIMO channels: a unified framework for convex optimization," *IEEE Transactions on Signal Processing*, vol. 51, no. 9, pp. 2381–2401, 2003.

[21] A. S. Behbahani, R. Merched, and A. M. Eltawil, "Optimizations of a MIMO relay network," *IEEE Transactions on Signal Processing*, vol. 56, no. 10, pp. 5062–5073, 2008.

[22] P. Wu and R. Schober, "Cooperative beamforming for single-carrier frequency-domain equalization systems with multiple relays," *IEEE Transactions on Wireless Communications*, vol. 11, no. 6, pp. 2276–2286, 2012.

[23] Y. Rong and F. Gao, "Optimal beamforming for non-regenerative MIMO relays with direct link," *IEEE Communications Letters*, vol. 13, no. 12, pp. 926–928, 2009.

[24] F.-S. Tseng, M.-Y. Chang, and W.-R. Wu, "Joint MMSE transceiver design in amplify-and-forward mimo relay systems with tomlinson-harashima source precoding," in *Proceedings of the IEEE 21st International Symposium on Personal Indoor and Mobile Radio Communications*, pp. 443–448, September 2010.

[25] Y. Rong, "Optimal joint source and relay beamforming for MIMO relays with direct link," *IEEE Communications Letters*, vol. 14, no. 5, pp. 390–392, 2010.

[26] C. Xing, S. Ma, M. Xia, and Y. C. Wu, "Cooperative beamforming for dual-hop amplify-and-forward multi-antenna relaying cellular networks," *Elsevier Signal Processing*, vol. 92, no. 11, pp. 2689–2699, 2012.

[27] R. Wang, M. Tao, and Y. Huang, "Linear precoding designs for amplify-and-forward multiuser two-way relay systems," *IEEE Transactions on Wireless Communications*, vol. 11, no. 12, pp. 4457–4469, 2012.

[28] J. Joung and A. H. Sayed, "Multiuser two-way amplify-and-forward relay processing and power control methods for beamforming systems," *IEEE Transactions on Signal Processing*, vol. 58, no. 3, pp. 1833–1846, 2010.

[29] Y. Rong, "Joint source and relay optimization for two-way MIMO multi-relay networks," *IEEE Communications Letters*, vol. 15, no. 12, pp. 1329–1331, 2011.

[30] C. Chen, L. Bai, B. Wu, and J. Choi, "Relay selection and beamforming for cooperative bi-directional transmissions with physical layer network coding," *IET Communications*, vol. 5, no. 14, pp. 2059–2067, 2011.

[31] Z. B. Wang, L. J. Xiang, L. H. Zheng, and H. Ding, "MSMSE-based optimal beamforming design and simplification on AF MIMO two-way relay channels," *Springer Journal of Central Southern University*, vol. 19, pp. 465–470, 2012.

[32] Z. Hui, Y. Longxiang, and Z. Hongbo, "Precoding and decoding design for two-way MIMO AF multiple-relay system," *Journal of Electronics*, vol. 29, no. 3, pp. 177–189, 2012.

[33] Y.-W. Liang and R. Schober, "Cooperative amplify-and-forward beamforming with multi-antenna source and relays," in *Proceedings of the 3rd IEEE International Workshop on Computational Advances in Multi-Sensor Adaptive Processing*, pp. 277–280, December 2009.

[34] B. Khoshnevis, W. Yu, and R. Adve, "Grassmannian beamforming for MIMO amplify-and-forward relaying," *IEEE Journal on Selected Areas in Communications*, vol. 26, no. 8, pp. 1397–1407, 2008.

[35] Y. Zhao, R. Adve, and T. J. Lim, "Beamforming with limited feedback in amplify-and-forward cooperative networks—[transactions letters]," *IEEE Transactions on Wireless Communications*, vol. 7, no. 12, pp. 5145–5149, 2008.

[36] B. K. Chalise, L. Vandendorpe, Y. D. Zhang, and M. G. Amin, "Local CSI based selection beamforming for amplify-and-forward MIMO relay networks," *IEEE Transactions on Signal Processing*, vol. 60, no. 5, pp. 2433–2446, 2012.

[37] R. H. Y. Louie, Y. Li, H. A. Suraweera, and B. Vucetic, "Performance analysis of beamforming in two hop amplify and forward relay networks with antenna correlation," *IEEE Transactions on Wireless Communications*, vol. 8, no. 6, pp. 3132–3141, 2009.

[38] Z. Zhou and B. Vucetic, "An optimized cooperative beamforming scheme in MIMO relay broadcast channels," in *Proceedings of the IEEE Global Telecommunications Conference*, pp. 1–6, December 2009.

[39] Z. Zhou and B. Vucetic, "A cooperative beamforming scheme in mimo relay broadcast channels," *IEEE Transactions on Wireless Communications*, vol. 10, no. 3, pp. 940–947, 2011.

[40] B. Zhang, Z. He, K. Niu, and L. Zhang, "Robust linear beamforming for MIMO relay broadcast channel with limited feedback," *IEEE Signal Processing Letters*, vol. 17, no. 2, pp. 209–212, 2010.

[41] E. Yilmaz, R. Zakhour, D. Gesbert, and R. Knopp, "Multi-pair two-way relay channel with multiple antenna relay station," in *Proceedings of the IEEE International Conference on Communications*, pp. 1–5, May 2010.

[42] A. El-Keyi and B. Champagne, "Adaptive linearly constrained minimum variance beamforming for multiuser cooperative relaying using the kalman filter," *IEEE Transactions on Wireless Communications*, vol. 9, no. 2, pp. 641–651, 2010.

[43] Y. Liu and A. P. Petropulu, "Cooperative beamforming in multi-source multi-destination relay systems with SINR constraints," in *Proceedings of the IEEE International Conference on Acoustics, Speech, and Signal Processing*, pp. 2870–2873, March 2010.

[44] Y. Fan and J. Thompson, "MIMO configurations for relay channels: theory and practice," *IEEE Transactions on Wireless Communications*, vol. 6, no. 5, pp. 1774–1786, 2007.

[45] X. Tang and Y. Hua, "Optimal design of non-regenerative MIMO wireless relays," *IEEE Transactions on Wireless Communications*, vol. 6, no. 4, pp. 1398–1407, 2007.

[46] E. Baccarelli, M. Biagi, C. Pelizzoni, and N. Cordeschi, "Maximum-rate node selection for power-limited multiantenna relay backbones," *IEEE Transactions on Mobile Computing*, vol. 8, no. 6, pp. 807–820, 2009.

[47] M. A. Torabi and J.-F. Frigon, "Semi-orthogonal relay selection and beamforming for amplify-and-forward MIMO relay channels," in *Proceedings of the IEEE Wireless Communications and Networking Conference*, pp. 48–53, April 2008.

[48] G. Okeke, W. A. Krzymien, and Y. Jing, "Beamforming in non-regenerative MIMO broadcast relay networks," *IEEE Transactions on Signal Processing*, vol. 60, no. 12, pp. 6641–6654, 2012.

[49] H. Wan, W. Chen, and X. Wang, "Joint source and relay design for MIMO relaying broadcast channels," *IEEE Communications Letters*, vol. 17, no. 2, pp. 345–348, 2013.

[50] K. T. Truong and R. W. Heath, "Joint transmit precoding for the relay interference broadcast channel," *IEEE Transactions on Vehicular Technology*, vol. 62, no. 3, pp. 1201–1215, 2013.

[51] K. Lee, S.-H. Park, J.-S. Kim, and I. Lee, "Degrees of freedom on mimo multi-link two-way relay channels," in *Proceedings of the 53rd IEEE Global Communications Conference*, pp. 1–5, December 2010.

[52] Z. Ding, I. Krikidis, J. Thompson, and K. K. Leung, "Physical layer network coding and precoding for the two-way relay channel in cellular systems," *IEEE Transactions on Signal Processing*, vol. 59, no. 2, pp. 696–712, 2011.

[53] N. Lee, C.-B. Chae, O. Simeone, and J. Kang, "On the optimization of two-way AF MIMO relay channel with beamforming," in *Proceedings of the 44th Asilomar Conference on Signals, Systems and Computers*, pp. 918–922, November 2010.

[54] R. Zhang, Y.-C. Liang, C. C. Chai, and S. Cui, "Optimal beamforming for two-way multi-antenna relay channel with analogue network coding," *IEEE Journal on Selected Areas in Communications*, vol. 27, no. 5, pp. 699–712, 2009.

[55] S. Mohajer, S. N. Diggavi, and D. N. C. Tse, "Approximate capacity of a class of gaussian relay-interference networks," in *Proceedings of the IEEE International Symposium on Information Theory*, pp. 31–35, July 2009.

[56] Y. Shi, J. Zhang, and K. B. Letaief, "Coordinated relay beamforming for amplify-and-forward two-hop interference networks," in *Proceedings of the IEEE Global Communications Conference*, pp. 2408–2413, December 2012.

[57] K. T. Truong and R. W. Heath Jr., "Relay beamforming using interference pricing for the two-hop interference channel," in *Proceedings of the 54th Annual IEEE Global Telecommunications Conference*, pp. 1–5, December 2011.

[58] T. M. Kim, B. Bandemer, and A. Paulraj, "Beamforming for network-coded MIMO two-way relaying," in *Proceedings of the 44th Asilomar Conference on Signals, Systems and Computers*, pp. 647–652, November 2010.

[59] G. Ye and R. Wang, "Transceiver designs for multiuser two-way relay system," in *Proceedings of the International Workshop on Information and Electronics Engineering*, pp. 4186–4191, March 2012.

[60] S. Borade, L. Zheng, and R. Gallager, "Amplify-and-forward in wireless relay networks: rate, diversity, and network size," *IEEE Transactions on Information Theory*, vol. 53, no. 10, pp. 3302–3318, 2007.

[61] Y.-W. Liang and R. Schober, "Cooperative amplify-and-forward beamforming with multiple multi-antenna relays," *IEEE Transactions on Communications*, vol. 59, no. 9, pp. 2605–2615, 2011.

[62] Z. Bai, Y. Xu, D. Yuan, and K. Kwak, "Performance analysis of cooperative MIMO system with relay selection and power allocation," in *Proceedings of the IEEE International Conference on Communications*, pp. 1–5, May 2010.

[63] C.-K. Wen, K.-K. Wong, and J.-C. Chen, "Precoding design in MIMO multiple-access cellular relay systems with partial CSI," in *Proceedings of the IEEE Wireless Communications and Networking Conference*, pp. 1–6, April 2010.

[64] F. Gao, T. Cuiy, B. Jiangz, and X. Gaoz, "On communication protocol and beamforming design for amplify-and-forward N-Way relay networks," in *Proceedings of the 3rd IEEE International Workshop on Computational Advances in Multi-Sensor Adaptive Processing*, pp. 109–112, December 2009.

[65] B. Xie, D. Munoz, and H. Minn, "A reduced overhead OFDM relay system with clusterwise TMRC beamforming," *IEEE Communications Letters*, vol. 16, no. 12, pp. 1913–1916, 2012.

[66] S. W. Peters and R. W. Heath, "Nonregenerative MIMO relaying with optimal transmit antenna selection," *IEEE Signal Processing Letters*, vol. 15, pp. 421–424, 2008.

[67] H.-N. Cho, J.-W. Lee, A.-Y. Kim, and Y.-H. Lee, "Cooperative interference mitigation with partial CSI in multi-user dual-hop MISO relay channels," in *Proceedings of the 20th IEEE Personal, Indoor and Mobile Radio Communications Symposium*, pp. 1211–1215, September 2009.

[68] H. A. Suraweera, H. K. Garg, and A. Nallanathan, "Beamforming in dual-hop fixed gain relay systems with antenna correlation," in *Proceedings of the IEEE International Conference on Communications*, pp. 1–5, May 2010.

[69] N. S. Ferdinand and N. Rajatheva, "Unified performance analysis of two-hop amplify-and-forward relay systems with antenna correlation," *IEEE Transactions on Wireless Communications*, vol. 10, no. 9, pp. 3002–3011, 2011.

[70] T. Riihonen, A. Balakrishnan, K. Haneda, S. Wyne, S. Werner, and R. Wichman, "Optimal eigenbeamforming for suppressing self-interference in full-duplex MIMO relays," in *Proceedings of the 45th Annual Conference on Information Sciences and Systems*, pp. 1–6, March 2011.

[71] S. M. Kim and M. Bengtsson, "Virtual full-duplex buffer-aided relaying—relay selection and beamforming," in *Proceedings of the IEEE International Symposium on Personal Indoor and Mobile Radio Communication*, September 2013.

[72] M. K. Maggs, S. G. O'Keefe, and D. V. Thiel, "Consensus clock synchronization for wireless sensor networks," *IEEE Sensors Journal*, vol. 12, no. 6, pp. 2269–2277, 2012.

[73] A. G. Kanatas, A. Kalis, and G. P. Efthymoglou, "A single hop architecture exploiting cooperative beamforming for wireless sensor networks," *Physical Communication*, vol. 4, no. 3, pp. 237–243, 2011.

[74] N. Nomikos, P. Makris, D. Vouyioukas, D. N. Skoutas, and C. Skianis, "Distributed joint relay-pair selection for buffer-aided successive opportunistic relaying," in *Proceedings of the IEEE International Workshop on Computer- Aided Modeling Analysis of Design of Communication Links and Networks*, September 2013.

[75] L. Chen, K.-K. Wong, H. Chen, J. Liu, and G. Zheng, "Optimizing transmitter-receiver collaborative-relay beamforming with perfect CSI," *IEEE Communications Letters*, vol. 15, no. 3, pp. 314–316, 2011.

[76] T. Luan, F. Gao, X. D. Zhang, J. C. F. Li, and M. Lei, "Rate maximization and beamforming design for relay-aided multiuser cognitive networks," *IEEE Transactions on Vehicular Technology*, vol. 61, no. 4, pp. 1940–1945, 2012.

[77] Q. Li, Q. Zhang, R. Feng, L. Luo, and J. Qin, "Optimal relay selection and beamforming in MIMO cognitive multi-relay networks," *IEEE Communications Letters*, vol. 17, no. 6, pp. 1188–1191, 2013.

[78] C. Jeong, I.-M. Kim, and D. I. Kim, "Joint secure beamforming design at the source and the relay for an amplify-and-forward MIMO untrusted relay system," *IEEE Transactions on Signal Processing*, vol. 60, no. 1, pp. 310–325, 2012.

[79] H. M. Wang, Y. Qinye, and X. G. Xia, "Distributed beamforming for physical-layer security of two-way relay networks," *IEEE Transactions on Signal Processing*, vol. 60, no. 7, pp. 3532–3545, 2012.

[80] G. Lim and L. J. Cimini, "Energy-efficient cooperative beamforming in clustered wireless networks," *IEEE Transactions on Wireless Communications*, vol. 12, no. 3, pp. 1376–1385, 2013.

Hindawi Publishing Corporation
International Journal of Antennas and Propagation
Volume 2013, Article ID 746831, 8 pages
http://dx.doi.org/10.1155/2013/746831

Research Article

The Effective Radiation Pattern Concept for Realistic Performance Estimation of LTE Wireless Systems

Dimitra Zarbouti,[1] George Tsoulos,[1] Georgia Athanasiadou,[1] and Constantinos Valagiannopoulos[2]

[1] *Department of Informatics and Telecommunications, University of Peloponnese, 22100 Tripoli, Greece*
[2] *School of Electrical Engineering, Aalto University, FI-00076 Helsinki, Finland*

Correspondence should be addressed to Dimitra Zarbouti; dzarb@uop.gr

Received 24 July 2013; Revised 24 September 2013; Accepted 26 September 2013

Academic Editor: Athanasios Kanatas

Radio channels induce distortions to the radiation pattern of beamforming systems such as beam broadening as well as sidelobe level and null rising. If these effects are ignored, the system performance is overestimated. This paper proposes the simple concept of an effective radiation pattern (ERP) calculated by optimally fitting the "real-world" radiation pattern to the ERP. The proposed ERP method is incorporated into a multicell bad urban 4G LTE operational scenario which employs beamforming for both the BSs and the RNs. The performed simulations provide evidence that the ideal instead of the real radiation pattern overestimates the SIR and capacity by almost 3 dB and 13 Mbps, respectively, for the reference scenario without RNs. It also proves that the ERP method produces almost identical performance results with the real radiation pattern, and hence it is a simple and viable option for realistic performance analysis. Finally, the network performance is studied as a function of the number of RNs with the help of the ERP method. Results show that a beamforming LTE network with RNs that also employ beamforming provides 3 dB SIR gain with the addition of 1 RN per cell and 15 dB gain with 4 RNs per cell.

1. Introduction

Beamforming and relays are two key techniques used by broadband wireless systems such as the 4th generation LTE wireless system, in order to help them confront interference, multipath, and poor signal strength that limit capacity and hence deliver the promised high data rates to users. Relays are used to extend coverage, fill in dead spots, and increase capacity for cell-edge users and wireless backhauling. Beamforming leverages the spatial dimension resulting from multiple antenna elements by focusing directional beams towards the desired users and reducing interference to and from unwanted users. The combination of beamforming with base station and relay nodes has been studied extensively in the literature and the benefits have been highlighted in several publications [1–4].

Nevertheless, the majority of the performed analyses for beamforming systems ignores or underestimates the significant effects on the produced "real" radiation patterns, from parameters such as multipath propagation, mutual coupling among the array elements, or other implementation mismatches (calibration, power amplifier linearity, etc.). However, it is known that in several cases (e.g., [5–9]), these effects dominate the radiation pattern characteristics, since they can broaden the main lobe, bring up the sidelobe level, and fill up the nulls. As a result, when these effects are overlooked, the estimated system performance is overoptimistic.

There are several techniques discussed in the open literature that avoid both the mutual coupling effects and the different implementation mismatches (see [10–14]), alas at some increased complexity and cost. On the other hand, it is more difficult to take into account the effects of the radio channel on the real radiation pattern, due to its volatility. This paper focuses on this issue and proposes the simple concept of the effective radiation pattern (ERP), in order to simplify the analysis and yet produce realistic performance estimations. The real radiation pattern, that is, the produced radiation pattern after the effect of the radio channel is taken

into account, is approximated by a simple step function with parameters the *effective* main lobe beamwidth (BW) and the *effective average* sidelobe level (SLL), (i.e., by a "flat-topped" beam pattern). The word *effective* is used here to reflect the modified beamwidth and average sidelobe level of an ideal radiation pattern, if multipath is taken into consideration, both calculated via a cost function minimization that best fits the ERP with the real radiation pattern. It must be mentioned here that the ERP concept generally assumes beamforming capability in a real environment, that is, an appropriate array geometry, the necessary number of antenna array elements, and adaptive algorithms that produce radiation patterns with the desired characteristics in terms of beamwidth and average sidelobe level.

Based on the ERP concept, [15] provides a closed form expression for the SIR cumulative distribution function (CDF) of a multitier OFDMA cellular network. That work is extended in this paper in order to prove that wireless system performance is overestimated when the effects of the radio channel to the radiation pattern of beamforming systems are ignored, while the use of the simple ERP concept can resolve this issue. For this reason, comparative simulations between systems employing ideal, real, and ERP radiation patterns are provided in this work. Hence, in the following analysis, the proposed ERP method is incorporated into a multicell, multicarrier beamforming 4G LTE system which employs Relay Nodes (RNs), in order to demonstrate the system level effects (SIR, capacity) from the radio channel, as well as the validity of the proposed method.

The paper is organised as follows: Section 2 provides the analysis on the ERP, Section 3 presents the deployment configuration of the network considered in our study, Section 4 outlines the simulations performed along with the results of our work, and finally Section 5 concludes the paper.

2. Effective Radiation Pattern Concept

According to [6], the measured azimuth (φ) radiation pattern ($G_{\text{real}}(\varphi)$) results from spreading the ideal antenna pattern ($G_{\text{ideal}}(\varphi)$) over the environment power azimuth pattern ($A(\varphi)$). In other words, the real radiation pattern is determined by the convolution of the ideal radiation pattern with the environment power azimuth pattern:

$$G_{\text{real}}(\varphi_0) = \oint_{\varphi} G_{\text{ideal}}(\varphi) \cdot A(\varphi - \varphi_0)\, d\varphi. \tag{1}$$

In [16], it was shown that the best way to model the power azimuth spectrum (PAS) around the base station for both urban and rural environments is the Laplacian distribution [17]. Replacing the power azimuth pattern in (1) with a Laplacian distribution leads to

$$G_{\text{real}}(\varphi_0) = \frac{1}{\sqrt{2}\sigma} \oint_{\varphi} G_{\text{ideal}} \cdot e^{-\sqrt{2}|\varphi-\varphi_0|/\sigma} d\varphi, \tag{2}$$

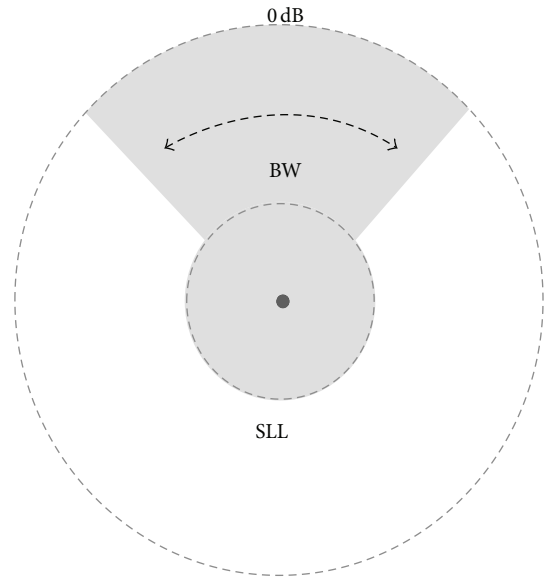

Figure 1: Graphical representation of the ERP.

where σ is the angular spread (AS). Let us assume now the array factor of an ideal N element linear antenna array with an element distance of $\lambda/2$ and bore-sight radiation:

$$G_{\text{ideal}}(\varphi) = \left| \frac{\sin\left((N/2)\,\pi\cos\varphi\right)}{(N/2)\,\pi\cos\varphi} \right|. \tag{3}$$

The impact of the environment azimuth power profile on $G_{\text{ideal}}(\varphi)$ can be calculated using (1)–(3) as follows:

$$G_{\text{real}}(\varphi_0) = \frac{1}{\sqrt{2}\sigma} \int_0^{\pi} \left| \frac{\sin\left((N/2)\,\pi\cos\varphi\right)}{(N/2)\,\pi\cos\varphi} \right| \cdot e^{-\sqrt{2}|\varphi-\varphi_0|/\sigma} d\varphi. \tag{4}$$

Note that when $\varphi \in (-\pi, \pi)$, the ideal antenna array is symmetrical. Hence, without loss of generality, for the analysis in this section, we consider only the "upper part" of the antenna array pattern; that is, $\varphi \in [0, \pi)$.

Our goal is to model the G_{real} diagram with an ERP given by a simple step function with parameters the effective beamwidth (BW) and sidelobe level (SLL):

$$G_{\text{ERP}}(\varphi) = \begin{cases} 1, & \varphi \in \left[\varphi_m - \dfrac{\text{BW}}{2}, \varphi_m + \dfrac{\text{BW}}{2}\right], \\ 10^{-\text{SLL}/10}, & \varphi \in \left[0, \varphi_m - \dfrac{\text{BW}}{2}\right) \cup \left(\varphi_m + \dfrac{\text{BW}}{2}, \pi\right), \end{cases} \tag{5}$$

where φ_m is the pointing angle of the main lobe. A graphic representation of the ERP is depicted in Figure 1.

In order to provide the best fit between G_{real} and G_{ERP} the BW and SLL parameters must be defined in a way that the cost function given in (6) is minimized. Consider

$$\left\{\text{BW}_{\text{opt}}, \text{SLL}_{\text{opt}}\right\} = \underset{\text{BW}\in(0,\pi),\text{SLL}\in(a,0)}{\text{argmin}} \int_0^{\pi} \left|G_{\text{ERP}}(\varphi) - G_{\text{real}}(\varphi)\right| d\varphi. \quad (6)$$

In (6), a is the minimum value of the side lobe level that is used to define the search area for the effective SLL (SLL_{opt}). The limiting case for the minimum value of side lobe level is when the angular spread is very low (almost zero) and the number of array elements is very large. As an example, when the angular spread is zero and the number of linear array elements is 750, the corresponding effective sidelobe level (SLL_{opt}) for the ERP is −30.5 dB. As a result, a value close to $a = -30$ dB can be chosen in order to cover all practical scenarios of cellular antenna systems, as well as cases for very large antenna arrays systems.

In order to demonstrate the validity of the proposed method we focus on the outdoor macro and RN operational environments and channel models in the context of a 4G LTE wireless system. Nevertheless, it must be mentioned here that the ERP method is valid for any channel model and system. Following the conclusions derived in [18], the Angular Spread (AS) at the BS of a bad urban macrocell is 17°, typically, while the AS for a bad urban microcell RN is 33°, typically. Therefore, we employ in the Laplacian distribution these values for the AS of the two network nodes and perform the analysis of (1)–(6) in order to find the appropriate BW_{opt} and SLL_{opt} that will help us model the real radiation patterns with $N = 8$ antenna elements.

Figures 2 and 3 show the ideal (3), the real (4), and the ERP (5) for $N = 8$ and AS = 17°/33°. The ERP parameters (e.g., $\text{BW}_{\text{opt}} = 31°$, $\text{SLL}_{\text{opt}} = 8.5$ dB for Figure 2) were calculated with (6). Note that since the focus of our analysis is on the effects of the propagation environment to the ideal radiation pattern and its modeling with an ERP, a fixed value of −20 dB is considered outside the azimuth area of interest for all the radiation patterns (important for the following system performance analysis). It can be seen from these figures that the environment induces considerable distortion on the ideal antenna diagram. Firstly, the nulls of the original radiation pattern (blue dotted line) are filled up (black solid line), raising the energy allocated to side lobes and hence the interference to/from unwanted users. Secondly, the main beam is broadened, for example, the original 12°3 dB beamwidth almost doubled for the case shown in Figure 2. Both these observations provide an insight into why the effective radiation pattern resulted in the BW_{opt} and SLL_{opt} values shown in Figures 2 and 3.

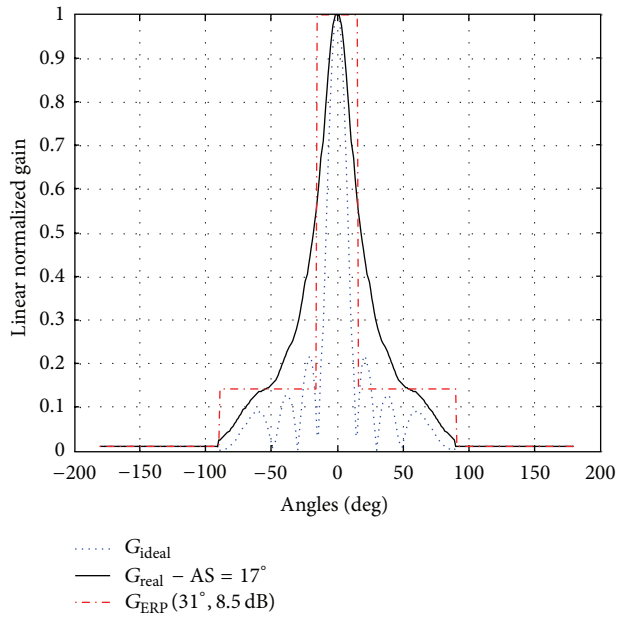

Figure 2: The radiation patterns produced by an $N = 8$ element linear array antenna when ideal and real propagation conditions (AS = 17°) are considered, along with the corresponding ERP.

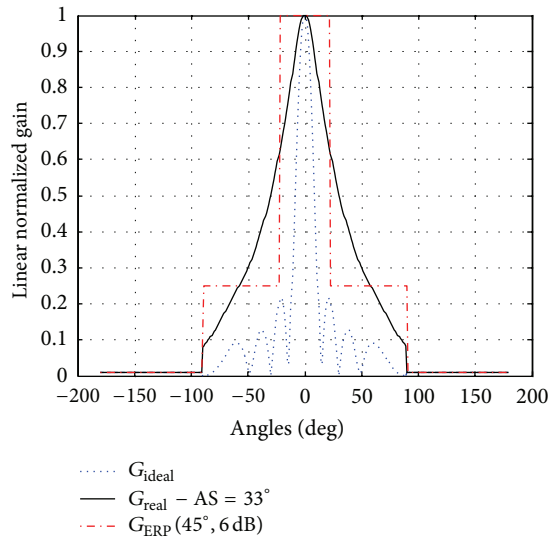

Figure 3: The radiation patterns produced by an $N = 8$ element linear array antenna when ideal and real propagation conditions (AS = 33°) are considered, along with the corresponding ERP.

3. Network Configuration

In the following analysis, we incorporate the ERP concept into the downlink of a multicell, multicarrier beamforming 4 G LTE system which employs RNs, in order to demonstrate the system level effects (SIR, capacity) from the channel AS and the validity of the proposed method. Users are uniformly distributed in the network area and their serving node (SN) is either a BS or an RN, according to the channel gain between the user and the respective network node. The same numbers of RNs per cell are considered with fixed predefined locations (an acceptable assumption due to the uniform user distribution; otherwise, in a real network deployment, the RN locations should be optimized according to the user distribution).

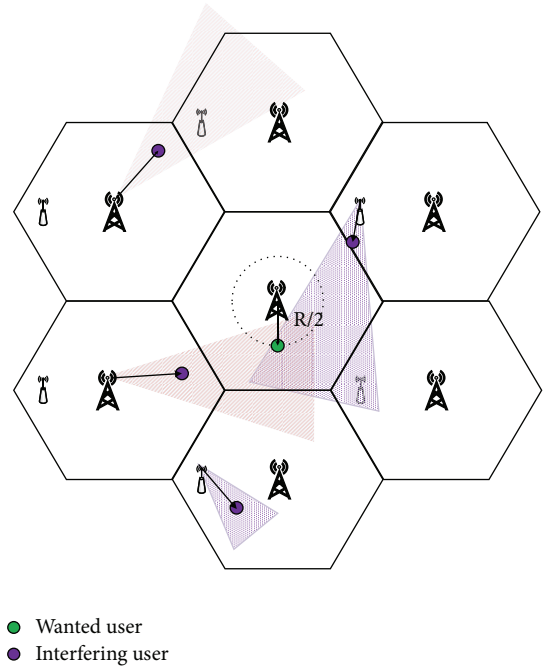

Figure 4: Layout of the downlink 4G LTE beamforming system (user snapshot).

The network nodes employ appropriate adaptive algorithms to perform optimum beam steering towards a user, if they are the SNs. A snapshot of the network layout is depicted in Figure 4 for a network configuration with 1 RN per BS (configurations with up to 4 RNs per BS are studied in the following).

The wanted user (u_w) is located in the central cell and at a distance $R/2$ from his server (R is the cell radius). The interference that the wanted user experiences (on each radio channel) depends on the number of downlink cochannel users and on the interfering node radiation pattern steering angle. As Figure 4 suggests, the u_w can either be in or out of the main lobe of an interfering node antenna, receiving higher/lower interference, respectively. A fully loaded network is considered, where each radio channel is reused in every BS (reuse factor 1). Under the fully loaded scenario, the u_w receives six interfering signals from the six interfering nodes (fixed BS or RN positions), and hence the amount of total interference depends only on the radiation patterns.

4. Simulations

The network configuration described above is analyzed via Monte Carlo simulations (10^4 iterations) in order to produce the empirical cumulative distribution function (ECDF) of the wanted user SIR and his achieved data rate.

4.1. Simulation Description. A simulation flow chart for each Monte Carlo iteration is given in Figure 5, while the simulation parameters are shown in Table 1.

Each simulation run starts with the arrival of a new user, u. The new user's location is randomly selected in the network

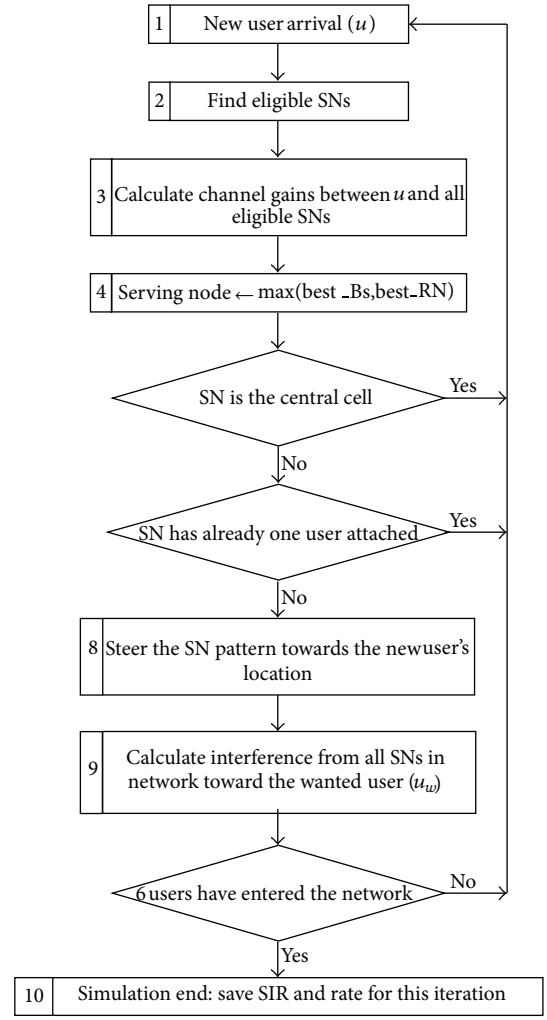

Figure 5: Simulation flow chart for each Monte Carlo iteration.

area and the list of eligible serving nodes is decided. More specifically, all the network BSs along with the RNs in line of sight (LOS) with the new user are considered in this list. For the purposes of this work, the LOS distance is set at 150 m; that is, the new user's eligible list of SNs includes all the BSs and the network RNs that are less than 150 m away from the new user. This way we avoid unrealistic situations where a user is located close to the BS but is served by the RN.

In step 3 of the simulation flow chart, the channel gains between the new user and the eligible network nodes are calculated based on the channel models and parameters proposed by [18], and the eligible SN is determined (step 4). If the eligible SN is the central cell or a cell that already serves a user, the new user is dropped. We study a system operating at the maximum 100% system load with full buffer traffic model, so for one radio channel this means one user per cell. Otherwise the new user is accepted and his SN steers its radiation pattern (any of the G_{ideal}, G_{real} or G_{ERP}) towards the new user's location. Finally, the total interference received by the wanted user at the central cell is calculated taking into account the individual radiation patterns.

Table 1: Simulation setup.

Network parameters	
Cell radius	0.5 Km
Frequency	2 GHz
Tiers	1
RN distance from BS	0.4 Km
Base station parameters	
BS height	25 m
BS antenna gain (omni)	8 dBi
BS transmit power	46 dBm
Relay node parameters	
RN height	5 m
RN antenna gain (omni)	5 dBi
RN transmit power	30 dBm
Channel models (Winner II, Table 4.4 in [4])	
BS $\rightarrow$ user: scenario C2 NLOS, $\sigma = 8$ dB	
RN_{SN} $\rightarrow$ user: scenario B1 LOS with $h_{BS} = h_{RN} = 5$ m, $\sigma = 3$ dB	
RN_{Interf} $\rightarrow$ user: scenario B1 NLOS with $h_{BS} = h_{RN} = 5$ m $d_{LOS} = 150$ m, $\sigma = 4$ dB	
Bad urban scenarios (Winner II, Tables 4–9 in [4])	
AS at BS	17°
AS at RN	33°

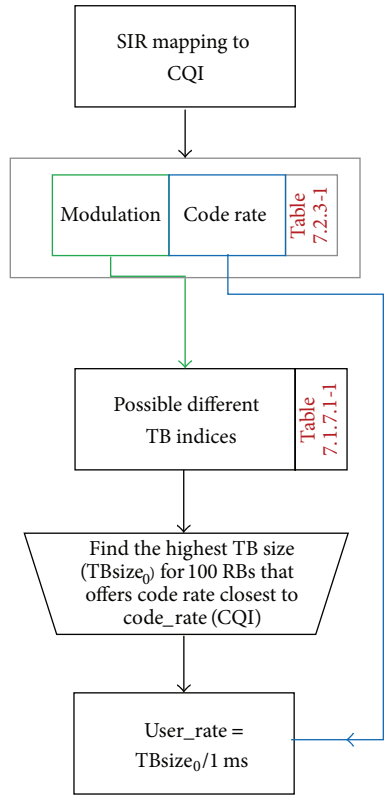

Figure 6: Flow chart for the data rate calculations. The mentioned tables can be found in [19].

Each simulation run ends when six users are served from six BSs or RNs. At this point, system level parameters such as the wanted user's SIR and data rate, are calculated and saved. In terms of the rate calculation we have considered a 4G/LTE system with 20 MHz bandwidth, and hence, Transport Block (TB) sizes for 100 Resource Blocks are taken into account. The data rate calculation methodology is briefly outlined in the flow chart of Figure 6. The detailed description of the rate calculation is out of the scope of this paper and for this reason [19] is cited.

4.2. Simulation Results. Each of the three different radiation patterns described in Section 2 (G_{ideal}, G_{real}, and G_{ERP}) was separately employed at the network nodes and the corresponding SIR ECDFs were derived for every network configuration. Our goal is first to prove that employing the ideal radiation pattern (see G_{ideal} in (3)) instead of the real one (G_{real} in (4)) in 4G networks like the one considered here produces overoptimistic results for the SIR and the achieved capacity. Then, we want to show that the simple concept of the ERP can produce the same performance results with the real radiation pattern, while it offers much greater flexibility in the analysis of such networks, for example, in [15].

Table 1 gives the basic simulation setup parameters, while the Winner II channel models with the corresponding large scale parameters that can be found in [18] were used for calculating the losses and channel gains between the network nodes and the users. It should be pointed out that cell radius of 0.5 Km was employed in the simulations in order to be in accordance with the Winner II recommendations. As mentioned in [18], the AS median values depend on the cell radius and the recommended values for bad urban scenarios were computed under the assumption of 0.5 Km cell radius.

First, a reference network scenario with no RNs was simulated, and Figure 7 presents the ECDF of the wanted user SIR. The "ideal" line shows the SIR ECDF when G_{ideal} of (3) with $N = 8$ is used at the BSs. The "real" line shows the achieved SIR when the radiation patterns of the BSs also consider the environment, that is, G_{real} of (4) with AS = 17°, and the "ERP" line is the SIR ECDF when the effective radiation pattern is employed with $BW_{opt} = 31°$ and $SLL_{opt} = 8.5$ dB (see Figure 2). As shown in Figure 8, employing the ideal radiation pattern instead of the real one leads to ~3 dB higher SIR (50% outage), which in terms of data rate corresponds to ~13 Mbps higher throughput estimation. At the same time, using the ERP method practically leads to the same SIR and data rate results with the real radiation pattern, as Figures 7 and 8 show.

For instance, in Figure 7, the difference between the "real" and the "ERP" radiation pattern for the 50% outage SIR is less than 0.4 dB. The ERP was further evaluated via simulations for different system characteristics (1 Km cell radius) but the results led to the same observations as with the results for the 0.5 Km radius presented herein; for example, for the reference scenario with no RNs the difference between the "real" and the "ERP" radiation pattern for the 50% outage SIR is ~0.3 dB (the difference for the 0.5 Km radius as previously mentioned was 0.4 dB). Hence, the obvious issue arising from the fact that a proper system analysis should take into account that

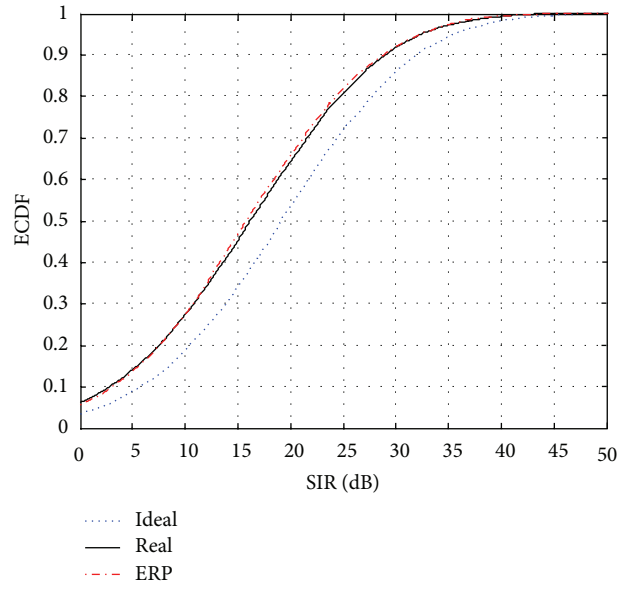

Figure 7: SIR ECDFs when the network employs no RNs (reference scenario).

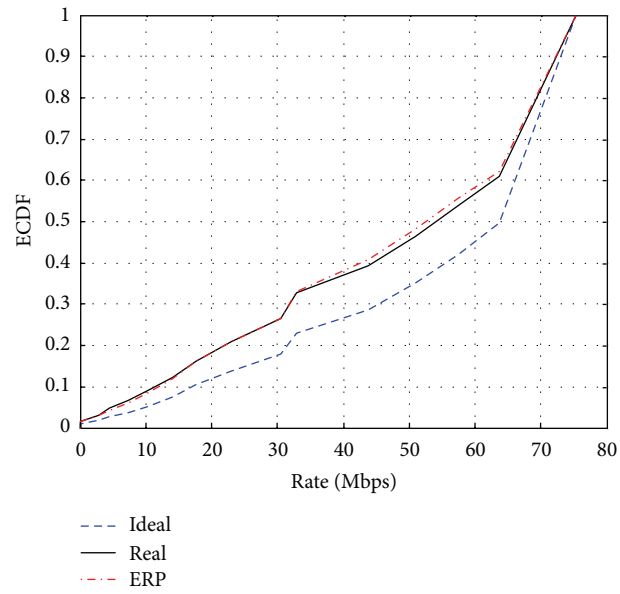

Figure 8: Rate ECDFs when the network employs no RNs (reference scenario).

the effect of the operational environment on the radiation pattern characteristics is resolved via the use of the simple method of the ERP.

It should be pointed out that the choice of 10^4 Monte Carlo iterations was validated for the reference scenario. Increasing the Monte Carlo iterations from 10^4 to 10^5 for all the radiation patterns shown in Figure 7 led to less than 0.3 dB difference for the 50% SIR outage. This difference is particularly low in the context of our problem, and hence 10^4 Monte Carlo iterations were employed in all simulations.

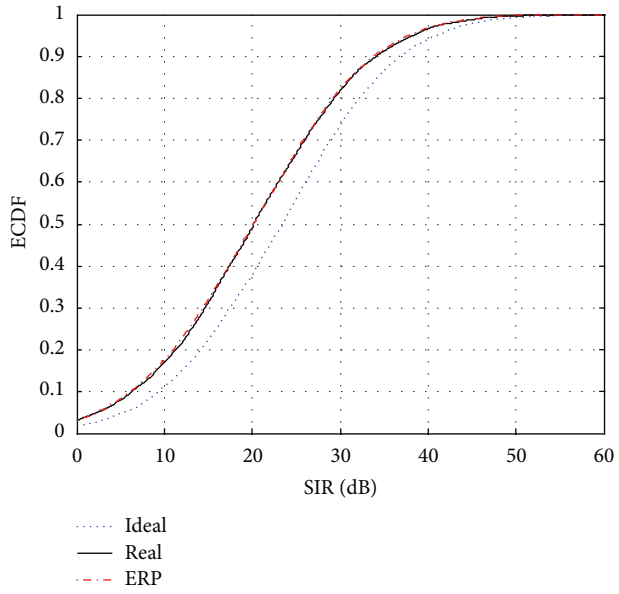

Figure 9: SIR ECDFs when the network employs 1 RN per BS.

Next, a network configuration with 1 RN per BS is simulated in order to prove the validity of the ERP method in mixed operational scenarios (different AS for BSs and RNs). Figure 9 presents the SIR ECDF for this network configuration. The "ideal" line shows the SIR ECDF when G_{ideal} of (3) with $N = 8$ is used at the BSs and the RNs. The "real" line shows the achieved SIR when the radiation patterns of the network nodes consider the environment, that is, G_{real} of (4) with AS = 17° for the BSs and G_{real} of (4) with AS = 33° for the RNs. The "ERP" line is the SIR ECDF when the ERPs are considered for the network nodes ($\text{BW}_{\text{opt}} = 31°$ and $\text{SLL}_{\text{opt}} = 8.5$ dB for the BSs and $\text{BW}_{\text{opt}} = 45°$ and $\text{SLL}_{\text{opt}} = 6$ dB for the RNs; see Figures 2 and 3, resp.). The same observations made for Figure 7 are also confirmed here. Using the ERP method at both the RNs and the BSs produces the same SIR results as with the real radiation patterns.

Figure 10 considers network configurations with 1, 2, and 4 RNs per BS. The "real" lines show the achieved SIR when the radiation patterns of the network nodes consider the environment, that is, G_{real} of (4) with AS = 17° for the BSs and G_{real} of (4) with AS = 33° for the RNs. The "ERP" lines are for the SIR when the ERPs are considered for the network nodes ($\text{BW}_{\text{opt}} = 31°$ and $\text{SLL}_{\text{opt}} = 8.5$ dB for the BSs and $\text{BW}_{\text{opt}} = 45°$ and $\text{SLL}_{\text{opt}} = 6$ dB for the RNs; see Figures 2 and 3, resp.). It can be easily seen that the ERP method can be used instead of the real radiation pattern with practically no divergence.

Figure 11 shows results for the achieved throughput in a 4G/LTE network when a different number of RNs per BS is employed. These results have been produced with the ERPs employed at the network nodes. The figure shows the ECDFs of the rate that the wanted user in the central cell can reach. Note that the ECDFs have the same peak value since the maximum TB size of TX mode 1 in LTE is ~75 Mbits (see Table 7.1.7.2.1-1 of [19]). There is an obvious performance boost in terms of throughput with the increase of RNs per cell.

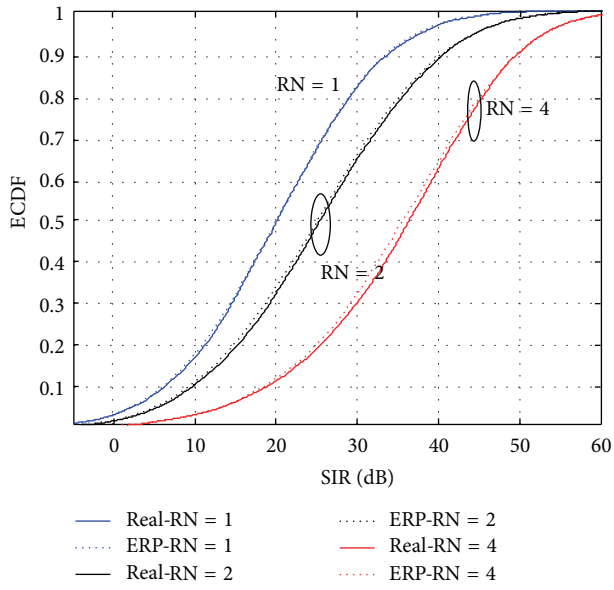

FIGURE 10: SIR ECDFs with 1, 2, and 4 RNs per BS and for both real and effective radiation patterns.

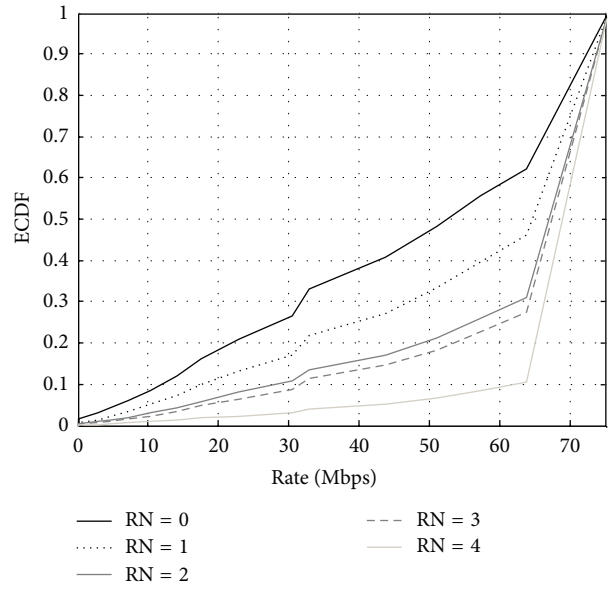

FIGURE 11: Rate ECDFs for all simulated networks with 0, 1, 2, and 4 RNs per BS. The ERPs are considered at the network nodes for $N = 8$ and AS = 17° for BSs and 33° for RNs.

This is seen more clearly in Figure 12 where the 10% outage rate and SIR are depicted for all networks configurations. Specifically, there is a 70% improvement in the wanted user rate with just the addition of one RN per BS, while there is a 500% improvement for the scenario with 4 RNs per cell (sixfold increase of the wanted user's throughput). In the same manner, one RN per BS adds 3 dB in the SIR while four RNs per BS lead to more than 15 dB SIR increase.

Comparable results for the performance gain from the deployment of RNs in 4G networks can be found, for instance, in [20] where the average cell throughput gain

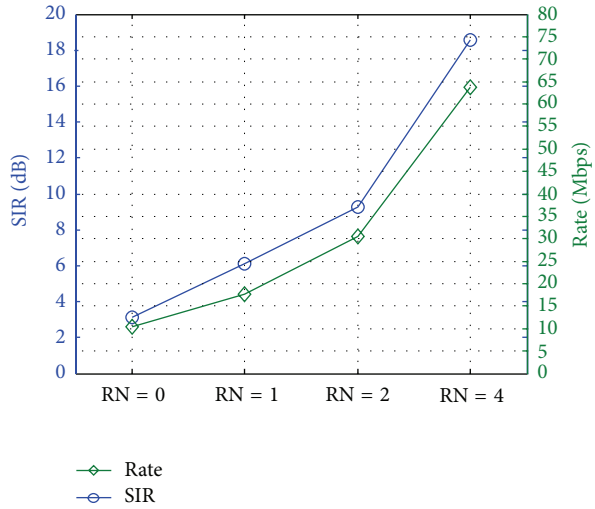

FIGURE 12: 10% outage SIR and rate for the different network configurations.

(5% outage) from one and four omnidirectional RNs per macrocell is shown to be 15% and 40%, respectively, and in [21] where 2, 3 and 6 omnidirectional RNs per cell are considered and the corresponding SIR ECDFs are provided. Specifically, in [21], the SIR gain for 10% outage when 2 omnidirectional RNs are employed is almost 4 dB, while the corresponding gain for our network with also 2 RNs per BS that however employ beamforming is more than 6 dB. At this point, it is worth noting that in the context of our work, we made the same observation with the authors in [21], concerning the performance of the network with 3 RNs per cell. The performance when 3 RNs per cell were used was only slightly better than that when 2 RNs per cell were used.

5. Conclusions

This paper proposes the simple concept of an effective radiation pattern with parameters the effective main lobe beamwidth and the effectiveaverage sidelobe level for realistic performance analysis of wireless systems. After the proposed ERP method has been described, it is incorporated into a 4G LTE beamforming system for both the base stations and the relay nodes, and simulation analysis demonstrates the system level effects (SIR, capacity) from the spatial characteristics of the radio channel, as well as the validity of the proposed method.

The performed simulations provide evidence that the ideal instead of the real radiation pattern overestimates the SIR (almost 3 dB for the reference network with no RNs) and subsequently leads to a significant over-estimation of the achieved data rates (over 13 Mbps for the reference network with no RNs). It is also proved that the ERP method produces almost identical performance results with the real radiation pattern, and hence it is a simple and viable option for designers and researches aiming at realistic performance analyses of wireless systems.

Finally, employing the ERP method the capacity of the network is studied as a function of the number of RNs. The results show that in a beamforming LTE network with RNs that also employ beamforming the usage of only one RN per cell leads to 70% throughput improvement, while increasing the number of RNs to four RNs per cell a throughput gain of 500% can be achieved.

Conflict of Interests

The authors declare that there is no conflict of interests regarding the publication of this paper.

Acknowledgments

This research has been cofinanced by the European Union (European Social Fund ESF) and the Greek National Funds through the Operational Program Education and Lifelong Learning of the National Strategic Reference Framework (NSRF)-Research Funding Program: THALIS NTUA, Novel Transmit, and Design Techniques for Broadband Wireless Networks (MIS 379489).

References

[1] V. Havary-Nassab, S. Shahbazpanahi, A. Grami, and Z. Q. Luo, "Distributed beamforming for relay networks based on second-order statistics of the channel state information," *IEEE Transactions on Signal Processing*, vol. 56, no. 9, pp. 4306–4316, 2008.

[2] Y. Jing and H. Jafarkhani, "Network beamforming using relays with perfect channel information," in *Proceedings of the IEEE International Conference on Acoustics, Speech and Signal Processing (ICASSP '07)*, pp. III473–III476, Honolulu, Hawaii, USA, April 2007.

[3] S. Fazeli-Dehkordy, S. Shahbazpanahi, and S. Gazor, "Multiple peer-to-peer communications using a network of relays," *IEEE Transactions on Signal Processing*, vol. 57, no. 8, pp. 3053–3062, 2009.

[4] Y. Zheng and S. Blostein, "Downlink distributed beamforming through relay networks," in *Proceedings of the IEEE Global Telecommunications Conference (GLOBECOM '09)*, Honolulu, Hawaii, USA, December 2009.

[5] O. Norklit, P. C. F. Eggers, and J. B. Andersen, "Jitter diversity in multipath environments," in *Proceedings of the IEEE 45th Vehicular Technology Conference*, vol. 2, pp. 853–857, July 1995.

[6] P. C. F. Eggers, "Angular dispersive mobile radio environments sensed by highly directive base station antennas," in *Proceedings of the 6th IEEE International Symposium on Personal, Indoor and Mobile Radio Communications (PIMRC '95)*, vol. 2, pp. 522–526, September 1995.

[7] G. V. Tsoulos, J. P. McGeehan, and M. A. Beach, "Space division multiple access (SDMA) field trials—part II: calibration and linearity issues," *IEE Proceedings: Radar, Sonar and Navigation*, vol. 154, no. 1, pp. 79–84, 1998.

[8] H. Xue, M. Beach, and J. McGeehan, "Non-linearity effects on adaptive antennas," in *Proceedings of the 9th International Conference on Antennas and Propagation*, vol. 1, pp. 352–355, Eindhoven, The Netherlands, April 1995.

[9] H. Steyskal, "Array error effects in adaptive beamforming," *Microwave Journal*, vol. 34, no. 9, pp. 101–112, 1991.

[10] J. Langston, S. Shashikant, K. Hinnman, K. Keisner, and D. Garcia, "Design definition for a digital beamforming processor," Tech. Rep., Rome Air Development Centre, Rome, NY, USA, 1988.

[11] P. B. Kenington and D. W. Bennett, "Linear distortion correction using a feedforward system," *IEEE Transactions on Vehicular Technology*, vol. 45, no. 1, pp. 74–81, 1996.

[12] K. R. Dandekar, H. Ling, and G. Xu, "Experimental study of mutual coupling compensation in smart antenna applications," *IEEE Transactions on Wireless Communications*, vol. 1, no. 3, pp. 480–487, 2002.

[13] H. Xue, V. Kezys, and J. Litva, "Smart antenna calibration for beamforming," in *Proceedings of the Antennas and Propagation Society International Symposium*, vol. 3, pp. 1458–1461, Atlanta, Ga, USA, June 1998.

[14] C. M. Simmonds and M. A. Beach, "Downlink calibration requirements for the TSUNAMI (II) adaptive antenna testbed," in *Proceedings of the 9th IEEE International Symposium on Personal, Indoor and Mobile Radio Communications (PIMRC '98)*, pp. 1260–1264, Boston, Mass, USA, September 1998.

[15] D. A. Zarbouti, G. V. Tsoulos, and G. E. Athanasiadou, "Theoretic SIR for multicarrier MISO beamforming cellular systems," in *Proceedings of the 7th European Conference on Antennas and Propagation (EuCAP '13)*, Goteburg, Sweden, April 2013.

[16] K. I. Pedersen, P. E. Mogensen, and B. H. Fleury, "Spatial channel characteristics in outdoor environments and their impact on BS antenna system performance," in *Proceedings of the 48th IEEE Vehicular Technology Conference (VTC '98)*, vol. 2, pp. 719–723, May 1998.

[17] A. Forenza, D. J. Love, and R. W. Heath Jr., "A low complexity algorithm to simulate the spatial covariance matrix for clustered MIMO channel models," in *Proceedings of the 59th IEEE Vehicular Technology Conference (VTC '04)*, vol. 2, pp. 889–893, May 2004.

[18] WINNER II WP1, "Channel models," Deliverable D1. 1.2, 2007, http://www.ist-winner.org/deliverables.html.

[19] 3GPP TS 36.213, "EVOLVED universal terrestrial radio access (E-UTRA), physical layer procedures," http://www.3gpp.org/ftp/Specs/html-info/36213.htm.

[20] "LTE-advanced: the advanced LTE toolbox for more efficient delivery of better user experience," Nokia Siemens Networks, 2011, http://www.nokiasiemensnetworks.com/sites/default/files/document/lte-advanced_technical_whitepaper_22032011_v03_low-res.pdf.

[21] M. Minelli, M. Coupechoux, J. M. Kelif, M. Ma, and P. Godlewski, "Relays-enhanced LTE-Advanced networks performance studies," in *Proceedings of the 34th IEEE Sarnoff Symposium (SARNOFF '11)*, pp. 1–5, Princeton, NJ, USA, May 2011.

Hindawi Publishing Corporation
International Journal of Antennas and Propagation
Volume 2013, Article ID 730710, 9 pages
http://dx.doi.org/10.1155/2013/730710

Research Article

Power Management in Multiuser Adaptive Modulation Transmission under QoS Requirements

Saud Althunibat,[1] Nizar Zorba,[2] Charalabos Skianis,[3] and Christos Verikoukis[4]

[1] *University of Jordan, Amman 11942, Jordan*
[2] *Qatar Mobility Innovations Center (QMIC), Doha 210531, Qatar*
[3] *University of the Aegean, 83200 Samos, Greece*
[4] *CTTC, 08860 Barcelona, Spain*

Correspondence should be addressed to Nizar Zorba; nizarz@qmic.com

Received 25 April 2013; Accepted 25 July 2013

Academic Editor: Athanasios Kanatas

A transmitter power management mechanism is presented in this paper where Multiple-Input Multiple-Output (MIMO) Multiuser Random Beamforming with Adaptive Modulation strategy is performed by the system. The objective of the proposed mechanism is quality of service (QoS) satisfaction for the scheduled user. The QoS is represented by the application demanded data rate and symbol error rate. The power outage problem is considered and a practical method to minimize the outage probability is proposed. The obtained results are encouraging as they show a great decrease in the system power budget. The multiuser system capability is also exploited to achieve larger power saving values and smaller probability of power outage by scheduling the user with the best channel characteristics at each time instant. The amount of saved power and the power outage probability are both presented through closed-form expressions. These theoretical results are compared to computer simulations, which show very good agreement in performance.

1. Introduction

Power efficiency in wireless systems is a very interesting and timely topic in the research arena. The wireless network interface consumes a significant amount of power that is continuously increasing mainly due to the transmitter operation at the base station (BS). Wireless operators consume a huge amount of power where the electric bill constitutes a large portion of the network running costs [1]. Therefore, if we decrease the consumed power in BSs, we will reduce the communication costs, and we will help in the environmental care by reducing the CO_2 emissions.

The main characteristic of the wireless channel is its variability over time, where several approaches have been implemented to tackle such channel variations. A strategy that has been already implemented in realistic systems is Adaptive Modulation (AM). By employing AM, the transmitter is continuously changing the employed modulation to match with the instantaneous channel conditions. AM is shown as a way to increase the system performance [2].

Such employment of the AM is mainly devoted to increase the average data rate in the system, but other system indicators, rather than the data rate, are also interesting to the system operator. One of such objectives relates to the requested quality of service (QoS) of the customers within the network. A potential measure of the QoS is through the minimum guaranteed data rate with the maximum allowed symbol error rate (SER) per user. Each served user is guaranteed a minimum signal-to-noise ratio (SNR), which provides its demanded rate and allows the user to properly decode its intended data with the predefined SER [3]. Regarding the minimum requirement per user, previous studies have shown that the user satisfaction is insignificantly increased by a performance higher than its demands, while on the other hand, if the provided resources fail to guarantee its requirements, the satisfaction drastically decreases [4].

Thus, an attractive transmission scheme is accomplished by meeting the minimum requirements for each scheduled user while minimizing the total transmitted power.

The availability of multiple antennas at the BS allows the implementation of multiple input multiple-output (MIMO) beamforming schemes at the transmitter side. To extract all the benefit from MIMO, awareness of the channel state information (CSI) is required at the transmitter side before the transmission starts. However, the required overhead to enable CSI is huge and impractical, especially in multiuser scenarios [3]. Partial CSI is the appropriate mechanism to enable beamforming with a feasible overhead on the system resources [5]. Multiuser random beamforming is an interesting beamforming strategy that only needs partial CSI and it provides an outstanding performance [5] by selecting, at each scheduling time, the user showing the best performance with respect to a randomly generated beam at the transmitter side. It remains to tackle its performance under QoS restrictions [3] in order to benefit from the scenario characteristics in the QoS achievement.

A cross-layer (XL) strategy will be proposed to employ information from the channel characteristics in the QoS management. Moreover, an XL power saving philosophy is regarded; as for a given QoS per user the system will be allowed to decrease the transmitted power by a continuous monitoring of the channel conditions. Therefore, it will be aware of the exact required power to meet the QoS-requirement of each user, with the consequent decrease in the overall transmitted power.

The minimization of the amount of transmitted power, while the QoS is achieved, is a challenge to system designers because of the nature of the wireless channel and the limitations on the power and spectrum resources. Moreover, the diverse requirements of QoS complicate the task, as several applications can coexist in the system at the same time. Several solutions have been presented in the literature to separately solve each research issue; [6, 7] propose adaptive subcarrier-bit allocation based on the QoS requirements while [8, 9] consider the QoS problem through admission control and scheduling algorithms. A power allocation over transmitting beams in MIMO system is presented in [10], where the required rate for each scheduled user is guaranteed. The rate maximization and QoS requirements are combined in [11] as the design objectives; and on the other hand, a proportional fair scheduler to tackle with different QoS requirement is designed in [12].

In the current paper, a power management mechanism based on the AM technique is presented for the MIMO Multiuser Random Beamforming scheme, where the user with the best channel characteristics is scheduled for transmission, and then the modulation is employed on the basis of its QoS-requirements represented by the demanded data rate and SER values. The transmitted power is allocated to the minimum value that satisfies the required QoS, obtaining a cross-layer framework to achieve both rate and SER demands. The required transmit power is presented in a closed-form expression, together with its statistical distributions. An important metric to identify the system performance in practical systems is the power outage [13] represented by the probability of exceeding the maximum allowed transmitted power. This metric is also obtained in a closed-form expression, where no previous contribution in the literature has obtained all these quantities through mathematical formulations. A practical solution of the power outage problem is presented, through a modification of the opportunistic beamforming decision to select another user that can be served without power outage probability. Computer simulations will validate the mathematically obtained results.

The remainder of this paper is organized as follows. Section 2 presents the system model, the MIMO opportunistic beamforming at the transmitter side, and a review of the Adaptive Modulation procedure. Section 3 discusses the proposed power management technique and its performance through a closed-form expression, followed by Section 4 with the discussion of the resultant resource power outage through the mathematical expressions. Section 5 proposes a modified opportunistic beamforming to overcome the power outage problem, followed by Section 6 with numerical results and simulations. The paper finally draws the conclusions in Section 7.

2. System Model

We focus on the downlink channel where K receivers, each one of them equipped with a single receiving antenna, are being served by a transmitter at the base station (BS) provided with n_t transmitting antennas. A channel $\mathbf{h}(t)_{[1\times n_t]}$ is considered between each user and the BS where a quasi static block fading model is assumed. The channel is kept constant through the coherence time and independently changes between consecutive time intervals with independent and identically distributed (i.i.d.) complex Gaussian entries ~CN(0,1). Let $\mathbf{w}_k(t)_{[n_t\times 1]}$ denotes the transmitted signal to the kth; then the received signal $y_k(t)$ is given by

$$y_k(t) = \mathbf{h}_k(t)\,\mathbf{w}_k(t) + z_k(t), \tag{1}$$

where $z_k(t)$ is an additive i.i.d. complex noise component with zero mean and $E\{|z_k|^2\} = \sigma^2$. A total transmission power of P_T is considered. To transmit the signal from the n_t antennas, a beamforming vector $\mathbf{g}_k(t)_{[n_t\times 1]}$ is required at the transmitter side, making the transmitted signal $\mathbf{w}_k(t) = \mathbf{g}_k(t)s_k(t)$, where $s_k(t)$ is the uncorrelated data symbol to the kth user with $E\{|s_k|^2\} = 1$. To simplify the notation, time index is dropped whenever possible.

We assume a heterogeneous system, where the K users run different applications. Each application has its own QoS requirements represented by a specified data rate and SER.

2.1. Opportunistic Beamforming. A main beamforming policy in multiuser MIMO scenarios is the random beamforming [5], where the transmitter accomplishes a maximization of the system average data rate. During the acquisition step, an i.i.d. complex Gaussian ~CN(0,1) unit-power random beam $\mathbf{g}_{[n_t\times 1]}$ is generated at the transmitter side and a known training sequence is transmitted using the generated beam for all the users in the system, and each user calculates the received SNR and feeds it back to the BS. The BS scheduler

chooses the user with the highest SNR value to benefit from its current channel situation, leading to improve the global system performance. As the user with the best channel conditions is selected for transmission, this scheme is known as the *Opportunistic Scheduler* [5]. A modified version of this scheduler has been already implemented in the cellular 3.5G HSDPA-HDR standard.

Besides its low complexity, the opportunistic beamforming only needs partial CSI which motivates its inclusion in commercial systems. The achieved throughput (TH) using opportunistic beamforming is given as follows:

$$\mathrm{TH} = E\left\{\log_2\left(1 + \max_{1\le k\le K} \mathrm{SNR}_k\right)\right\}, \tag{2}$$

where $E\{\cdot\}$ is the expectation operator to denote the average value. Notice that the value of $\max_{1\le k\le K}\mathrm{SNR}_k$ reflects the serving SNR (i.e., the SNR that the user k obtains when it is selected for transmission). The SNR value γ_k calculated at each user as follows:

$$\gamma_k = \frac{P_T\left|\mathbf{h}_k\mathbf{g}s_k\right|^2}{\sigma^2} = \frac{P_T\left|\mathbf{h}_k\right|^2}{\sigma^2}, \tag{3}$$

where the transmitted power value is usually set to unity, except for power saving mechanisms as we will later see in Section 3.

Based on such selection philosophy to deliver service to the users, the serving SNR distribution can be obtained from the SNR probability distribution function (pdf) $b(\gamma)$ of i.i.d. complex Gaussian channels [5, 14], which is stated as

$$b(\gamma) = \sigma^2 e^{-(\gamma\cdot\sigma^2)}, \tag{4}$$

and its cumulative distribution function (cdf) $B(\gamma)$ is formulated [14] as

$$B(\gamma) = 1 - e^{-(\gamma\cdot\sigma^2)}, \tag{5}$$

and since the serving SNR is the maximum over all the users' SNR values, then the cdf of the serving SNR $F(\gamma)$ is stated as [15]

$$F(\gamma) = (B(\gamma))^K = \left[1 - e^{-(\gamma\cdot\sigma^2)}\right]^K, \tag{6}$$

and the pdf $f(\gamma)$ of the serving SNR is therefore obtained as

$$f(\gamma) = K\left[1 - e^{-(\gamma\cdot\sigma^2)}\right]^{K-1}\left[\sigma^2 e^{-(\gamma\cdot\sigma^2)}\right]. \tag{7}$$

Considering the cdf of the serving rate, the probability P_r for the serving SNR to be above some predefined threshold γ^* is given as

$$P_r = 1 - \left[1 - e^{-(\sigma^2\cdot\gamma^*)}\right]^K, \tag{8}$$

where the value of γ^* can be the lowest acceptable SNR value in each modulation step, as now will be explained.

2.2. Adaptive Modulation (AM). The wireless channel is continuously fluctuating. Adaptation to these changes is required to achieve good performance in the wireless systems. The AM strategy [16] is accomplished by an instantaneous change in the employed modulation level to match the BS transmitter parameters to the channel conditions subject to the required QoS of the served user.

Notice that the selection of the user with the best SNR value is actually another way to adapt the transmitter processing to the channel properties. In this aspect, it follows the same strategy as AM schemes [16], with both strategies looking towards improving the wireless channel performance. This paper concentrates on the opportunistic scheduler and we consider it together with AM for the transmitter adaptation to the channel characteristics. We will later employ this scenario to present a power management strategy in a closed-form expression.

Consider an AM scheme that offers M available rates $\{R_1, \ldots, R_M\}$ in ascending order [2]. Each rate will be used for transmission when the QoS guarantee of the served user is implied using the corresponding modulation type. The threshold for any modulation type represents the lowest SNR value that can satisfy the required SER value by the corresponding modulation.

3. Power Management Mechanism

As the considered scenario with the AM transmission and the opportunistic beamforming has been discussed, we now present the power management mechanism along with its closed form mathematical expression. The paper will exploit the characteristics of the AM strategy that are defined in terms of intervals.

Once the user with the highest SNR is scheduled, its required rate and SER are determined and the total SNR range is divided into modulation regions according to the required SER. Each region supports one modulation type. To achieve the required rate and SER, the received SNR must be within the corresponding modulation region. After that, the transmitted power P_t must be allocated to adjust the SNR to within the modulation region.

Due to the division into regions, in each region the same modulation is employed with the same required SER satisfaction, a matter that we will exploit to achieve power saving. For example, suppose that the QoS of the scheduled user is satisfied by SER $= 10^{-3}$ and QPSK modulation; then, according to the SER, the total range is divided into regions. Table 1 presents the modulation thresholds for (SER $= 10^{-3}$) calculated upon the SER equations in [17]. Based on Table 1, and as the QoS is guaranteed by QPSK modulation, the required data rate is achieved by any SNR value between 10.34 and 14.20. In the case of SNR = 10.34, however, the allocated power is less than that of the power for SNR = 14.20. Hence, for the purpose of power saving, the allocated power must be decreased to make the SNR expression (3) to match the exact SNR threshold (10.34 in our example) of the required modulation.

Table 1: SNR thresholds for SER = 10^{-3}.

Modulation type	SNR threshold γ (dB)
BPSK	6.78
QPSK	10.34
8QAM	14.21
16QAM	17.62
32QAM	20.84
64QAM	23.96

Notice that each application requires one of the N SER values and one of M rates (i.e., modulation types), so the QoS for any application is given by two values (R_m, SER_n), where $(n = 1, 2, \ldots, N)$ and $(m = 1, 2, \ldots, M)$. Following the proposed philosophy, the resultant required transmit power, denoted by P_x, considers the ratio between the measured SNR (γ) and the SNR threshold, making it to be formulated as

$$P_x = P_T \frac{\gamma_{m,n}}{\gamma}, \tag{9}$$

where $\gamma_{m,n}$ is the threshold of the required modulation type m obtained based on the required SER_n. For the assumed heterogeneous system with possibility of having M rates with N SER values, we formulate the average required transmit power as

$$E\{P_x\} = \sum_{m,n=1}^{M,N} P_{m,n} \int_0^{\infty} \frac{\gamma_{m,n}}{\gamma} f(\gamma) \cdot d\gamma, \tag{10}$$

where $P_{m,n}$ is the probability that the QoS guarantee of the scheduled user is satisfied by SER_n and R_m. Using the power series expansion and integration by parts for (7), (10) can be solved in a closed-form expression as (see Appendix A):

$$E\{P_x\} = \sum_{m,n=1}^{M,N} P_{m,n} \gamma_{m,n} \sigma^2 K \times \sum_{k=0}^{K-1} \binom{K-1}{k} (-1)^k \ln\left(\sigma^2 (k+1)\right). \tag{11}$$

4. Power Saving under Resources Outage

The previous section introduced a power management technique that can perfectly fulfill the QoS requirements for all users with the lowest amount of transmit power. In commercial systems, the transmit power is limited to a maximum value (e.g., 1 Watt) defined by the corresponding standard. Such a limiting factor will definitely affect our proposal, so in this section we deal with the power limitation problem and we obtain its probability through mathematical expressions. We then present the amount of saved power under the maximum power restriction.

4.1. Resource Outage Probability. If the required power P_x is lower than the total available power P_T, obviously the QoS will be satisfied and we can apply the power saving proposed algorithm described in the previous section. On the other hand, the amount of required transmit power P_x that satisfies the required QoS may be larger than the maximum allowed power P_T by the system. Therefore, the QoS will not be satisfied and the user suffers from a power outage. By referring to (9), the power outage occurs only if the measured SNR (γ) is less than the required modulation threshold $(\gamma_{m,n})$ within the demanded modulation region (i.e., corresponding to the demanded rate and SER values). The probability of power outage equals to the integral of the PDF of the serving SNR from zero to the threshold of the required modulation $\gamma_{m,n}$ multiplied by the probability of the modulation threshold. Mathematically, such resource power outage probability (Pr_o) we give it by

$$\mathrm{Pr}_o = \sum_{m,n=1}^{M,N} P_{m,n} \int_0^{\gamma_{m,n}} f(\gamma) \cdot d\gamma = \sum_{m,n=1}^{M,N} P_{m,n} F(\gamma_{m,n}), \tag{12}$$

which will be employed in later formulations.

4.2. Saved Power under the Power Outage. Once the probability of the power resource outage has been calculated, we present the amount of saved power, when the proposed technique is applied. These calculations are very useful to the system designer to precisely adjust the power supply at the BS.

The amount of saved power P_s is defined as the difference between the total available power P_T and the actual transmitted power P_x, when the measured SNR is larger than the required modulation threshold (i.e., no outage). Therefore, the saved power P_s is given by

$$P_s = P_T - P_T \frac{\gamma_{m,n}}{\gamma} \quad \text{for } \gamma \geq \gamma_{m,n}, \tag{13}$$

and the average saved power over all AM regions for the N SER values and M rates is given by

$$E\{P_s\} = \sum_{m,n=1}^{M,N} P_{m,n} P_T \int_{\gamma_{m,n}}^{\infty} \left(1 - \frac{\gamma_{m,n}}{\gamma}\right) f(\gamma) \cdot d\gamma, \tag{14}$$

where the integration starts from $\gamma_{m,n}$ to overcome the probability of outage. Equation (14) can be solved in a closed-form expression and we present it as follows (see Appendix B):

$$E\{P_s\} = \sum_{m,n=1}^{M,N} P_{m,n} P_T \left[1 - F(\gamma_{m,n}) - K\sigma^2 \gamma_{m,n} \times \sum_{k=0}^{K-1} \binom{K-1}{k} (-1)^k E_1 \times \left(\sigma^2 \gamma_{m,n} (k+1)\right)\right], \tag{15}$$

where E_1 is the exponential integral function defined as $E_1(x) = \int_x^{\infty} (e^{-t}/t) \cdot dt$ [18].

5. Modified Opportunistic Beamforming

The QoS satisfaction is the main objective of our power management proposal. However, the power limitation in real systems is the main problem that affects our proposal. Therefore, we propose a method to overcome this problem and minimize the power outage probability. It is based on a modified users scheduling rather than the opportunistic one. Notice that once the user with the best channel characteristics (i.e., with the highest SNR) is selected, (9) indicates that the power outage problem occurs only if the measured SNR is less than the threshold of the required modulation for a predefined QoS satisfaction.

If another user is scheduled with another SNR value lower than the maximum and with lower QoS demands, there exists the probability that the BS could satisfy its demands. Therefore, a new scheduling strategy is now proposed based on such philosophy.

Each user knows its measured SNR value as well as its QoS demands. Therefore, only the users that can satisfy their QoS with their respective SNR values are allowed to feedback. These users can be called the "QoS potential users." Hence, the modified opportunistic beamforming is performed only among the QoS potential users, and not over all the users. Such modified strategy will reduce the feedback load, it avoids the power outage, and it guarantees that the BS will always be able to apply the power saving mechanism.

The probability that a user feeds his SNR back to the BS (i.e., being a QoS potential user) ($\Pr_f$) is defined as the probability that the required power is lower than the total available power at the BS. We formulate it as

$$\Pr_f = \sum_{m,n=1}^{M,N} P_{m,n} \int_{\gamma_{m,n}}^{\infty} b(\gamma) \cdot d\gamma \tag{16}$$

which can be simplified through (5) as

$$\Pr_f = 1 - \sum_{m,n=1}^{M,N} P_{m,n} B(\gamma_{m,n}). \tag{17}$$

The feedback load F_L is defined as the number of feedback users k out of the total number of users K, which follows the binomial distribution as

$$F_L = \binom{K}{k} \left(\Pr_f\right)^k \left(1 - \Pr_f\right)^{K-k}, \tag{18}$$

and the average number of feedback users $\overline{K}$ can be given as

$$\overline{K} = K \cdot \Pr_f. \tag{19}$$

To show the amount of saved power using this modified scheduling, we must obtain the cdf representing the modified serving SNR based in this proposal. The cdf of the kth maximum user can be easily derived using the order statistics cdf, considering that the cdf of the kth maximum user is the cdf of the $(K-k)$th order statistics [15]. Hence, the kth maximum user has a modified cdf obtained as

$$F^{(k)}(\gamma) = \sum_{j=0}^{k-1} \binom{K}{j} (B(\gamma))^{K-j} (1 - B(\gamma))^j. \tag{20}$$

The amount of saved power can be derived by referring to (14) and replacing the pdf $f(\gamma)$ by a modified pdf $f^{(k)}$ representing the new serving SNR, which we obtain by

$$E\{P_s^*\} = \sum_{m,n=1}^{M,N} P_{m,n} P_T \times \sum_{k=1}^{K} \Pr^{(k)} \int_{\gamma_{m,n}}^{\infty} \left(1 - \frac{\gamma_{m,n}}{\gamma}\right) f^{(k)}(\gamma) \cdot d\gamma, \tag{21}$$

where $\Pr^{(k)}$ is the probability that the serving SNR is the kth maximum SNR, which we give as

$$\Pr^{(k)} = \left(1 - F^{(k)}(\gamma_{m,n})\right) \prod_{i=1}^{k-1} F^{(i)}(\gamma_{m,n}). \tag{22}$$

Equation (21) represents the amount of saved power P_S^* for the modified opportunistic beamforming scheme. By using the equations in Appendix B, it can be represented in a closed form as

$$E\{P_s^*\} = \sum_{m,n=1}^{M,N} P_{m,n} P_T \sum_{k=1}^{K} \Pr^{(k)} \left[1 - F^{(k)}(\gamma_{m,n}) + A_{ijk} \sigma^2 \gamma_{m,n} E_1\left(\sigma^2 \gamma_{m,n}(i+j)\right)\right], \tag{23}$$

where the constant A_{ijk} is defined through

$$A_{ijk} = \sum_{i=0}^{k-1} \sum_{j=0}^{K-i} \binom{K}{i} \binom{K-i}{j} (-1)^j (i+j). \tag{24}$$

Notice that applying this modified scheduling leads to zero power-outage probability. It is worth noting that there is a small probability of not serving any user. This probability occurs when all users cannot satisfy their QoS demands, and hence, none of the users will feed back its SNR. To get that probability, we substitute ($k = 0$) in (18) as follows:

$$P_{\text{no}} = \left(1 - \Pr_f\right)^K. \tag{25}$$

6. Simulations

To assess the performance of the proposed power management technique, a heterogeneous scenario is set up where users with different QoS requirements coexist in the system. The results are obtained by Monte Carlo simulations. In the considered scenario, the BS intends to communicate with a single user at a time. A total of $K = 10$ users are available in the system with i.i.d. channel characteristics. A noise variance of $\sigma^2 = 1$ is also assumed together with a total antenna gain at transmitter and receiver of 15 dBi. At the BS, after all users report their SNRs, the user with the maximum SNR is scheduled and the power saving mechanism is then applied. Table 2 presents the assumed QoS requirements for each user, and the mapping between these different QoS requirements

Table 2: QoS requirements and SNR thresholds for all users.

User index	SER	Modulation type	SNR threshold $\gamma_{m,n}$ (dB)
User 1	10^{-3}	BPSK	6.79
User 2	10^{-3}	QPSK	10.34
User 3	10^{-4}	QPSK	11.80
User 4	10^{-3}	8QAM	14.21
User 5	10^{-3}	8QAM	14.21
User 6	10^{-4}	8QAM	15.62
User 7	10^{-5}	8QAM	16.69
User 8	10^{-3}	16QAM	17.62
User 9	10^{-4}	16QAM	19.00
User 10	10^{-5}	16QAM	20.06

and the minimum required SNR for QoS guarantee. The calculation of these values is based on the SER equations in [17]. In theoretical results, since we assume i.i.d users, the probability of serving a user with specific QoS requirements is equal among users; that is, $P_{m,n}$ is equal for all users.

The average amount of required transmit power versus the average SNR of the system is shown in Figure 1. Remember that the required transmit power is the amount of power that can satisfy the QoS for any user. Figure 1 shows that the average required power decreases for an increasing SNR value because as the average scheduled SNR increases, the required power to satisfy a QoS demand will decrease from (9). Also from Figure 1, notice that the required transmitted power decreases with the number of users. The multiuser gain has always been presented to enhance the average data rate of the system [5], while here we see in our case that it can be also employed to achieve a great power reduction in the system. Comparing the results obtained by simulation to the mathematical expression that we previously formulated in (11), we notice the exact match between them as the obtained mathematical results were not based on approximation but on the exact system pdf and cdf expressions.

Regarding the power limitation fact in practical systems, our proposed technique generates outage in the power resource. Figure 2 shows the probabilities of power outage versus the average SNR for 10 and 20 users. As the power outage occurs only if the required power is larger than the available power, while the required transmit power decreases for an increasing SNR value, then the power outage probability will consequently decrease as the SNR value enlarges, as confirmed in Figure 2. Here also, the multiuser diversity provides helpful properties to the system, as it enhances the reduction in the power outage probabilities. Notice the exact match between the simulation and the theoretical results (see (12)), which support our previously presented theoretical analysis.

To overcome the power outage problem, a modified opportunistic beamforming scheme was proposed in Section 5. Following this proposed algorithm, Figure 3 plots the percentage of saved power versus the average SNR. Notice that the percentage of saved power reaches up to 95% for

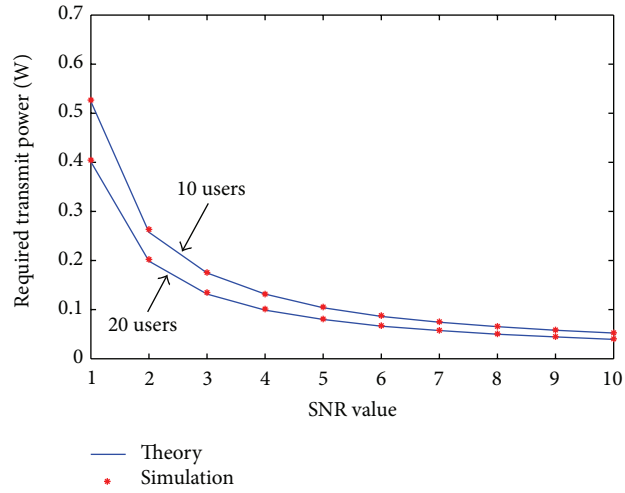

Figure 1: The required transmit power versus the average SNR.

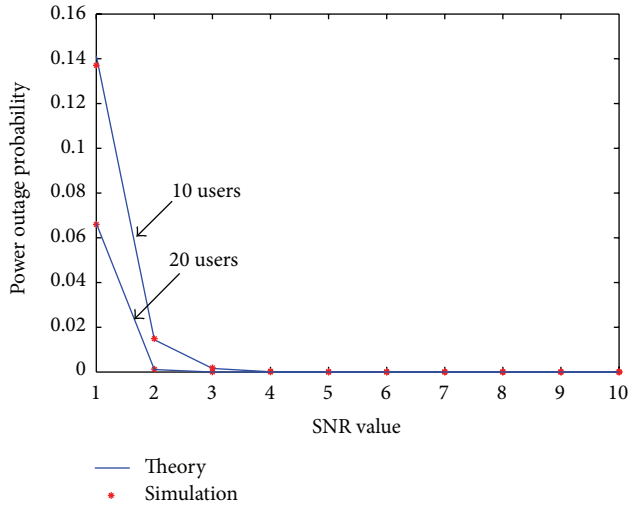

Figure 2: The probability of power outage versus the average SNR.

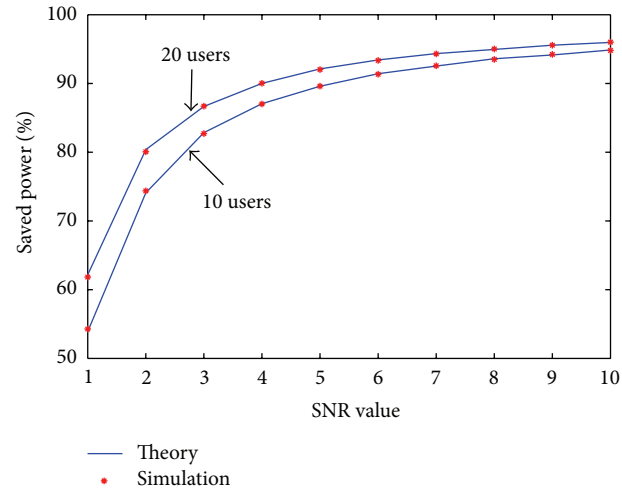

Figure 3: The percentage of saved power versus the average SNR by applying the modified opportunistic beamforming.

high SNR values, showing the large power saving that can be obtained by allowing feedback only to the users who could satisfy their QoS demands. The results are plotted for 10 and 20 users to show the multiuser gain within our proposal. It is worthy to mention that our proposed scheduling always requires an equal or smaller transmitted power compared to the classical opportunistic beamforming. This is because the proposed scheduling serves users with lower QoS requirements. The analytical results are obtained using (23).

7. Conclusions

The paper proposes a cross-layer power management strategy that benefits from the Adaptive Modulation intervals, where a quality of service indicator is defined in terms of the minimum data rate with the maximum allowed SER value. The transmitted power is decreased to the minimum required level to match the QoS demands while a multiuser scheduling is used to select the user with the best channel characteristics at each time instant. Closed-form mathematical expressions are obtained for the amounts of transmitted and saved power. The power limitation problem is also considered, where the power resource outage probability is introduced in a closed-form expression. A modified opportunistic beamforming is proposed to overcome the power resource outage problem in practical systems. Simulations show an exact match with the theoretical expressions. The system multiuser gain is presented as a potential resource to enhance the power efficiency of the system.

The analysis of the proposed mechanism of power management sheds light on more advanced mechanisms to be applied for Multiple-Input Multiple-Output (MIMO) Beamforming strategies [19] and MIMO Relay [20] scenarios, as the same philosophy of power management could be applied.

Appendices

A. Derivation of (11)

Using (7), we can rewrite (10) as

$$E\{P_x\} = \sum_{m,n=1}^{M,N} P_{m,n} \left[\int_0^{\infty} \frac{K\sigma^2\gamma_{m,n} e^{-\sigma^2\gamma}}{\gamma} \times \left(1 - e^{-\sigma^2\gamma}\right)^{K-1} \cdot d\gamma \right]. \tag{A.1}$$

Using the binomial power series, we write

$$E\{P_x\} = \sum_{m,n=1}^{M,N} P_{m,n} \left[\int_0^{\infty} \frac{K\sigma^2\gamma_{m,n}}{\gamma} \times \sum_{k=0}^{K-1} \binom{K-1}{k} (-1)^k e^{-\sigma^2\gamma(k+1)} \cdot d\gamma \right], \tag{A.2}$$

which we rearrange as

$$E\{P_x\} = \sum_{m,n=1}^{M,N} P_{m,n} \left[K\sigma^2\gamma_{m,n} \times \sum_{k=0}^{K-1} \binom{K-1}{k} (-1)^k \int_0^{\infty} \frac{e^{-\sigma^2\gamma(k+1)}}{\gamma} \cdot d\gamma \right]. \tag{A.3}$$

The integral can be divided into two integrals as follows:

$$E\{P_x\} = \sum_{m,n=1}^{M,N} P_{m,n} \left[K\sigma^2\gamma_{m,n} \times \sum_{k=0}^{K-1} \binom{K-1}{k} (-1)^k \times \left(\int_0^1 \frac{e^{-\sigma^2\gamma(k+1)}}{\gamma} \cdot d\gamma + \int_1^{\infty} \frac{e^{-\sigma^2\gamma(k+1)}}{\gamma} \cdot d\gamma \right) \right], \tag{A.4}$$

where we replace the second integral by the exponential integral, defined as $E_1(x) = \int_1^{\infty} (e^{-xt}/t) \cdot dt$ [18], so that our last expression becomes

$$E\{P_x\} = \sum_{m,n=1}^{M,N} P_{m,n} \left[K\sigma^2\gamma_{m,n} \times \sum_{k=0}^{K-1} \binom{K-1}{k} (-1)^k \times \left(\int_0^1 \frac{e^{-\sigma^2\gamma(k+1)}}{\gamma} \cdot d\gamma + E_1\left(\sigma^2(k+1)\right) \right) \right]. \tag{A.5}$$

It remains to solve the first integral which is an improper integral, using the power series representation of the exponential function, we rewrite it as follows:

$$E\{P_x\} = \sum_{m,n=1}^{M,N} P_{m,n} \left[K\sigma^2\gamma_{m,n} \times \sum_{k=0}^{K-1} \binom{K-1}{k} (-1)^k \times \left(\int_0^1 \sum_{i=0}^{\infty} \frac{\left(-\sigma^2(k+1)\gamma\right)^i}{i!\gamma} \cdot d\gamma + E_1\left(\sigma^2(k+1)\right) \right) \right], \tag{A.6}$$

that is simplified as

$$E\{P_x\} = \sum_{m,n=1}^{M,N} P_{m,n}\left[K\sigma^2\gamma_{m,n} \times\left(\int_0^1 \sum_{i=0}^{\infty}\frac{\left(-\sigma^2(k+1)\right)^i(\gamma)^{i-1}}{i!}\cdot d\gamma + E_1\left(\sigma^2(k+1)\right)\right)\right]. \tag{A.7}$$

Performing the integration, we obtain

$$E\{P_x\} = \sum_{m,n=1}^{M,N} P_{m,n}\left[K\sigma^2\gamma_{m,n}\times\sum_{k=0}^{K-1}\binom{K-1}{k}(-1)^k \times\sum_{k=0}^{K-1}\binom{K-1}{k}(-1)^k \times\left(\sum_{i=0}^{\infty}\frac{\left(-\sigma^2(k+1)\right)^i\gamma^i}{i\cdot i!}\Bigg|_0^1 + E_1\left(\sigma^2(k+1)\right)\right)\right], \tag{A.8}$$

that by substituting the integral limits, we state it as

$$E\{P_x\} = \sum_{m,n=1}^{M,N} P_{m,n}\left[K\sigma^2\gamma_{m,n}\times\sum_{k=0}^{K-1}\binom{K-1}{k}(-1)^k \times\left(\sum_{i=0}^{\infty}\frac{\left(-\sigma^2(k+1)\right)^i}{i\cdot i!} + E_1\left(\sigma^2(k+1)\right)\right)\right]. \tag{A.9}$$

The first term ($i = 0$) in the third summation is constant, through the identity $\sum_{h=0}^{H}\binom{H}{h}(-1)^h a = 0$ when a = constant [18], we reformulate the last equation as

$$E\{P_x\} = \sum_{m,n=1}^{M,N} P_{m,n}\left[K\sigma^2\gamma_{m,n}\times\sum_{k=0}^{K-1}\binom{K-1}{k}(-1)^k \times\left(\sum_{i=1}^{\infty}\frac{\left(-\sigma^2(k+1)\right)^i}{i\cdot i!} + E_1\left(\sigma^2(k+1)\right)\right)\right], \tag{A.10}$$

where we evaluate the last summation as follows:

$$E\{P_x\} = \sum_{m,n=1}^{M,N} P_{m,n}\left[K\sigma^2\gamma_{m,n} \times\sum_{k=0}^{K-1}\binom{K-1}{k}(-1)^k \times\left(-\delta-\ln\left(\sigma^2(k+1)\right)-E_1\left(\sigma^2(k+1)\right) + E_1\left(\sigma^2(k+1)\right)\right)\right], \tag{A.11}$$

where δ is Euler constant. Using the previous identity where δ is a constant, we obtain the amount of required transmit power as

$$E\{P_x\} = \sum_{m,n=1}^{M,N} P_{m,n}K\sigma^2\gamma_{m,n} \times\sum_{k=0}^{K-1}\binom{K-1}{k}(-1)^k\left(\ln\left(\sigma^2(k+1)\right)\right) \tag{A.12}$$

as given in (11).

B. Derivation of (15)

We expand the integral of (14) into two integrals as follows:

$$E\{P_s\} = \sum_{m,n=1}^{M,N} P_{m,n}P_T \times\left[\int_{\gamma_{m,n}}^{\infty} f(\gamma)\cdot d\gamma - \int_{\gamma_{m,n}}^{\infty}\frac{\gamma_{m,n}}{\gamma}f(\gamma)\cdot d\gamma\right], \tag{B.1}$$

where the first integral equals to $1 - F(\gamma_{m,n})$. Using (7), we rewrite it as

$$E\{P_s\} = \sum_{m,n=1}^{M,N} P_{m,n}P_T\left[1-F(\gamma_{m,n}) - \int_{\gamma_{m,n}}^{\infty}\frac{K\sigma^2\gamma_{m,n}}{\gamma}e^{-\sigma^2\gamma}\left(1-e^{-\sigma^2\gamma}\right)^{K-1}\cdot d\gamma\right]. \tag{B.2}$$

Using power series expansion, we simplify (B.2) as

$$E\{P_s\} = \sum_{m,n=1}^{M,N} P_{m,n}P_T\left[1-F(\gamma_{m,n}) - \int_{\gamma_{m,n}}^{\infty}\frac{K\sigma^2\gamma_{m,n}}{\gamma} \times\sum_{k=0}^{K-1}\binom{K-1}{k}(-1)^k e^{-\sigma^2(k+1)\gamma}\cdot d\gamma\right], \tag{B.3}$$

which we rearrange as

$$E\{P_s\} = \sum_{m,n=1}^{M,N} P_{m,n}P_T \left[1 - F(\gamma_{m,n}) - K\sigma^2\gamma_{m,n} \times \sum_{k=0}^{K-1} \binom{K-1}{k} (-1)^k \int_{\gamma_{m,n}}^{\infty} \frac{e^{-\sigma^2(k+1)\gamma}}{\gamma} \cdot d\gamma\right]. \tag{B.4}$$

Using the exponential integral [18], we provide the amount of saved power as the closed-form expression

$$E\{P_s\} = \sum_{m,n=1}^{M,N} P_{m,n}P_T \left[1 - F(\gamma_{m,n}) - K\sigma^2\gamma_{m,n} \times \sum_{k=0}^{K-1} \binom{K-1}{k} (-1)^k E_1\left(\sigma^2\gamma_{m,n}(k+1)\right)\right] \tag{B.5}$$

as given in (15).

Acknowledgments

This work has been funded by the Research Projects GREENET (PITN-GA-2010-264759), CO2GREEN (TEC2010-20823), and GREEN-T (CP8-006).

References

[1] W. Vereecken, W. Van Heddeghem, M. Deruyck et al., "Power consumption in telecommunication networks: Overview and reduction strategies," *IEEE Communications Magazine*, vol. 49, no. 6, pp. 62–69, 2011.

[2] J. Choi and J. Ha, "On the energy efficiency of AMC and HARQ-IR with QoS constraints," *IEEE Transactions on Vehicular Technology*, vol. 99, no. 1, 2013.

[3] N. Zorba, A. I. Pérez-Neira, A. Foglar, and C. Verikoukis, "Cross layer qoS guarantees in multiuser wlan systems," *Wireless Personal Communications*, vol. 51, no. 3, pp. 549–563, 2009.

[4] P. Svedman, S. K. Wilson, L. J. Cimini Jr., and B. Ottersten, "Opportunistic beamforming and scheduling for OFDMA systems," *IEEE Transactions on Communications*, vol. 55, no. 5, pp. 941–952, 2007.

[5] T. Samarasinghe, H. Inaltekin, and J. Evans, "Optimal selective feedback policies for opportunistic beamforming," *IEEE Transactions on Information Theory*, vol. 59, no. 5, 2013.

[6] C.-H. Choi, H.-J. Lim, T.-K. Kim, G.-H. Im, and V. B. Lawrence, "Spectral efficient multiuser technique with channel-dependent resource allocation schemes," *IEEE Transactions on Wireless Communications*, vol. 11, no. 3, pp. 990–999, 2012.

[7] S. Bashar and Z. Ding, "Admission control and resource allocation in a heterogeneous OFDMA wireless network," *IEEE Transactions on Wireless Communications*, vol. 8, no. 8, pp. 4200–4210, 2009.

[8] G. I. Tsiropoulos, D. G. Stratogiannis, P. G. Cottis, T. D. Lagkas, and P. Chatzimisios, "Adaptive resource allocation and dynamic call admission control in wireless networks," in *Proceedings of the IEEE Global Communications Conference (GLOBECOM '10)*, pp. 1217–1221, Miami, Fla, USA, December 2010.

[9] C. W. Leong, W. Zhuang, Y. Cheng, and L. Wang, "Optimal resource allocation and adaptive call admission control for voice/data integrated cellular networks," *IEEE Transactions on Vehicular Technology*, vol. 55, no. 2, pp. 654–669, 2006.

[10] N. Zorba and A. I. Pérez-Neira, "Robust power allocation schemes for multibeam opportunistic transmission strategies under quality of service constraints," *IEEE Journal on Selected Areas in Communications*, vol. 26, no. 6, pp. 1025–1034, 2008.

[11] C.-F. Tsai, C.-J. Chang, F.-C. Ren, and C.-M. Yen, "Adaptive radio resource allocation for downlink OFDMA/SDMA systems with multimedia traffic," *IEEE Transactions on Wireless Communications*, vol. 7, no. 5, pp. 1734–1743, 2008.

[12] Y. Long, H. Li, M. Pan, Y. Fang, and T. F. Wong, "A fair QoS-aware resource allocation scheme for multi-radio multi-channel networks," *IEEE Transactions on Vehicular Technology*, no. 99, 2013.

[13] K. Son, B. C. Jung, S. Chong, and D. K. Sung, "Power allocation for OFDM-based cognitive radio systems under outage constraints," in *Proceedings of the IEEE International Conference on Communications (ICC '10)*, Cape Town, South Africa, May 2010.

[14] L. Yang and M.-S. Alouini, "Performance analysis of multiuser selection diversity," in *Proceedings of the IEEE International Conference on Communications*, pp. 3066–3070, Paris, France, June 2004.

[15] B. C. Arnold, N. Balakrishnan, and H. N. Nagaraja, *A First Course in Order Statistics*, John Wiley & Sons, 1992.

[16] R. Fantacci, D. Marabissi, D. Tarchi, and I. Habib, "Adaptive modulation and coding techniques for OFDMA systems," *IEEE Transactions on Wireless Communications*, vol. 8, no. 9, pp. 4876–4883, 2009.

[17] J. Proakis, *Digital Communications*, McGraw-Hill, New York, NY, USA, 4th edition, 2000.

[18] I. S. Gradshteyn and I. M. Ryzhik, *Table of Integrals, Series, and Products*, Academic Press, New York, NY, USA, 4th edition, 1994.

[19] A. Kalis, A. G. Kanatas, and G. P. Efthymoglou, "A co-operative beamforming solution for eliminating multi-hop communications in wireless sensor networks," *IEEE Journal on Selected Areas in Communications*, vol. 28, no. 7, pp. 1055–1062, 2010.

[20] E. T. Michailidis, P. Theofylakos, and A. G. Kanatas, "Three-dimensional modeling and simulation of MIMO mobile-to-mobile via stratospheric relay fading channels," *IEEE Transactions on Vehicular Technology*, vol. 62, no. 5, pp. 2014–2030, 2012.